

HYDROLOGY AND LANDSCAPE STRUCTURE CONTROL SUBALPINE  
CATCHMENT CARBON EXPORT

by

Vincent Jerald Pacific

A dissertation submitted in partial fulfillment  
of the requirements for the degree

of

Doctor of Philosophy

in

Ecology and Environmental Sciences

MONTANA STATE UNIVERSITY  
Bozeman, Montana

April, 2009

©COPYRIGHT

by

Vincent Jerald Pacific

2009

All Rights Reserved

APPROVAL

of a dissertation submitted by

Vincent Jerald Pacific

This dissertation has been read by each member of the dissertation committee and has been found to be satisfactory regarding content, English usage, format, citation, bibliographic style, and consistency, and is ready for submission to the Division of Graduate Education.

Dr. Brian L. McGlynn

Approved for the Department Land Resources and Environmental Sciences

Dr. Bruce D. Maxwell

Approved for the Division of Graduate Education

Dr. Carl A. Fox

## STATEMENT OF PERMISSION TO USE

In presenting this dissertation in partial fulfillment of the requirements for a doctoral degree at Montana State University, I agree that the Library shall make it available to borrowers under rules of the Library. I further agree that copying of this dissertation is allowable only for scholarly purposes, consistent with “fair use” as prescribed in the U.S. Copyright Law. Requests for extensive copying or reproduction of this dissertation should be referred to ProQuest Information and Learning, 300 North Zeeb Road, Ann Arbor, Michigan 48106, to whom I have granted “the exclusive right to reproduce and distribute my dissertation in and from microform along with the non-exclusive right to reproduce and distribute my abstract in any format in whole or in part.”

Vincent Jerald Pacific

April, 2009

## ACKNOWLEDGEMENTS

First and foremost, I am extremely grateful to have worked with my major adviser, Brian McGlynn. He has been exceptionally motivating and intellectually stimulating, and his support and guidance was endless. I do not know of another advisor as willing to stay on campus until 2 am, or spend countless hours in the field under the harshest of Montana field conditions. On a more personal level, I have become a devoted follower of his “work hard, play hard” motto and think my experience as a graduate student has prospered because of it. I am thankful for support, advice, and guidance from my committee members Danny Welsch, Lucy Marshall, and Wyatt Cross. Howie Epstein was also an exceptional asset, and the only reason he was not on my graduate committee was due to the fact that he was located over 2,000 miles away. A special thanks goes out to Ward McCaughey of the US Forest Service for logistical support. I am grateful to my “partners-in-crime,” Diego and Kelsey, with whom I spent countless hours in the field and engaged in many discussions, both about research and life in general. I thank my labmates and friends, particularly Becca, Tim, Austin, Kelley, Rob, Dan, Jen, John, Galena, and Josh for their friendship and motivation. I am very grateful for my girlfriend Monica, who put up with all the late nights and long weekends and was always understanding, supportive, and motivating. Finally, I would like to thank my parents, Frank and Wendy, and my brother, Daniel, for their love, support, and encouragement. This dissertation has been a wonderful experience, and I would undoubtedly spend another 5 years as a graduate student if given the chance.

## VITA

Vincent Jerald Pacific was born in Pittsburg, PA on November 13, 1979 to Francis John Pacific and Wendy Ann Pacific. He grew up in Richmond, VA and graduated from James River High School in 1998. Vincent received a B.S. in Integrated Science and Technology (2003) from James Madison University in Harrisonburg, VA. During the following year, Vincent worked as an Environmental Technician for Joyce Engineering, Inc. in Richmond, VA. He began graduate school in 2004 at Montana State University, working with Dr. Brian McGlynn, and received a M.S. in Land Resources and Environmental Sciences in May, 2007.

## TABLE OF CONTENTS

|   |    |
|---|----|
| 1. INTRODUCTION .....   | 1  |
| Site Description .....  | 4  |
| Dissertation Organization .....   | 5  |
| References Cited .....  | 8  |
| <br>  |    |
| 2. SOIL RESPIRATION ACROSS RIPARIAN-HILLSLOPE<br>TRANSITIONS: BIOPHYSICAL CONTROLS AND THE<br>ROLE OF LANDSCAPE POSITION .....      | 13 |
| Abstract .....  | 13 |
| Introduction .....  | 14 |
| Methods .....   | 17 |
| Site Description .....  | 17 |
| Landscape Characterization .....  | 19 |
| Terrain Analysis .....  | 19 |
| Environmental Measurements .....  | 20 |
| Soil and Vegetation Carbon and Nitrogen Content .....   | 21 |
| Soil Bulk Density and Root Density .....  | 22 |
| Hydrologic Measurements .....   | 22 |
| Soil CO <sub>2</sub> Concentrations .....   | 22 |
| Surface CO <sub>2</sub> Efflux .....  | 23 |
| Soil Gas Diffusivity .....  | 24 |
| Statistical Analyses .....  | 25 |
| Results .....   | 26 |
| Landscape Analysis .....  | 26 |
| Soil Carbon, Nitrogen, and C:N Ratios .....   | 26 |
| Vegetation C:N Ratios .....   | 27 |
| Soil Bulk Density and Root Density .....  | 27 |
| Soil Temperature .....  | 27 |
| Soil Water Content .....  | 28 |
| Soil Gas Diffusivity .....  | 28 |
| Soil CO <sub>2</sub> Concentrations .....   | 28 |
| Surface CO <sub>2</sub> Efflux .....  | 29 |
| Discussion .....  | 31 |
| How does the Variability of Surface CO <sub>2</sub> Efflux differ within and between<br>Eight Riparian-Hillslope Transitions? ..... | 31 |
| Within Transects .....  | 31 |
| Cumulative Growing Season Efflux .....  | 32 |
| Between Transects .....   | 34 |

## TABLE OF CONTENTS – CONTINUED

|  |     |
|--|-----|
| Can Relationships between Efflux and Soil Water Content or Soil Temperature be Applied across Multiple Riparian and Hillslope Positions? ..... | 36  |
| How does Landscape Position and Attributes (e.g. Slope, Upslope Accumulated Areas, and Aspect) Impact Soil Respiration? .....                  | 37  |
| Implications for Up-scaling Soil Respiration Measurements .....  | 40  |
| Conclusions .....  | 42  |
| Acknowledgements .....   | 43  |
| References Cited .....   | 45  |
| <br>   |     |
| 3. DIFFERENTIAL SOIL RESPIRATION RESPONSES TO CHANGING HYDROLOGIC REGIMES.....   | 71  |
| Abstract .....   | 71  |
| Introduction .....   | 71  |
| Methods .....  | 73  |
| Results .....  | 75  |
| Discussion .....   | 76  |
| Conclusions .....  | 80  |
| Acknowledgements .....   | 81  |
| References Cited .....   | 82  |
| <br>   |     |
| 4. VARIABLE FLUSHING MECHANISMS AND LANDSCAPE STRUCTURE CONTROL STREAM DOC EXPORT DURING SNOWMELT IN A SET OF NESTED CATCHMENTS .....          | 89  |
| Abstract .....   | 89  |
| Introduction .....   | 90  |
| Methods .....  | 93  |
| Site Description .....   | 93  |
| Terrain Analysis .....   | 95  |
| Measurement Locations .....  | 96  |
| Hydrometric Monitoring .....   | 97  |
| Water Sampling .....   | 99  |
| DOC Analysis .....   | 99  |
| Cumulative DOC Export .....  | 100 |
| Results .....  | 100 |
| Landscape Analysis .....   | 100 |
| Snowmelt and Precipitation .....   | 101 |
| Transect Water Table Dynamics and DOC Concentrations .....   | 101 |
| ST1-East .....   | 101 |
| ST1-E1 .....   | 102 |

## TABLE OF CONTENTS - CONTINUED

|  |     |
|--|-----|
| ST1-E2 .....   | 102 |
| ST1-E3 .....   | 102 |
| ST1-West .....   | 103 |
| ST1-W1 .....   | 103 |
| ST1-W2 .....   | 104 |
| ST1-W3 .....   | 104 |
| ST5-West .....   | 104 |
| ST5-W1 .....   | 104 |
| ST5-W2 .....   | 105 |
| ST5-W3 .....   | 105 |
| ST5-W4 .....   | 106 |
| Stream Discharge and DOC Dynamics .....  | 106 |
| Stream Discharge .....   | 106 |
| Stream DOC Concentration .....   | 107 |
| Stringer Creek .....   | 107 |
| Tenderfoot Creek .....   | 109 |
| Spring Park Creek .....  | 110 |
| Sun Creek .....  | 110 |
| Bubbling Creek .....   | 110 |
| Cumulative Stream DOC Export .....   | 111 |
| Discussion .....   | 111 |
| What are the Dominant DOC Mobilization and Stream Delivery Mechanisms<br>during Snowmelt, and how do they Vary with Respect to Landscape Setting? .. | 111 |
| Conceptual Model .....   | 117 |
| What is the Spatial Extent/Frequency of Dominant Landscape Settings,<br>and what does this mean for DOC Export at the Catchment Scale? .....         | 120 |
| Conclusions .....  | 125 |
| Acknowledgements .....   | 127 |
| References Cited .....   | 128 |
| 5. SUMMARY .....   | 145 |

## LIST OF TABLES

| Table | Page   |
|-------|--|
| 2.1   | Landscape characterization of upslope accumulated area (UAA), riparian zone width, predominate slope of hillslope, approximate vegetative groundcover (visually estimated in 3 m <sup>2</sup> area surrounding each measurement nest), and topographic wetness index (TWI). UAA and slope were calculated using 3 m digital elevation models (Seibert and McGlynn, 2007) .....52   |
| 2.2   | Analysis of variance statistics ( $\alpha = 0.05$ ) for riparian versus hillslope 20 and 50 cm soil carbon and nitrogen content, and respective soil C:N ratios. Bold numbers indicate statistically significant differences, and $n = 8$ for all analyses. Riparian and hillslope average and standard deviation across all transects are provided.....52   |
| 2.3   | Analysis of variance statistics ( $\alpha = 0.05$ ) for transect-versus-transect comparisons A) soil carbon content; B) soil nitrogen content; and C) respective soil C:N ratios at 20 and 50 cm in both riparian and hillslope zones. Shaded boxes indicate significant differences. A dashed line indicates that statistical analysis could not be performed due to only one sample in each zone. $n$ ranged from 3 to 8 due to reclassification of some nests as riparian or hillslope.....53 |
| 2.4   | Analysis of variance statistics ( $\alpha = 0.05$ ) for riparian versus hillslope soil CO <sub>2</sub> concentrations (20 and 50 cm), soil temperature, soil water content, surface CO <sub>2</sub> efflux, and soil gas diffusivity during A) June; B) July; and C) August, 2005. Bold numbers indicate statistically significant differences.....54  |
| 2.5   | Analysis of variance statistics ( $\alpha = 0.05$ ) for transect-versus-transect comparisons of riparian and hillslope soil temperature during A) June; B) July; and C) August, 2005. Shaded boxes indicate significant differences. $n$ ranged from 24 for T7 versus T8 in June to 80 for T1 versus T2 in July.....55   |
| 2.6   | Analysis of variance statistics ( $\alpha = 0.05$ ) for transect-versus-transect comparisons of riparian and hillslope soil water content during A) June; B) July; and C) August, 2005. Shaded boxes indicate significant differences. $n$ ranged from 24 for T7 versus T8 in June to 80 for T1 versus T2 in July.....56   |

## LIST OF TABLES – CONTINUED

| Table | Page  |
|-------|---|
| 2.7   | Analysis of variance statistics ( $\alpha = 0.05$ ) for transect-versus-transect comparisons of riparian and hillslope soil water content during A) June; B) July; and C) August, 2005. Shaded boxes indicate significant differences. n ranged from 24 for T7 versus T8 in June to 80 for T1 versus T2 in July.....57  |
| 2.8   | Analysis of variance statistics ( $\alpha = 0.05$ ) for transect-versus-transect comparisons of riparian and hillslope soil CO <sub>2</sub> concentrations (20 cm) during A) June; B) July; and C) August, 2005. Shaded boxes indicate significant differences. n ranged from 24 for T7 versus T8 in June to 80 for T1 versus T2 in July.....58   |
| 2.9   | Analysis of variance statistics ( $\alpha = 0.05$ ) for transect-versus-transect comparisons of riparian and hillslope soil CO <sub>2</sub> concentrations (50 cm) during A) June; B) July; and C) August, 2005. Shaded boxes indicate significant differences. n ranged from 24 for T7 versus T8 in June to 80 for T1 versus T2 in July.....59   |
| 2.10  | Analysis of variance statistics ( $\alpha = 0.05$ ) for transect-versus-transect comparisons of riparian and hillslope soil surface CO <sub>2</sub> efflux during A) June; B) July; and C) August, 2005. Shaded boxes indicate significant differences. n ranged from 24 for T7 versus T8 in June to 80 for T1 versus T2 in July.....60   |
| 4.1   | Stringer Creek transect characteristics of upslope accumulated area (UAA), hillslope-riparian-stream connectivity, riparian width, and slope of hillslope. Hydrologic connectivity across the hillslope-riparian-stream (HRS) continuum was calculated by dividing the number of days that a hillslope water table was present by the total snowmelt period (April 15 - July 15) .....133 |
| 4.2   | Ratio of riparian:upland area and cumulative stream DOC export from April 15 to July 15, 2007 for the sub-catchments within the Tenderfoot Creek Watershed .....133   |

LIST OF TABLES – CONTINUED

| Table |  | Page |
|-------|--|------|
| 4.3   | Percentage of stream network with hillslope-riparian-stream (HRS) hydrologic connectivity, ratio of riparian:upland area, and cumulative stream DOC export from April 15 - July 15, 2007 for 4 sections of Stringer Creek: the headwaters to ST1, ST1 to the Middle Stringer Creek Flume (MSC), MSC to ST5, and ST5 to the Lower Stringer Creek Flume (LSC)..... | 134  |

## LIST OF FIGURES

| Figure |  | Page |
|--------|--|------|
| 1.1    | Location of the Tenderfoot Creek Experimental Forest, in the Little Belt Mountains of the Lewis and Clark National Forest, Montana. The sub-catchments are delineated, and the upper Stringer Creek Watershed is highlighted, where a significant portion of the research took place .....   | 12   |
| 2.1    | LIDAR (ALSM) topographic image (resolution < 1 m for bare earth and vegetation) of the upper-Stringer Creek Watershed within the Tenderfoot Creek Experimental Forest (Lewis and Clark National Forest), MT. Transect and soil respiration measurement locations are shown.....  | 61   |
| 2.2    | Bar graphs of: a) 20 cm soil C content; b) 50 cm soil C content; c) 20 cm soil N content; d) 50 cm soil N content; e) 20 cm soil C:N ratio; and f) 50 cm soil C:N ratio in hillslope (black) and riparian (grey) zones along each transect. Very small or large values are written instead of plotted as they affected the bar graph scale .....   | 62   |
| 2.3    | Bar graphs of vegetation C:N ratios in hillslope (black) and riparian (grey) zones: a) lodgepole pine (roots, twigs, and needles); b) vaccinium (roots, twigs, leaves); c) grass in the hillslopes (roots, and above-ground); d) grass in the riparian zones (roots and above-ground); and e) broad leaf plants (roots and above-ground). Whiskers represent one standard deviation based upon 3 replications. Average 20 cm soil C:N ratios (26:1 and 14:1 in the hillslope and riparian zone, respectively) are indicated by solid black (hillslope) and grey (riparian) lines ..... | 63   |
| 2.4    | Box-plots of a) soil temperature; b) soil water content; c) soil CO <sub>2</sub> concentration – 20 cm; d) soil CO <sub>2</sub> concentration – 50 cm; e) soil gas diffusivity; and f) surface CO <sub>2</sub> efflux along each transect from June 14 to August 31, 2005.....   | 64   |

## LIST OF FIGURES - CONTINUED

| Figure | Page   |
|--------|--|
| 2.5    | Bivariate plots of soil temperature and surface CO <sub>2</sub> efflux at a) riparian, and b) hillslope zones; and SWC and surface CO <sub>2</sub> efflux at c) riparian, and d) hillslope zones from all transects collected from June 9 to August 31, 2005. Solid line denotes linear regression, and p-values are provided for $\alpha = 0.05$ . Circles show data from T1N2 and T2N3, boxes show $r^2$ and p-values, and dashed line denotes linear regression, with these nests removed from analysis .....65   |
| 2.6    | Bivariate plots of soil temperature and surface CO <sub>2</sub> efflux at riparian and hillslope zones along each transect, collected from June 9 to August 31, 2005. Solid line denotes linear regression, and p-values are provided for $\alpha = 0.05$ . Dark boxes indicate a statistically significant relationship.....66  |
| 2.7    | Bivariate plots of soil water content and surface CO <sub>2</sub> efflux at riparian and hillslope zones along each transect, collected from June 9 to August 31, 2005. Solid lines denote linear regression, and p-values are provided for $\alpha = 0.05$ . Dark boxes indicate a statistically significant relationship.....67  |
| 2.8    | Box plots of cumulative growing season efflux (June 9 - August 31, 2005) from all riparian and hillslope locations .....68   |
| 2.9    | Cumulative growing season efflux (June 9 - August 31, 2005) plots for hillslope (dashed lines) and riparian (solid lines) zones across each transect.....6.9   |
| 2.10   | Cumulative growing season efflux (June 9 – August 31, 2005) from riparian and hillslope locations versus distance from channel head .....70  |
| 3.1    | Streamflow and cumulative water inputs (rain and snowmelt). a), Streamflow during 2005 (solid line), 2006 (dashed line), and 1997-2006 data record (grey lines). b) cumulative water inputs (rain and snowmelt) during 2005 (solid line), 2006 (dashed line), and 1994-2006 data record (grey lines). Peak snowmelt occurred on June 6 in 2005, and May 19 in 2006 (10-year average was May 29). Cumulative water inputs were slightly higher in 2005 than 2006 (74.4 versus 69.3 cm), however a higher percentage fell as rain during the 2005 growing season (34% versus 20%).....86 |

## LIST OF FIGURES - CONTINUED

| Figure | Page  |
|--------|---|
| 3.2    | <p>Riparian and hillslope precipitation, soil water content (SWC), and soil temperature during the 2005 (wet) and 2006 (dry) growing season. j) SWC, k) soil temperature, and l) efflux. m-p: dry growing season hillslope zone m) precipitation, n) SWC, o) soil temperature, and p) efflux. Measurements were collected between June 9 and August 31 during both 2005 and 2006 from 14 riparian and 18 hillslope measurement locations across 8 transects. Symbols indicate average values, and error bars indicate one standard deviation. n ranged from 8-32 on each sampling day. Across the 2005 and 2006 growing seasons, n = 366 and 252 in the riparian zones, respectively, and 450 and 292 in the hillslopes. Grey boxes denote intermediate SWC (optimal for soil respiration), defined as 40-60% in the TCEF (Pacific et al., 2008). Precipitation was 91% higher in 2005 than 2006.....</p> |
| 87     |   |
| 3.3    | <p>Cumulative riparian and hillslope growing season soil CO<sub>2</sub> efflux during the wet and dry growing seasons. Cumulative growing season efflux (measurements collected from June 9 - August 31) at riparian (black) and hillslope (grey) zones during the a) wet growing season (2005) and b) the dry growing season (2006). Boxes represent inter-quartile range, lines denote the cumulative median, and whiskers 1.5 times the inter-quartile range. Measurements are from 14 riparian and 18 hillslope locations across 8 transects. Total number of measurements (n) were 366 and 450 in the riparian and hillslope zones, respectively, in 2005, and 252 and 292 in 2006. The relative difference between riparian and hillslope efflux was 25% in 2005, and 79% in 2006.....</p>  |
| 88     |   |
| 4.1    | <p>Conceptual model of DOC export from the soil to the stream. At times of low flow (baseflow) (A), groundwater travels through low DOC mineral soil, and stream DOC concentrations are low. As flow begins to increase (beginning of snowmelt) (B), the water table rises into shallow organic-rich riparian soil, and inputs of DOC from the soil to the stream increase, which we refer to as a one-dimensional process (1D flushing). As flow continues to increase (C), a hydrologic connection develops across the hillslope-riparian-stream continuum and initiates 2D flushing. A large pulse of DOC can occur as high DOC water from the hillslopes is transmitted.....</p>  |
| 135    |   |

## LIST OF FIGURES - CONTINUED

| Figure |   | Page |
|--------|---|------|
| 4.2    | Location of the Tenderfoot Creek Experimental Forest (TCEF), with delineations of the sub-catchments, and locations of the flumes (at the outlet of each sub-catchment) and the Lower Stringer Creek SNOTEL site. Transect locations are denoted by rectangles, and the 3 utilized for this study within the Stringer Creek Watershed are shown in black .....  | 136  |
| 4.3    | Stringer Creek Transect 1E: a) snow water equivalent (black line) and soil water inputs from snowmelt (black bars) and precipitation (grey bars); b) ST1-E1 (riparian) 10 cm, surface, and well DOC concentrations and groundwater height; c) ST1-E2 (riparian) lysimeter (20 cm), 10 cm and well DOC concentrations and groundwater height; d) ST1-E3 (hillslope) lysimeter (20 cm) and well DOC concentrations and groundwater height; and e) stream DOC concentrations and discharge from April 15 to July 15, 2007. The percentage of the study period that hillslope-riparian-stream connectivity existed, and upslope accumulated area (UAA) at the toeslope measurement location (E2) are listed at the top of the figure. Stream discharge is from the Lower Stringer Creek Flume .....           | 137  |
| 4.4    | Stringer Creek Transect 1W: a) snow water equivalent (black line) and soil water inputs from snowmelt (black bars) and precipitation (grey bars); b) ST1-W1 (riparian) 10 cm, surface, and well DOC concentrations and groundwater height; c) ST1-W2 (riparian) lysimeter (L1 = 20 cm; L2 = 50 cm) and well DOC concentrations and groundwater height; d) statement of no hillslope water table development above the bedrock interface at 100 cm; and e) stream DOC concentrations and discharge from April 15 to July 15, 2007. The percentage of the study period that hillslope-riparian-stream connectivity existed, and upslope accumulated area (UAA) at the toeslope measurement location (W2) are listed at the top of the figure. Stream discharge is from the Lower Stringer Creek Flume ..... | 138  |

## LIST OF FIGURES - CONTINUED

| Figure | Page  |
|--------|---|
| 4.5    | Stringer Creek Transect 5W: a) snow water equivalent (black line) and soil water inputs from snowmelt (black bars) and precipitation (grey bars); b) ST5-W1 (riparian) surface and well DOC concentrations and groundwater height; c) ST5-W2 (riparian) well DOC concentrations and groundwater height; d) ST5-W3 (riparian) surface and well DOC concentrations and groundwater height; e) ST5-W4 (hillslope) well DOC concentration and groundwater height; and h) stream DOC concentrations and discharge from April 15 to July 15, 2007. Note the difference in scale for DOC at (c) and (d). The percentage of the study period that hillslope-riparian-stream connectivity existed, and upslope accumulated area (UAA) at the toeslope measurement location (W3) are listed at the top of the figure. Stream discharge is from the Lower Stringer Creek Flume.....139   |
| 4.6    | Stringer Creek and Tenderfoot Creek: a) snow water equivalent (black line) and soil water inputs from snowmelt (black bars) and precipitation (grey bars); b) discharge and DOC concentrations at ST1 on Stringer Creek; c) snow water equivalent and snowmelt; and d) stage height and DOC concentrations at Upper Tenderfoot Creek (Onion Park) from April 15 to July 15, 2007. Discharge could not be calculated at Onion Park as no flume was installed.....140   |
| 4.7    | Conceptual model of 1D and 2D flushing mechanisms. Part (a) is adapted from Jencso et al. (2009), which shows data for the entire 2007 water year. Part (b) focuses on the snowmelt period, denoted by the grey box in Part (a). For 1D flushing to occur, a hydrologic connection is necessary between the riparian zone and the stream (RS). In contrast, a hydrologic connection across the entire hillslope-riparian-stream (HRS) continuum is requisite for 2D flushing. At baseflow and/or areas of high UAA, only a small portion of the stream network has HRS hydrologic connectivity, and 1D flushing is the dominant DOC mobilization and delivery mechanism to the stream. However, the relative importance of 2D flushing increases at areas of high UAA and during times of high wetness status (such as snowmelt or precipitation events). The greatest influence of 2D flushing on stream DOC export occurs at peak snowmelt when HRS hydrologic connectivity is highest .....141 |

LIST OF FIGURES - CONTINUED

| Figure |  | Page |
|--------|--|------|
| 4.8    | Stringer Creek: a-d) upstream to downstream Stringer Creek DOC concentrations at a) Transect 1; b) Middle Stringer Creek Flume (MSC); c) Transect 5; and d) Lower Stringer Creek Flume (LSC) from April 15 to July 15, 2007. e-h) cumulative DOC export from each sub-catchment. The percentage of riparian to upland area within each sub-catchment is also shown.....    | 142  |
| 4.9    | Cumulative DOC export between April 15 and July 15, 2007 at each of the sub-catchments in the Tenderfoot Creek Watershed (including the 4 catchments within the Stringer Creek Watershed - see Figure 8) as a function of riparian:upland ratio .....  | 143  |
| 4.10   | Comparison of discharge and DOC concentrations at the catchment outlet of a) Spring Park Creek; b) Upper Tenderfoot Creek; c) Sun Creek; d) Bubbling Creek; e) Lower Tenderfoot Creek; f) Lower Stringer Creek, and g) Middle Stringer Creek from April 15 to July 15, 2007. Riparian:upland extent and cumulative stream DOC export is given for each sub-catchment. .... | 144  |

## ABSTRACT

Carbon export from high elevation ecosystems is a critical component of the global carbon cycle. Ecosystems in northern latitudes have become the focus of much research due to their potential as large sinks of carbon in the atmosphere. However, there exists limited understanding of the controls of carbon export from complex mountain catchments due to strong spatial and temporal hydrologic variability, and large heterogeneity in landscape structure. The research presented in this dissertation investigates the control of hydrology and landscape structure and position on two major avenues of carbon loss from mountain watersheds: soil respiration and stream dissolved organic carbon (DOC) export. Measurements of soil respiration and its biophysical controls (soil water content, soil temperature, vegetation, soil organic matter, and soil physical properties) and stream and groundwater DOC dynamics are presented across three years and multiple riparian-hillslope transitions within a complex subalpine catchment in the northern Rocky Mountains, Montana. Variability in soil respiration was related to hydrologic dynamics through space and time and was strongly influenced by topography and landscape structure. Cumulative soil CO<sub>2</sub> efflux was significantly higher from wet riparian landscape positions compared to drier hillslope locations. Changes in hydrologic regimes (e.g. snowmelt and precipitation timing and magnitude) also impacted soil respiration. From a wet to a dry growing season, there were contrasting and disproportionate changes in cumulative growing season surface CO<sub>2</sub> efflux at wet and dry landscape positions. Stream DOC export was also influenced by landscape structure and hydrologic variability. The mobilization and delivery mechanisms of DOC from the soil to the stream were dependent upon the size of DOC source areas and the degree of hydrologic connectivity between the stream and the riparian and hillslope zones, which varied strongly across the landscape. This dissertation provides fundamental insight into the controls of hydrology and landscape structure on carbon export from complex mountain watersheds. The results of this research have large implications for the carbon source/sink status of high elevation mountain ecosystems, the influence of changing hydrologic regimes on soil respiration, and the use of landscape analysis to determine the locations of large source areas for carbon export.

## CHAPTER 1

## INTRODUCTION

The carbon cycle is at the forefront of environmental science research due to the large rise in atmospheric carbon over past decades, which can strongly impact the Earth's climate. It has long been understood that the carbon and water cycles are intrinsically intertwined (*Schlesinger, 1997; Chapin et al., 2002*), however their interdependence through space and time remains poorly understood. Soil respiration and stream dissolved organic carbon (DOC) export are two major avenues of ecosystem carbon loss and are important components of the global carbon cycle (*Raich and Schlesinger, 1992; Laudon et al., 2004; Johnson et al., 2006; Lee et al., 2006; Jonsson et al., 2007*). Investigation of the spatiotemporal variability of soil respiration and stream DOC export requires examination of the interactions between the carbon and water cycle due to strong relationships between carbon export and hydrologic variables, such as soil water content (SWC) and fluctuations in the groundwater table, both of which are influenced by landscape structure and organization.

The hydrologic influence on soil respiration or DOC export is often examined at the ecosystem or global scale (*Oechel et al., 1993; Hope et al., 1994; Aitkenhead and McDowell, 2000; Lee et al., 2006; Heimann and Reichstein, 2008*), and can therefore overlook the controls on carbon export at smaller plot level or catchment scales. Studies of soil respiration that do occur at smaller scales are often conducted in relatively homogeneous terrain (*Parkin et al., 2005; Tang and Baldocchi, 2005; Baldocchi et al.,*

2006), or are limited to subtle biophysical gradients (*Kang et al.*, 2006; *Ohashi and Gyokusen*, 2007; *Xu and Wan*, 2008), and are therefore limited in their ability to account for the influence of landscape structure and associated strong biophysical gradients. Similarly, stream DOC export studies (*Hornberger et al.*, 1994; *Boyer et al.*, 1997, 2000) often ignore the influence of landscape structure on the spatial and temporal variability of DOC source areas and mobilization and delivery mechanisms to the stream. Consideration of landscape structure in carbon export studies in complex terrain is essential, as 70% of the western U.S. carbon sink potentially occurs at elevations greater than 750 m (*Schimel et al.*, 2002).

CO<sub>2</sub> in soil air is the sum of microbial and root respiration and is controlled in part by SWC, soil temperature, and soil organic matter (SOM) availability (*Raich and Schlesinger*, 1992; *Davidson et al.*, 1998, 2000; *Schuur and Trumbore*, 2006; *Scott-Denten et al.*, 2006). These drivers of soil respiration can vary significantly across the landscape. For example, SWC is often high in convergent and lower slope positions (*Dunne and Black*, 1970; *McGlynn and Seibert*, 2003; *Pacific et al.*, 2008), which generally occur in areas of high upslope accumulated area (UAA – a measure of the amount of land draining to a particular location) (*Jencso et al.*, 2009). Soil temperature is often dependent upon aspect and elevation, and higher soil temperatures are generally found on south-facing slopes in the northern hemisphere (*Kang et al.*, 2006). Wet areas of the landscape often have a larger accumulation of SOM because frequent saturation can retard microbial decomposition (*Schlesinger*, 1997; *Sjogersten et al.*, 2006). Given the large variability in these topographically influenced drivers of soil respiration,

landscape position needs to be accounted for in studies of CO<sub>2</sub> export from the soil to the atmosphere.

Similar to soil respiration, the influence of landscape structure on watershed hydrology can exert a strong influence on stream DOC export from mountain catchments. Past studies have often focused on DOC dynamics from riparian and wetland areas (*Hope et al.*, 1994; *Creed et al.*, 2003, 2008; *Bishop et al.*, 2004; *Agren et al.*, 2007, 2008), which generally have high organic matter content and are therefore rich DOC source areas (*Hornberger et al.*, 1994; *Boyer et al.*, 1997; *Hood et al.*, 1996), as compared to upslope positions with lower DOC mineral soil (*Boyer et al.*, 1997). However, the importance of upland DOC source areas on stream DOC export has recently been documented (*McGlynn and McDonnell*, 2003; *Hood et al.*, 2006). The transport of DOC from these source areas to the stream requires a hydrologic connection between the uplands and the riparian zone and stream (*McGlynn and McDonnell*, 2003), which is strongly influenced by the structure and organization of the landscape (*Jencso et al.*, 2009). However, our understanding of hydrologic and landscape structure controls on the spatial and temporal variability of DOC mobilization and delivery mechanisms from the soil to the stream is limited and necessitates further attention. High elevations mountain watersheds present an ideal location to examine the control of landscape structure and hydrology on carbon export due to great spatial and temporal variability in hydrologic dynamics, strong biophysical gradients, and topographic complexity.

### Site Description

The study site was the U.S. Forest Service Tenderfoot Creek Experimental Forest (TCEF) (3,591 ha; lat. 46°55' N., long. 110°52' W.) in the Little Belt Mountains of central Montana (Figure 1.1). Tenderfoot Creek drains into the Smith River, a tributary of the Missouri River. All research was conducted in the upper Tenderfoot Creek Watershed (2,280 ha), with a significant portion in the upper Stringer Creek sub-catchment (380 ha). Average elevation is 2,205 m and ranges from 1,840 to 2,421 m. The TCEF is characteristic of subalpine watersheds in the northern Rocky Mountains due to a wide range of slope, aspect, UAA, topographic convergence/divergence, and strong seasonality, and is therefore an ideal location for studies of carbon export in complex terrain.

Mean annual temperature is 0°C, and mean daily temperatures range from -8.4°C in December to 12.8°C in July (*Farnes et al.*, 1995). Mean annual precipitation is 880 mm, with ~70% falling as snow from November through May (*Farnes et al.*, 1995). Monthly precipitation generally peaks in December or January (100 to 120 mm per month), and declines to 45 to 55 mm per month from July through October. Two snow survey telemetry (SNOTEL) stations are located in the TCEF (Onion Park – 2,259 m, and Stringer Creek – 1,996 m), which provide real-time data for snow depth, snow water equivalent, precipitation, temperature, radiation, and wind speed. Peak flows in Tenderfoot Creek typically occur in late May or early June, and runoff averages 250 mm per year.

TCEF geology is characterized by granite gneiss, shales, quartz porphyry, and quartzite (*Farnes et al.*, 1995). The major soil group is mixed Aquic Cryoboralfs in the riparian zones (*Holdorf*, 1981), where the groundwater tables are generally at or near the soil surface and soil depths range from 1-2.0 m (*Jencso et al.*, 2009). In the hillslopes, Loamy skeletal, mixed Typic Cryochrepts are the predominant soil group (*Holdorf*, 1981), and soil depths range from 0.5-1 m (*Jencso et al.*, 2009). *Farnes et al.* (1995) and *Mincemoyer and Birdsall* (2006) characterized the vegetation in the TCEF. The riparian zones are generally composed of Bluejoint reedgrass (*Calamagrostis canadensis*), sedges (*Carex spp.*), rushes (*Juncaceae spp.*), and Willows (*Salix spp.*). Lodgepole pine (*Pinus contorta*) is the dominant overstory vegetation, and Grouse whortleberry (*Vaccinium scoparium*) primarily composes the understory vegetation.

### Dissertation Organization

The following chapters address in the influence of hydrology and landscape structure on the export of carbon from a subalpine catchment in the northern Rocky Mountains, Montana, with a specific focus on soil respiration and stream DOC export. The following chapters are organized to build upon and progress from the previous chapters. The objectives of this dissertation are to:

- 1) Examine the biophysical controls and the role of landscape position on soil respiration across riparian and hillslope zones,
- 2) Assess the impact of changing hydrologic regimes on soil respiration at wet and dry landscape positions, and

- 3) Evaluate the control of landscape structure on stream DOC export at both the plot and catchment scale.

Integration of these chapters herein provide a synthesis of primary controls on soil respiration and stream DOC export in a complex, snowmelt-dominated catchment. This dissertation examines the dynamic interactions between carbon export, landscape structure, and hydrology across a range of spatial and temporal scales and seeks to elucidate their fundamental linkages.

Chapter 2, “Soil respiration across riparian-hillslope transitions: Biophysical controls and the role of landscape position,” examines the control of landscape structure and soil respiration driving variables on soil surface CO<sub>2</sub> efflux. Specifically, it investigates the control of soil water content, soil temperature, and soil organic matter on soil respiration across a range of riparian-hillslope transitions with large differences in UAA, slope, aspect, and vegetation cover. This chapter highlights the need for consideration of landscape position and attributes in soil respiration studies and provides insight into the controls of the spatial variability of soil respiration across a range of riparian and hillslope zones.

Chapter 3, “Differential soil respiration responses to changing hydrologic regimes,” assesses the impact that changes in the timing and magnitude of snowmelt and precipitation can have on soil respiration across wet and dry landscape positions. It expands upon the information presented in Chapter 2 by examining the response of riparian and hillslope soil respiration across contrasting wet and dry growing seasons. The results presented in Chapter 3 demonstrate that changes in hydrologic regimes can

lead to opposing and disproportionate soil respiration responses at wet and dry landscape positions.

Chapter 4, “Variable flushing mechanisms and landscape structure control stream DOC export during snowmelt in a set of nested catchments,” builds upon the information presented in Chapters 2 and 3 by examining the control of landscape structure on DOC export. Similar to soil respiration, the export of DOC can represent a significant component of the carbon cycle and is strongly influenced by landscape structure. The mobilization and delivery mechanisms of DOC to the stream were dependent upon the degree of hydrologic connectivity across the hillslope-riparian-stream continuum, and the distribution and size of DOC source areas, which varied strongly across the landscape. The greatest DOC export occurred from areas with both high hydrologic connectivity and large DOC source areas.

Finally, Chapter 5 provides a brief summary of the main findings of each chapter of this dissertation, addresses their implications, and offers recommendations for future studies of carbon export from topographically complex catchments.

This dissertation addresses the spatial and temporal variability of soil respiration and stream DOC export, which are at the forefront of carbon cycle research. The results of each chapter demonstrate an underlying principle: landscape structure and hydrologic variability can be significant controls of carbon export from complex mountain watersheds.

References Cited

- Agren, A., I. Buffam, M. Jansson, and H. Laudon (2007) Importance of seasonality and small streams for the landscape regulation of dissolved organic carbon export. *Journal of Geophysical Research*, 112, G03003, doi: 10.1029/2006JG000381.
- Agren, A., I. Buffam, M. Berggren, K. Bishop, M. Jansson, and H. Laudon (2008) Dissolved organic carbon dynamics in boreal streams in a forest-wetland gradient during the transition between winter and summer, *Journal of Geophysical Research*, 113, G03031, doi: 10.1029/2007JG000674.
- Bishop, K., C. Pettersson, B. Allard, and Y. H. Lee (1994) Identification of the riparian sources of aquatic dissolved organic carbon, *Environmental International*, 20, 11-19.
- Aitkenhead, J. A. and W. H. McDowell (2000) Soil C:N ratios as a predictor of annual riverine DOC flux at local and global scales. *Global Biogeochemical Cycles*, 14, 127-138.
- Baldocchi, D., J. Tang, and L. Xu (2006) How switches and lags in biophysical regulators affect spatial-temporal variation of soil respiration in an oak-grass savanna, *Journal of Geophysical Research*, 111, G02008, doi: 10.1029/2005JG000063.
- Boyer, E. W., G. M. Hornberger, K. E. Bencala, and D. M. McKnight (1997) Response characteristics of DOC flushing in an alpine catchment, *Hydrological Processes*, 11, 1635-1647.
- Boyer, E. W., G. M. Hornberger, K. E. Bencala, and D. M. McKnight (2000) Effects of asynchronous snowmelt on flushing of dissolved organic carbon: a mixing model approach, *Hydrological Processes*, 14, 3291-3308.
- Chapin, F. S., P. A. Mattson, H. A. Mooney (2002) Principles of Terrestrial Systems Ecology. Springer, New York. 472 pp.
- Creed, I. F., S. E. Sanford, F. D. Beall, L. A. Molot, and P. J. Dillon (2003) Cryptic wetlands: Integrating hidden wetlands in regression models of the export of dissolved organic carbon from forested landscapes, *Hydrological Processes*, 17, 3629-3648.
- Creed, I. F., F. D. Beall, T. A. Clair, P. J. Dillon, and R. H. Hesslein (2008) Predicting export of dissolved organic carbon from forested catchments in glaciated landscapes with shallow soils, *Global Biogeochemical Cycles*, 22, GB4024, doi: 10.1029/2008GB003294.

- Davidson, E. A., E. Belk, and R. D. Boone (1998) Soil water content and temperature as independent or confounded factors controlling soil respiration in a temperate mixed hardwood forest, *Global Change Biology*, 4, 217-227.
- Davidson, E. A., L. V. Verchot, J. H. Cattanio, I. L. Ackerman, and J. E. M. Carvalho (2000) Effects of soil water content on soil respiration in forests and cattle pastures of eastern Amazonia, *Biogeochemistry*, 48, 53-69.
- Dunne, T., and R. D. Black (1970) Partial area contributions to storm runoff in a small New England watershed, *Water Resources Research*, 6, 1296-1311.
- Farnes, P.E., R. C. Shearer, W. W. McCaughey, and K. J. Hanson (1995) Comparisons of Hydrology, Geology and Physical Characteristics between Tenderfoot Creek Experimental Forest (East Side) Montana, and Coram Experimental Forest (West Side) Montana. Final Report RJVA-INT-92734. USDA Forest Service, Intermountain Research Station, Forestry Sciences Laboratory, Bozeman, Montana, 19 pp.
- Heimann, M. and M. Reichstein (2008) Terrestrial ecosystem carbon dynamics and climate feedbacks, *Nature*, 451, 289-292, doi: 10.1038/nature06591.
- Holdorf, H. D. (1981) Soil Resource Inventory, Lewis and Clark National Forest – Interim In-Service Report. On file with the Lewis and Clark National Forest, Forest Supervisor's Office, Great Falls, MT.
- Hood, E., M. N. Gooseff, and S. L. Johnson (2006) Changes in the character of stream water dissolved organic carbon during flushing in three small watersheds, Oregon, *Journal of Geophysical Research*, 111, G01007, doi: 10.1029/2005JG000082.
- Hope, D., M. F. Billet, and M. S. Cressner (1994) A review of the export of carbon in rivers: Fluxes and processes, *Environmental Pollution*, 84, 301-324.
- Hornberger, G. M., K. E. Bencala, D. M. McKnight (1994) Hydrologic controls on dissolved organic carbon during snowmelt in the Snake River near Montezuma, Colorado, *Biogeochemistry*, 25, 147-165.
- Jencso, K. G., B. L. McGlynn, M. N. Gooseff, S. M. Wondzell, K. E. Bencala, and L. A. Marshall (2009) Hydrologic connectivity between landscapes and streams: Transferring reach and plot scale understanding to the catchment scale, *Water Resources Research*, doi:10.1029/2008WR007225.
- Johnson, M. S., J. Lehmann, E. C. Selva, M. Abdo, S. Riha, and E. Guimarães Couto (2006) Organic carbon fluxes within and streamwater exports from headwater catchments in the southern Amazon, *Hydrological Processes*, 20, 2599-2614.

- Jonsson, A., G. Algesten, A. K. Bergstrom, K. Bishop, S. Sobek, L. J. Tranvik, and M. Jansson (2007) Integrating aquatic carbon fluxes in a boreal catchment carbon budget, *Journal of Hydrology*, 334, 141-150.
- Kang, S., D. Lee, J. Lee, and S. Running (2006) Topographic and climatic controls on soil environments and net primary production in a rugged temperate hardwood forest in Korea, *Ecological Resources*, 21, 64-74.
- Laudon, H., S. Kohler, and I. Buffam (2004) Seasonal TOC export from seven boreal catchments in northern Sweden, *Aquatic Science*, 66, 223-230.
- Lee, M., W. H. Mo, and H. Koizumi (2006) Soil respiration of forest ecosystems in Japan and global implications. *Ecological Resources*, 21, 828-839, doi: 10.1007/s11284-006-0038-4.
- McGlynn, B. L., and J. Seibert (2003) Distributed assessment of contributing area and riparian buffering along stream networks, *Water Resources Research*, 39, doi:10.1029/2002WR001521.
- McGlynn, B. L. and J. J. McDonnell (2003) Role of discrete landscape units in controlling catchment dissolved organic carbon dynamics, *Water Resources Research*, 39, doi:10.1029/2002WR001525.
- Mincemoyer, S. A., and J. L. Birdsall (2006) Vascular flora of the Tenderfoot Creek Experimental Forest, Little Belt Mountains, Montana, *Madrono*, 53, 211-222.
- Oechel, W. C., S. J. Hastings, G. Vourlitis, M. Jenkins, G. Riechers, and N. Grulke (1993) Recent change of Arctic tundra ecosystems from a net carbon dioxide sink to a source, *Nature*, 361, 520-523.
- Ohashi, M., and K. Gyokusen (2007) Temporal change in spatial variability of soil respiration on a slope of Japanese cedar (*Cryptomeria japonica* D. Don) forest, *Soil Biology and Biochemistry*, 39, 1130-1138.
- Pacific, V. J., B. L. McGlynn, D. A. Riveros-Iregui, D. L. Welsch, and H. E. Epstein (2008) Variability in soil respiration across riparian-hillslope transitions, *Biogeochemistry*, doi: 10.1007/s10533-008-9258-8.
- Parkin, T. B., T. C. Kasper, Z. Senwo, J. H. Prueger, and J. L. Hatfield (2005) Relationship of soil respiration to crop and landscape in the Walnut Creek Watershed, *Journal of Meteorology*, 6, 812-824.
- Raich, J. W., and W. H. Schlesinger (1992) The global carbon dioxide flux in soil respiration and its relationship to vegetation and climate, *Tellus*, 44B, 81-99.

- Schimel, T. G. F. Kittel, S. Running, R. Monson, A. Turnipseed, and D. Anderson (2002) Carbon sequestration studies in western U.S. mountains. *Eos Transactions, American Geophysical Union*, 83, 445-446.
- Schuur, E. A. G., and S. E. Trumbore (2006) Partitioning sources of soil respiration in boreal black spruce forest using radiocarbon, *Global Change Biology*, 12, 165-176.
- Scott-Denton, L. E., K. L. Sparks, R. K. Monson (2003) Spatial and temporal controls of soil respiration rate in a high-elevation, subalpine forest, *Soil Biology and Biochemistry*, 35, 525-534.
- Sjogersten, S., R. van der Wal, and S. J. Woodin (2006) Small-scale hydrological variation determines landscape CO<sub>2</sub> fluxes in the high Arctic, *Biogeochemistry*, 80, 205-216.
- Tang, J., and D. D. Baldocchi (2005) Spatial-temporal variation in soil respiration in an oak-grass savanna ecosystem in California and its partitioning into autotrophic and heterotrophic components, *Biogeochemistry*, 73, 183-207.
- Xu, W., and S. Wan (2008) Water- and plant-mediated response of soil respiration to topography, fire, and nitrogen fertilization in semiarid grassland in northern China, *Soil Biology and Biochemistry*, 40, 679-687.

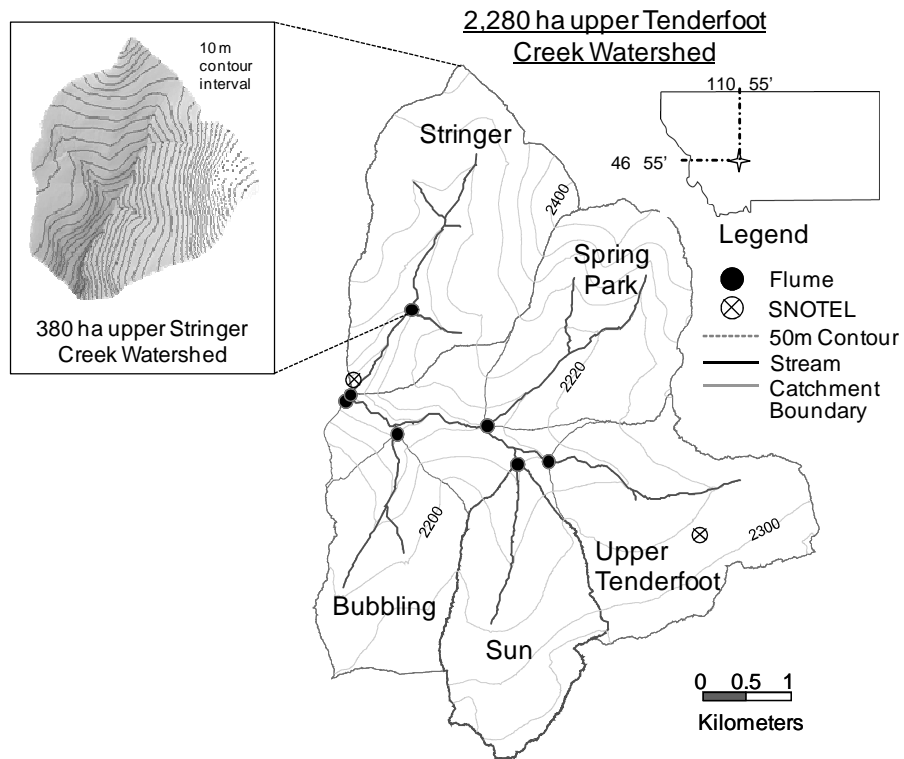


Figure 1.1: Location of the Tenderfoot Creek Experimental Forest, in the Little Belt Mountains of the Lewis and Clark National Forest, Montana. The sub-catchments are delineated, and the upper Stringer Creek Watershed is highlighted, where a significant portion of the research took place.

## CHAPTER 2

SOIL RESPIRATION ACROSS RIPARIAN-HILLSLOPE TRANSITIONS:  
BIOPHYSICAL CONTROLS AND THE ROLE OF LANDSCAPE POSITION

*Adapted from: Pacific, V.J., B.L. McGlynn, D.A. Riveros-Iregui, D.L. Welsch, and H.E. Epstein (in review) Soil respiration across riparian-hillslope transitions: Biophysical controls and the role of landscape position. Submitted for publication in Journal of Geophysical Research – Biogeosciences.*

Abstract

Soil respiration spatial variability has been the focus of much research, however, most investigations have been limited to small spatial extent or have taken place in areas of limited topographic and biophysical complexity. We investigated growing season (June-August) soil respiration across eight riparian-hillslope transitions in the subalpine upper-Stringer Creek Watershed in Montana (~380 ha). The eight transition locations differed in slope, upslope accumulated area (UAA), aspect, and vegetation cover during the 2005 growing season. Riparian-hillslope transitions are ideal for investigating the controls on soil CO<sub>2</sub> dynamics due to strong, natural biophysical gradients in soil water content (SWC), temperature, and organic matter, which largely drive soil respiration. We analyzed daily-to-weekly measurements of SWC, soil temperature, soil CO<sub>2</sub> concentrations, surface CO<sub>2</sub> efflux, and soil and vegetation C and N content (collected once) at 32 locations across eight transects. Instantaneous soil surface CO<sub>2</sub> efflux was not significantly different both within and between riparian and hillslope zones at monthly timescales according to ANOVA analysis. However, cumulative growing

season comparisons indicated that riparian zones had on average 25% greater efflux than adjacent hillslopes, and that cumulative efflux decreased downstream concurrent with decreasing UAA and vegetation cover, and increasing slopes. This study provides fundamental insight into controls on soil CO<sub>2</sub> efflux across strong biophysical gradients, offers implications for up-scaling point scale measurements of soil respiration, and highlights the need for consideration of landscape position in soil respiration studies.

### Introduction

Soil respiration constitutes the largest terrestrial flux of CO<sub>2</sub> to the atmosphere, contributing over an order of magnitude more CO<sub>2</sub> than anthropogenic sources (*Raich et al.*, 2002). While past research has examined the spatial variability of soil respiration, most studies have been limited to small spatial extent (*Fang et al.*, 1998; *Rayment and Jarvis*, 2000; *Scott-Denton et al.*, 2003), have not been conducted in areas of complex terrain (*Parkin et al.*, 2005; *Tang and Baldocchi*, 2005; *Baldocchi et al.*, 2006), or have been limited to only one or two hillslopes and subtle biophysical gradients (*Kang et al.*, 2006; *Ohashi and Gyokusen*, 2007; *Xu and Wan*, 2008). We define complex terrain as having a broad range of slopes (e.g. 5 to 45% in our study), aspects, landscape elements (e.g. riparian and hillslope zones), topographic convergence and divergence, and landcover (e.g. forests and meadows). Seventy percent of the western U.S. carbon sink potentially occurs at elevations greater than 750 m (*Schimel et al.*, 2002), and often in complex topography; therefore it is essential to understand and consider the role of landscape position and biophysical gradients in soil respiration.

CO<sub>2</sub> in soil air is the sum of autotrophic (root) and heterotrophic (microbial) respiration. Soil temperature and soil water content (SWC) (*Raich and Schlesinger, 1992; Fang and Moncrieff, 1999; Tang and Baldocchi, 2005*), as well as the availability of soil organic matter (SOM) (*Schuur and Trumbore, 2006; Scott-Denton et al., 2006*), are considered to be the primary controls on soil CO<sub>2</sub> production. Traditionally, it is accepted that increases in both soil temperature (*Fang and Moncrieff, 2001; Yuste et al., 2007; Xu and Wan, 2008*) and SWC (*Davidson et al., 1998, 2000; Liu and Li, 2005; Risch and Frank, 2007*) promote higher soil CO<sub>2</sub> production. However, soil respiration rates can quickly decrease when soils become very wet (*Happell and Chanton, 1993; Davidson et al., 1998; Gulege and Schimel, 2000*) or very dry (*Conant et al., 1998; Welsch and Hornberger, 2004; Riveros-Iregui et al., 2007, 2008a*).

The efflux of CO<sub>2</sub> from the soil to the atmosphere is the balance between soil CO<sub>2</sub> production and soil gas diffusivity (i.e. transport through the soil column). An increase in SWC often leads to higher soil CO<sub>2</sub> production (*Davidson et al., 1998, 2000*), but simultaneously reduces soil gas transport (*Millington, 1959; Washington et al., 1994; Moldrup et al., 2000, 2001*). This production-transport balance can result in short term efflux equifinality (i.e. comparable outcomes with different combinations of the variables) across landscapes where SWC-mediated CO<sub>2</sub> production and transport are spatially variable (*Pacific et al., 2008*). For example, *Pacific et al. (2008)* found that despite concentration gradients that were nearly an order of magnitude higher in riparian versus hillslope zones, efflux was similar across short timescales. *McCarthy and Brown (2006)* and *Sotta et al. (2006)* also found similar efflux across upland and lowland

positions, even though SWC was significantly different. These results indicate efflux equifinality at short timescales can result from different combinations of production and transport controlling variables.

Significant differences in the drivers of soil respiration can exist as a function of landscape position. For example, higher SWC is often observed in convergent (*Dunne and Black, 1970; Anderson and Burt, 1978; McGlynn and Seibert, 2003*), depressional (*Parkin et al., 2005*), lower slope positions (*Sotta et al., 2006; Xu and Wan, 2008; Pacific et al., 2008*), and locations with high upslope accumulated area (UAA, a measure of the area of land draining to a particular location) (*Jencso et al., 2009*). This variability in SWC can in turn affect other soil respiration driving variables, such as the abundance of SOM (*Ostendorf, 1996; Sjogersten et al., 2006*) and magnitude of soil gas diffusivity (*Millington, 1959; Schwendenmann et al., 2004; Moldrup et al., 2001; Sotta et al., 2007*). Aspect can be a strong control on soil temperature, with higher soil temperatures generally found on south-facing slopes in the northern hemisphere (*Kang et al., 2006*). Spatial variability in vegetation can also influence soil respiration due to differences in root respiration and the quantity and quality of detritus (*Raich and Tufekcioglu, 2000*). These biophysical gradients across landscape positions can lead to strong spatial heterogeneity in soil respiration.

Riparian and hillslope zones are two dominant landscape elements in headwater watersheds and generally have distinct SWC and groundwater table regimes, leading to differences in soil and vegetation characteristics (*Hill, 1996; McGlynn and Seibert, 2003*). The riparian zone can be defined as the near-stream area between the hillslope

and stream channel (*Seibert and McGlynn, 2005*), and is often characterized by hydromorphic soils (*Phillips et al., 2001; Cosanday et al., 2003; Mourier et al., 2008*), high SOM (*McGlynn and McDonnell, 2003; Hill and Cardaci, 2004; Hill et al., 2004; Gurwick et al., 2008*), and sharp decrease in slope from the adjacent hillslope zone (*Merot et al., 1995; Jencso et al., in press*). Riparian-hillslope transitions are useful for investigating the role of landscape position and biophysical variables on soil respiration due to strong gradients of SWC, soil temperature, soil gas diffusivity, and SOM.

We present measurements of growing season (June-August) surface CO<sub>2</sub> efflux, soil CO<sub>2</sub> concentrations, SWC, soil temperature, and soil and vegetation C and N content at thirty-two positions along eight riparian-hillslope transitions in a complex subalpine watershed in the northern Rocky Mountains to address the following questions:

- 1) How does the variability of surface CO<sub>2</sub> efflux differ within and between eight riparian-hillslope transitions?
- 2) Can relationships between efflux and SWC or temperature be applied across multiple riparian and hillslope positions?
- 3) How do landscape positions and attributes (e.g. slope, upslope accumulated area, and aspect) impact soil respiration?

## Methods

### Site Description

This research was conducted in the United States Forest Service Tenderfoot Creek Experimental Forest (TCEF, lat. 46°55' N., long. 110°52' W.) within the upper-Stringer Creek Watershed (~380 ha). The TCEF is located in the Little Belt Mountains within the

Lewis and Clark National Forest of central Montana (Figure 2.1), and is characteristic of subalpine watersheds in the northern Rocky Mountains (wide range of slope, aspect, and topographic convergence/divergence). Elevation ranges from 1,840 to 2,421 m, with a mean of 2,205 m.

The mean annual temperature is 0°C, with mean daily temperatures ranging from -8.4°C in December to 12.8°C in July (*Farnes et al.*, 1995). Annual precipitation averages 880 mm, with ~70% falling as snow from November through May with typical snow depths of 1-2 m. The growing season for the TCEF is 45 to 75 days (but can decrease to 30 to 45 days on the ridges). For this study, we define the growing season as June 15 – August 31.

Lodgepole pine (*Pinus contorta*) is the dominant overstory vegetation (*Farnes et al.*, 1995); subalpine fir (*Abies lasiocarpa*), Douglas fir (*Pseudotsuga menziesii*), Englemann spruce (*Picea engelmannii*), and whitebark pine (*Pinus albicaulis*) are also present. Trees are present on the hillslopes along each transect and are generally not found in the riparian areas. Grouse whortleberry (*Vaccinium scoparium*) is the dominant understory species in the uplands, while riparian vegetation is mainly composed of bluejoint reedgrass (*Calamagrostis canadensis*) (*Mincemoyer and Birdsall*, 2006). In general, west-aspect hillslopes often have a denser canopy cover and later snowmelt. The geology is characterized by granite gneiss, shales, quartz porphyry, and quartzite (*Farnes et al.*, 1995), and the most extensive soil types are Loamy skeletal, mixed Typic Cryochrepts, and clayey, mixed Aquic Cryoboralfs (*Holdorf*, 1981).

### Landscape Characterization

Eight transects (approximately 50 m long) were installed within the upper-Stringer Creek Watershed (Figure 2.1). Each transect originated at Stringer Creek, which flows north to south, and extended up the fall line through the riparian zones and adjacent hillslopes. The transects were labeled 1 through 8, and located in east-west pairs (odd = west, even = east along 4 stream reaches along Stringer Creek. T1 and T2 were the northern-most (upstream) transects, and T7 and T8 the southern-most (downstream) transects. The riparian-hillslope transition was defined by a break in slope, higher and more sustained groundwater tables in the riparian zones (often leading to saturated conditions), difference in soil depth (0.5-1 m in the hillslopes and 1-2 m in the riparian zones), and change in soil properties (more organic soils in the riparian zones and mineral soils in the hillslopes) (*Seibert and McGlynn, 2007; Jencso et al., 2009*) and vegetation (predominantly bluejoint reedgrass in the riparian zones and grouse whortleberry in the hillslopes) (*Mincemoyer and Birdsall, 2006*). Four instrumentation nests were installed along each transect, two each in the riparian and hillslope zones. The nests were labeled 1-4, with 1 being furthest up the hillslope, and 4 closest to Stringer Creek. Some nests were reclassified as either riparian or hillslope once data collection began due to groundwater table dynamics (T3-2 as riparian, and T2-3, T5-3, and T7-3 as hillslope) (*Seibert and McGlynn, 2007*).

### Terrain Analysis

An ALSM (airborn laser swath mapping, commonly known as LIDAR) 3 m digital elevation model (DEM) was used to calculate UAA (amount of land area draining

to a particular location, calculated from the instrument nest closest to the stream on each transect; e.g. T1-4, T2-4) and slope (average slope along the fall line from the highest to lowest hillslope location; e.g. T1-1 to T1-2) along each transect (*Seibert and McGlynn, 2007*). Riparian zone width was calculated from a GPS survey (Trimble GPS 5700 receiver) (*Jencso et al., 2009*), and vegetation cover was visually estimated in a 3 m<sup>2</sup> area surrounding each measurement nest. The topographic wetness index (TWI), which can be interpreted as a relative wetness index, indicated landscape position wetness propensity with the following equation (*Beven and Kirkby, 1979*):

$$TWI = \ln(a/\tan\beta) \quad (1)$$

where  $a$  is the upslope contributing area (area of land draining to a particular location, defined as the measurement location closest to String Creek on each transect) and  $\tan\beta$  is the local slope

### Environmental Measurements

Along each transect, environmental measurements were collected every 1-5 days from June 9 – August 31, 2005. Both volumetric SWC (cm<sup>3</sup> H<sub>2</sub>O/cm<sup>3</sup> soil, integrated over the top 20 cm of soil; Hydrosense portable SWC meter, Campbell Scientific Inc., Utah, USA) and soil temperature (12 cm soil thermometer, Reotemp Instrument Corporation, San Diego, California, USA; measurement range of -20°C to 120°C) were manually collected within a 1 m<sup>2</sup> measurement area at each nest location. SWC was measured three times due to potential spatial variability of SWC, and measurements were averaged for data analysis.

The Hydrosense portable SWC meter was calibrated using a time domain reflectometry (TDR) system developed following *Robinson et al. (2003)*. The TDR sensor was tested in the laboratory by comparing TDR and gravimetric measurements over a wide range of SWC. Approximately 300 SWC measurements were collected in the field with both instruments. Measurements were comparable in the mineral upland soil ( $r^2 = 0.99$ ), but overestimated by the Hydrosense in the organic riparian soil. The following equation was therefore used to adjust Hydrosense SWC measurements in the organic riparian soil:

$$\text{SWC} = (0.7704 * \text{Hydrosense measurement}) + 0.8774$$
$$(r^2 = 0.986) \quad (2)$$

#### Soil and Vegetation Carbon and Nitrogen Content

Soil samples were collected at both 20 and 50 cm depths at all nest locations along each transect with a hand auger (7.5 cm diameter, 10 cm height, with center of sample at depth of interest) from July 26-30, 2005. Vegetation samples (3 replicates) were collected along T1 and T2 from lodgepole pine (roots, needles, and twigs), vaccinium (roots, stems, leaves) and grass (roots and above-ground vegetation) from the hillslopes, and broad leaf plants and grass (roots and above-ground vegetation) from the riparian zones. The samples were dried, sieved (60-mesh, 250  $\mu\text{m}$  screen), ground into a fine powder using a mortar and pestle, and weighed and analyzed for total C and N content using a C and N analyzer (LECO TruSpec CN, Leco Corporation, St. Joseph, Michigan, USA).

### Soil Bulk Density and Root Density

Bulk density of the upper 5 cm of soil was measured with a 5 cm diameter bulk density sampler. Soil root density was measured from soil samples collected from the upper 20 cm of soil using a hand auger (5 cm diameter). The samples were dried, and the roots were manually separated and weighed in the lab.

### Hydrologic Measurements

Groundwater wells (screened from the completion depth of [0.5 to 2 m] to within 0.2 m of the ground surface) were installed at both riparian and the lower hillslope nests (i.e. 4, 3, 2) along each transect. Groundwater levels were recorded every 30 min using capacitance rods (+/- 1 mm resolution, Trutrack, New Zealand).

### Soil CO<sub>2</sub> Concentrations

Following the methods described by *Andrews and Schlesinger* (2001) and *Welsch and Hornberger* (2004), soil air gas wells (15-cm section of 5.25 cm [inside diameter] PVC) were installed at completion depths of 20 and 50 cm at each nest (total of two gas wells per nest). The top of each gas well was capped with a size 11 rubber stopper through which passed two pieces of PVC tubing (4.8 mm inside diameter Nalgene 180 clear PVC, Nalge Nunc International, Rochester, New York, USA) that extended above the ground surface. To ensure that no gas escaped while measurements were not being collected, the tubing was joined with plastic connectors (6-8 mm HDPE FisherBrand tubing connectors, Fisher Scientific, USA).

Soil air CO<sub>2</sub> concentrations were measured by attaching the two sections of gas well tubing to a portable infrared gas analyzer (IRGA) (model EGM-3, accurate to within

1% of calibrated range [0 to 50,000 ppm]; PP Systems, Massachusetts, USA;) or (model GM70 with M170 pump and GMP 221 CO<sub>2</sub> probe, accurate to within 1% of calibrated range [0 to 50,000 ppm]; Vaisala, Finland), as performed by *Pacific et al.* (2008). Two IRGAs were available in case one needed to be recalibrated, and measurements were routinely compared in the field to ensure validity. The air from the gas well was circulated through the IRGA and returned to the gas well, creating a closed loop and minimizing pressure changes during sampling. Both instruments were allowed a 30 min warm-up time (per the manufacturer's recommendations), and after which remained on for the duration of measurements. The CO<sub>2</sub> concentration measurement required 2-5 minutes (recirculation time) before stabilized values were recorded. Recirculation time did not affect soil CO<sub>2</sub> concentrations in our experimental design or similar designs (*Andrews and Schlesinger, 2000; Welsch and Hornberger, 2004; Pacific et al., 2008*). Soil CO<sub>2</sub> concentration measurements were internally corrected for air temperature and pressure with the EGM-3 and compensated for air temperature and pressure for the GMP 221 following recommendations by the manufacturer and described in detail by *Tang et al.* (2003).

#### Surface CO<sub>2</sub> Efflux

A 0.5 m<sup>2</sup> surface CO<sub>2</sub> efflux plot, roped off to minimize soil trampling, was selected at each nest location. To minimize the effect of above-ground autotrophic respiration inside the chamber, vegetation within the efflux plot was clipped approximately once per week after a round of measurements was collected. Plant roots were left intact to minimize disturbance to belowground root respiration. A soil

respiration chamber (SRC-1 chamber with a footprint of 314.2 cm<sup>2</sup>, accurate to within 1% of calibrated range [0 to 9.99 g CO<sub>2</sub> m<sup>-2</sup> hr<sup>-1</sup>] in conjunction with an IRGA (EGM-4, accurate to within 1% of calibrated range [0 to 2,000 ppm]; PP Systems, Massachusetts, USA) was used to measure surface CO<sub>2</sub> efflux (three measurements per nest location, averaged for data analysis). The chamber was flushed with ambient air for 15 s then inserted 3 cm into the soil before each measurement began. We estimated cumulative efflux from June 9 to August 31, 2005, by linearly interpolating between measurements collected every 2-7 days. *Riveros-Iregui et al.* (2008a) demonstrated that this was a robust approach for comparison of efflux measurements across multiple locations over extended periods of time at this site, and that sampling frequency did not bias cumulative efflux estimates.

### Soil Gas Diffusivity

We inversely calculated “effective” soil gas diffusivity for the upper 20 cm of the soil profile (which provided an estimate of  $D$  in the following equation) using Fick’s Law and measured values of surface CO<sub>2</sub> efflux, 20 cm soil CO<sub>2</sub> concentrations, and an assumed atmosphere CO<sub>2</sub> concentrations of 400 ppm:

$$\text{Flux} = -D \frac{\partial C}{\partial z} \quad (3)$$

where  $D$  is the diffusivity (m<sup>2</sup> s<sup>-1</sup>),  $C$  is the CO<sub>2</sub> concentration (ppm), and  $z$  is the depth (m).

### Statistical Analyses

Analysis of variance (ANOVA) statistics ( $\alpha = 0.05$ ) were used to test for differences between the drivers of soil respiration both within transects (riparian versus hillslope) and between transects (riparian versus riparian, and hillslope versus hillslope). For analysis of riparian versus hillslope soil C and N content and respective soil C:N ratios,  $n = 8$ , as samples were collected once at each nest location over the course of the study (Table 2). For comparisons between transects,  $n$  ranged from 3 to 8 due to reclassification of some nests as either riparian or hillslope. ANOVA analysis was also employed to test for differences in soil CO<sub>2</sub> concentrations, soil temperature, SWC, soil gas diffusivity, and surface CO<sub>2</sub> efflux within transects (riparian versus hillslope) and between transects (riparian versus riparian, and hillslope versus hillslope). For these variables, separate analyses were performed each month due to the temporal dynamics at our research site. For within-transect analyses,  $n$  was higher on T1-T4 (ranging from 52 in June to 80 in July on T1-T4 versus 24 in August to 44 in June on T5-T8, Table 4) as these transects had a higher sampling frequency (to increase temporal resolution). For comparisons between transects,  $n$  ranged from 24 for T7 versus T8 in June to 80 for T1 versus T2 in July. Three measurements of SWC and surface CO<sub>2</sub> efflux were collected at each nest location on all sampling days and averaged for data analysis. To test the validity of the ANOVA approach and test for autocorrelation problems, we performed autocorrelation tests, which showed that our measurements had little to no temporal dependence over the monthly timescales used for the ANOVA analysis.

## Results

### Landscape Analysis

Landscape characterization results are summarized in Table 2.1. UAA ranged from 1023 m<sup>2</sup> on T7 to 14,783 m<sup>2</sup> on T4, with the lowest values on downstream transects. The slope of the hillslopes generally increased moving downstream, with a minimum of 13.6% on T2 and maximum of 42.5% on T8. Riparian zone width ranged from 12.7 m on T1 to 4.7 m on T7, and was typically wider on upstream transects. Vegetation cover was lowest on downstream transects, ranging from 20% on T5 to 90% on T2. TWI was in general highest on upstream transects, with the highest values of 11.5 on T3, and lowest of 8.0 on T8.

### Soil Carbon, Nitrogen, and C:N Ratios

In general, soil C content was not significantly different between riparian and hillslope landscape positions within each transect (Table 2.2, Figure 2.2). Significant differences between riparian zones across transects were not found, while a small number of differences were observed between hillslopes across transects (Table 2.3, Figure 2.2). Riparian and hillslope soil N content were generally not significantly different within each transect (Table 2.2), and few significant differences were found between transects (Table 2.2, Figure 2.2).

However, there were differences in riparian versus hillslope soil C:N ratios within transects, with significantly higher ratios in the hillslopes on T1, T3, and T4 at 20 cm, and on T3 and T4 at 50 cm (Table 2.2, Figure 2.2). There was also a general trend of decreasing soil C:N ratios from hillslope to riparian zones along each transect (Figure

2.2). Few significant differences in 20 and 50 cm soil C:N ratios were observed when comparing hillslope zones between transects, while many differences were found between riparian zones at both 20 and 50 cm across transects (Table 2.3). T2, T4, and T7 had significantly higher, and T3, T6, and T8 significantly lower C:N ratios than other transects (Figure 2.2), consistent with differences in SWC and groundwater regimes.

#### Vegetation C:N Ratios

Vegetation C:N ratios were highest in hillslope vegetation, with the highest values in lodgepole pine roots and twigs, and lowest values in *vaccinium* leaves (Figure 2.3). In the riparian zones, the highest vegetation C:N ratios were found in grass roots, and the lowest values in above-ground broad leaf vegetation.

#### Soil Bulk Density and Root Density

Soil bulk density was slightly higher in the riparian zones, with an average and standard deviation of 0.962 and 0.046 g cm<sup>-3</sup>, respectively, versus 0.911 and 0.076 g cm<sup>-3</sup> in the hillslopes. Riparian zone soil root density was also higher than in the hillslopes, with an average and standard deviation of 11.5 and 2.5 g root kg<sup>-1</sup> soil, respectively, in the riparian zones, and 9.6 and 4.2 g root kg<sup>-1</sup> soil in the hillslopes.

#### Soil Temperature

Soil temperature (12 cm) was not significantly different between riparian and hillslope zones within each transect (with the exception of localized differences on T3, T4, and T8 during June and July) (Table 2.4, Figures 2.4-2.6). There were however significant differences in both riparian and hillslope zones between transects (Table 2.5).

Colder soil temperatures were found during June and July on transects with a west aspect (even numbered transects), where snow was observed up to 3 weeks later than transects with an east aspect (particularly in the hillslopes). The number of significant differences in soil temperature between transects decreased from June to August (Table 2.5).

#### Soil Water Content

SWC (integrated over top 20 cm) was significantly higher in the riparian zones within each transect during the entire period of this study (Table 2.4; Figures 2.4, 2.5, and 2.7). There were also significant differences when comparing both riparian and hillslope zones across transects (Table 2.6), with higher SWC generally measured on upstream transects (i.e. T1-T4 versus T5-T8). A general downstream decrease in SWC was observed, with a more pronounced trend in the riparian zones (Figure 2.6).

#### Soil Gas Diffusivity

Soil gas diffusivity was significantly higher in the riparian zones within nearly all transects during both June and July (Table 2.4, Figures 2.4 and 2.7). Riparian zone soil gas diffusivity varied significantly between most transects, while few differences were found between hillslopes (Table 2.7).

#### Soil CO<sub>2</sub> Concentrations

There were significant differences between riparian and hillslope soil CO<sub>2</sub> concentrations within each transect (Table 2.4). Higher concentrations were measured at 20 cm in the riparian zones (Figure 2.4), with the exception of T8, where higher mean values were found in the hillslopes during June and July, coincident with riparian zone

saturation. At 50 cm, the highest concentrations were found in the hillslopes, consistent with frequent riparian zone groundwater saturation.

There were also significant differences in soil CO<sub>2</sub> concentrations across transects in both riparian and hillslope zones (Table 2.8, Figure 2.4). At 20 cm, soil CO<sub>2</sub> concentrations in the riparian zone along T8 were always lower than other transects (with a few exceptions in August), and higher concentrations were often observed on T1. In the hillslopes, there were significant differences in 20 cm soil CO<sub>2</sub> concentrations between many transects in June, with fewer observed during July and August (Table 2.8). Many 50 cm riparian zone soil CO<sub>2</sub> gas wells remained saturated by groundwater over the course of this study, and soil CO<sub>2</sub> concentrations could not be measured at these locations (denoted by flat lines in Figure 2.4D). Fifty cm soil CO<sub>2</sub> concentrations could therefore not be compared between many transects (indicated by dashed lines in Table 2.9). In general, there was a downstream decrease in soil CO<sub>2</sub> concentrations in the riparian and hillslope zones at both 20 and 50 cm (Figure 2.4). The downstream decrease of soil CO<sub>2</sub> concentration magnitude and variability was much more pronounced in the riparian zones, particularly at 20 cm.

#### Surface CO<sub>2</sub> Efflux

In general monthly averaged soil surface CO<sub>2</sub> efflux was not significantly different between riparian and hillslope zones within each transect based upon ANOVA analysis (Table 2.4). With the exception of T1, similar ranges and median values were observed in riparian and hillslope zones within each transect when grouping all data from June through August (Figure 2.4). For example, differences in median efflux between

riparian and hillslope zones within each transect were generally less than  $0.1 \text{ g CO}_2 \text{ m}^{-2}$ , and similar minimum and maximum values were observed (Figure 2.4). However, significantly higher riparian zone efflux ( $p \ll 0.01$ ) (25% higher in the riparian zones) becomes apparent when examining median growing season cumulative efflux across all transects ( $1135$  versus  $819 \text{ g CO}_2 \text{ m}^{-2}$  in the riparian and hillslope zones, respectively; Figure 2.8). The range of riparian cumulative efflux was  $649$  to  $1918 \text{ g CO}_2 \text{ m}^{-2}$ , with a standard deviation of  $354 \text{ g CO}_2 \text{ m}^{-2}$ . In contrast, hillslope cumulative efflux ranged from  $432$  to  $1246 \text{ g CO}_2 \text{ m}^{-2}$ , with a standard deviation of  $222 \text{ g CO}_2 \text{ m}^{-2}$  (note that T1-2 was excluded due to local site disturbance leading to unusually high efflux of  $1774 \text{ g CO}_2 \text{ m}^{-2}$ ) (Figure 2.9). When comparing riparian and hillslope cumulative efflux within each transect, higher values were found at riparian nest locations on nearly all transects, except for T1 and T3 (Figure 2.9) where values were similar or more variable.

Significant differences in efflux between transects were observed in both riparian and hillslope zones during June, July, and August (Table 2.10). For example, lower efflux was found along T4 and T8 in the riparian zones in both July and August, and higher efflux was often measured along T1 over the duration of this study in the hillslopes. In contrast, lower efflux was observed along T2 during June, and on T8 during July and August. Median cumulative growing season efflux tended to decrease with distance from channel head (but was not significantly different between upstream [T1-T4] and downstream [T5-T8] transects,  $p = 0.11$ ), ranging from  $1160 \text{ g CO}_2 \text{ m}^{-2}$  on T1/T2 (200 m from channel head) to  $810 \text{ g CO}_2 \text{ m}^{-2}$  on T7/T8 (1400 m from channel head) (Figure 2.10).

There was not a consistent relationship between surface CO<sub>2</sub> efflux and growing season soil temperature or SWC across all transects (Figure 2.5). While statistically significant ( $p < 0.01$ ) in both riparian and hillslope zones when all data were grouped together (Figure 2.5), these relationships were very weak, as denoted by low  $r^2$  values. Further, when hillslope measurement nests with unusually high efflux and SWC were removed from data analysis (e.g. T1-2 and T2-3, Figure 2.5), the relationships became weaker (dashed regression line in Figure 5), and in the case of hillslope efflux versus SWC, insignificant (Figure 2.5C). When examining the data by individual transects, there were often significant relationships between surface CO<sub>2</sub> efflux and soil temperature, particularly in the riparian zones (Figure 2.6). However, the relationships were weak (low  $r^2$  values), and one relationship could not be applied across all transects. Few significant relationships were found between efflux and SWC in both the riparian and hillslope zones across each transect (Figure 2.7).

## Discussion

### How Does the Variability of Surface CO<sub>2</sub> Efflux Differ within and between Eight Riparian-Hillslope Transitions?

Within Transects: In general, monthly surface CO<sub>2</sub> efflux was not significantly different between riparian and hillslope zones according to ANOVA analysis (Table 2.4). This was likely a result of strong temporal heterogeneity in instantaneous efflux at monthly timescales, as well as tradeoffs between the relative control of SWC on soil CO<sub>2</sub> production and transport (at shorter timescales) across the landscape. For example, SWC was significantly different between riparian and hillslope zones (Table 2.4), which can

lead to variations in soil CO<sub>2</sub> production (*Davidson et al.*, 2000; *Schwendenmann et al.*, 2003; *Sjogersten et al.*, 2006) and soil gas transport (*Millington*, 1959; *Washington et al.*, 1994; *Moldrup et al.*, 2000, 2001). Riparian zone SWC was often in the intermediate range (defined as 40-60% in the TCEF) (Figure 2.4) optimal for soil CO<sub>2</sub> production (*Davidson et al.*, 2000; *Schwendenmann et al.*, 2003; *Sjogersten et al.*, 2006). However, increased riparian SWC also led to decreased soil gas transport (*Millington*, 1959; *Washington et al.*, 1994; *Moldrup et al.*, 2000, 2001), where gas diffusivity rates were up to nearly an order of magnitude lower than the adjacent hillslopes (Figure 2.4). In contrast, low hillslope SWC (median values of ~20%, Figure 2.4) likely led to decreased soil CO<sub>2</sub> production relative to the riparian zones, but higher soil gas transport. We suggest this tradeoff between the relative control of SWC on soil CO<sub>2</sub> production and transport resulted in equifinality in surface CO<sub>2</sub> efflux at monthly timescales (see conceptual model in *Pacific et al.*, 2008). Because soil temperature was not significantly different between riparian and hillslope positions (Table 2.4, Figure 2.4), it is likely that soil temperature had little control on the spatial variability of soil respiration. This is consistent with previous investigations (*Pinol et al.*, 1995; *Xu and Qi*, 2001; *Scott-Denton et al.*, 2003).

*Cumulative Growing Season Efflux:* While riparian and hillslope instantaneous surface CO<sub>2</sub> efflux was in general not significantly different within each transect at monthly timescales (Table 4), higher riparian zone efflux ( $p \ll 0.01$ ) becomes apparent when integrating to cumulative growing season (June-August) efflux (Figure 2.8).

Cumulative efflux was on average 25% higher in the riparian zones within each transect.

Higher riparian zone cumulative efflux was likely due to increased riparian zone soil CO<sub>2</sub> production in response to higher SWC. Our results show surface efflux can exhibit equifinality at short timescales across a wide range of SWC. However, comparisons of cumulative efflux demonstrate large differences existed between wet and dry landscape positions, and highlights the importance of cumulative analysis in studies of soil respiration across strong SWC gradients. Our results also indicate that surface CO<sub>2</sub> efflux was impacted by differences in riparian and hillslope SOM (*Ostendorf, 1996; Ju and Chen, 2005; Sjogersten et al., 2006*). Soil C:N ratios, which can be a strong indicator of the availability of SOM, often approached 10:1 to 12:1 in the riparian zones within each transect (Figure 2.2), which are optimal ratios for microbial decomposition (*Pierzynski et al., 2000*). In contrast, hillslope soil C:N ratios were generally above 20:1, and up to 105:1 on T8 (Figure 2.2). It is likely that SOM in the upper soil horizons (note that measurements of soil C and N content were not collected above 20 cm) were more optimal for microbial decomposition in the riparian zones due to differences in above and below ground vegetation litter (*Raich and Tufekcioglu, 2000; Smith and Johnson, 2004; Kellman et al., 2007*). The riparian zones are mainly composed of bluejoint reedgrass and smaller amounts of broadleaf vegetation, both of which have C:N ratios under 30:1 (for both roots and above-ground vegetation) (Table 2.3, Figure 2.3). In contrast, hillslope vegetation is predominantly grouse whortleberry (*vaccinium*) and lodgepole pine, which have much higher C:N ratios. With the exception of *vaccinium* leaves, hillslope plant material (roots, twigs, needles, and stems) had C:N ratios above 50:1 (and up to 172:1 in lodgepole pine twigs) (Table 2.3, Figure 2.3). This variation in plant

material C:N ratios, as well as higher allocation of photosynthate below ground by grass in the riparian zones (*Raich and Tufekcioglu, 2000*), likely led to increased microbial respiration in the riparian zones within each transect (*Raich and Nadelhoffer, 1989; Raich and Tufekcioglu, 2000*). We suggest that differences in riparian and hillslope cumulative growing season efflux were the result of higher riparian zone soil CO<sub>2</sub> production in response to significantly higher SWC, as well as differences in vegetation. These differences illustrate that large variability in efflux can exist across the landscape when measurements are integrated over longer time periods (e.g. growing season), supporting the analysis of cumulative efflux as a useful tool in multi-site, landscape-scale comparisons of soil respiration (*Pacific et al., 2008; Riveros-Iregui et al., 2008a*).

Between Transects: Similar to comparisons of riparian and hillslope surface CO<sub>2</sub> efflux within each transect, instantaneous efflux was in general not significantly different between transects at monthly timescales according to ANOVA analysis. However, differences in surface CO<sub>2</sub> efflux between transects become apparent when integrating to cumulative growing season (June-August) efflux (Figure 2.8). For example, cumulative growing season efflux decreased downstream from 1190 g CO<sub>2</sub> m<sup>-2</sup> on T1/T2 to 850 g CO<sub>2</sub> m<sup>-2</sup> on T7/T8 (Figure 2.10). This downstream decrease was likely due to the downstream decrease in SWC (Figure 2.4), which resulted in lower soil CO<sub>2</sub> production (*Davidson et al., 2000; Schwendenmann et al., 2003; Sjogersten et al., 2006*), as reflected by the downstream decrease in soil CO<sub>2</sub> concentrations (Figure 2.4). In contrast, soil gas diffusivity increased downstream, but only in the riparian zones (Table 2.7, Figure 2.4). We infer that significant differences in only riparian zone soil gas diffusivity were due to

the wider range of riparian SWC (35-85% in the riparian zones versus 10-40% in the hillslopes; Figure 2.4), as even small changes in SWC can significantly impact soil gas transport (*Millington, 1959; Washington et al., 1994; Moldrup et al., 2000, 2001*). This relationship between soil gas transport and SWC is supported by *Risk et al. (2002)*, who observed differences in soil gas diffusivity of up to a factor of  $10^4$  across a similar range of riparian SWC. Further, a wider range of cumulative riparian surface CO<sub>2</sub> efflux was observed (Figure 2.4 versus Figure 2.8), where riparian cumulative efflux ranged from 649 to 1918 g CO<sub>2</sub> m<sup>-2</sup>, versus hillslope efflux of 432 to 1246 g CO<sub>2</sub> m<sup>-2</sup> (note that T1-2 was excluded from calculation due to unusually high cumulative efflux of 1774 g CO<sub>2</sub> m<sup>-2</sup>, see upcoming discussion). We infer the wide range of riparian cumulative efflux was also due to the wide range of riparian SWC. Our results again highlight the importance of examining cumulative efflux in studies of soil respiration heterogeneity across the landscape.

Similar to variability of soil respiration within transects, it is likely that inter-transect heterogeneity in surface CO<sub>2</sub> efflux was partially in response to differences in vegetation cover. In general, transects with more dense vegetation (upstream transects) had low soil C:N ratios, which are an indicator of the availability of SOM for microbial decomposition (*Pierzynski et al., 2000*). The lowest riparian zone soil C:N ratios were found on T3 (10.4:1 to 14.2:1, Figure 2.2), where vegetation cover was greatest (90%, Table 2.1). In contrast, the highest riparian zone soil C:N ratio (49.5:1) was measured on T7, where vegetation cover was only 40% (Table 2.1). As previous research has suggested a positive correlation between litter production and soil respiration (*Raich and*

*Nadelhoffer, 1989; Raich and Tufekcioglu, 2000*), lower efflux was expected on downstream transects where vegetation cover was lowest, and root respiration likely lower. Our results support this premise, as cumulative growing season surface CO<sub>2</sub> efflux decreased with distance from the channel head (Figure 9), ranging from a median of 1190 g CO<sub>2</sub> m<sup>-2</sup> on T1/T2 (average vegetation cover of 70%, Table 2.1) to 850 g CO<sub>2</sub> m<sup>-2</sup> on T7/T8 (average vegetation cover of 35%, Table 2.1). This research suggests that variations in groundcover (vegetated versus barren ground) may lead to differences in efflux across the landscape due to litterfall and respiration and should be accounted for in studies of the spatial variability of soil respiration.

#### Can Relationships between Efflux and SWC or Soil Temperature be Applied across Multiple Riparian and Hillslope Positions?

Our results demonstrate that consistent relationships between surface CO<sub>2</sub> efflux and growing season soil temperature or SWC do not exist in the upper-Stringer Creek Watershed and suggest caution for application of relationships across complex terrain. While there were significant relationships between efflux and soil temperature or SWC across some transects (Figures 2.6 and 2.7), the relationships were very weak (low  $r^2$  values), and one relationship could not be applied to all riparian and hillslope zones within and between transects. This lack of consistent relationships between efflux and soil temperature or SWC was likely due to the complication of confounding interactions between soil temperature, SWC, and soil physical properties and substrate, which can vary both spatially and temporally (*Davidson et al., 1998; Xu and Qi, 2001; Khomik et al., 2006; Sotta et al., 2006*). The results of our study also demonstrate that the wide range of SWC and efflux observed across riparian and hillslope zones at our study site

(Figure 2.5) can impact efflux and SWC or soil temperature relationships. For example, groundwater saturation inhibited soil respiration at some riparian zone locations (e.g. T1-4) early in the growing season (see *Pacific et al.*, 2008), however, efflux increased by up to an order of magnitude as SWC decreased, and the groundwater table declined. Similarly, in the hillslopes, T1-2 had unusually high efflux and SWC (likely in response to a fallen tree and increased litterfall, see upcoming discussion), and T2-3 often had very high SWC in response to its low slope position. When these nests were removed from data analysis (denoted by dashed regression line in Figure 2.5), the relationships became weaker, and in the case of surface CO<sub>2</sub> efflux versus SWC, insignificant. Our results demonstrate the need to collect measurements across a wide range of landscape positions and to exercise caution when applying soil temperature-SWC-efflux relationships in models of soil respiration to ensure validity of model assumptions.

#### How does Landscape Position and Attributes (e.g. Slope, Upslope Accumulated Area, and Aspect) Impact Soil Respiration?

Our results indicate that slope and UAA impacted soil respiration due to their influence on SWC. The relationship between slope, UAA, and SWC can be described by the topographic wetness index (TWI) (Equation 1; *Beven and Kirkby*, 1979), which suggests that the wettest landscape positions will occur in areas with large UAAs and gentle slopes (which therefore have high TWI values) (*Bonell*, 1998). This relationship was applicable in the upper-Stringer Creek Watershed, as significantly higher SWC was observed on upstream transects (Figure 2.10) where UAA was greatest and slopes the most gentle (Table 2.1). For example, T3, which has the largest UAA (14,304 m<sup>2</sup>) of all transects and a very gentle slope (14.6%), had both the highest TWI (11.5) and SWC

(Figure 2.4). Conversely, T7, where UAA is small (1373 m<sup>2</sup>) and slope is steep (41.7%), had the lowest TWI (8.0) and very low SWC (Figure 2.4). Therefore, based upon the TWI, higher efflux was expected along T3, where SWC was highest, as increases in SWC generally promote higher rates of soil respiration (*Davidson et al.*, 1998, 2000; *Liu and Li*, 2005; *Risch and Frank*, 2007). Cumulative growing season efflux was 1300 g CO<sub>2</sub> m<sup>-2</sup> on T3, while only 926 g CO<sub>2</sub> m<sup>-2</sup> on T7, confirming expectations based on topographic analysis. We suggest that the concept of the TWI may be useful as an indicator of soil respiration across complex landscapes and highlights the value of interpreting surface CO<sub>2</sub> efflux in the landscape context.

In contrast to slope and UAA, aspect (east versus west) generally did not impact growing season soil respiration within or between riparian and hillslope zones in the upper-Stringer Creek Watershed (Figure 2.4). While there were some significant differences in soil temperature between transects (Table 2.5), these occurred early in the growing season and were likely the result of differences in snowpack persistence as well as the influence of the high specific heat of water in saturated areas (*Pacific et al.*, 2008). As all landscape positions became snow-free and SWC declined in many saturated areas, variability in soil temperature between east and west aspects became insignificant (Table 2.6) and suggests that aspect had little impact on the spatial variability of soil respiration. However, our results contrast with those of other studies of soil respiration in complex terrain. *Kang et al.* (2006) found higher soil temperatures on south versus north facing slopes, likely in response to greater differences in incoming solar radiation between north and south aspects compared to west versus east in our study site. *Riveros-Iregui* (2008b)

found higher soil temperature on NE versus NW aspects in the same watershed as this study. However, *Riveros-Iregui* (2008b) collected measurements over much larger spatial extents (e.g. transects of hundreds of meters in length versus ~50 m in our study), and it is possible that the smaller spatial extent of our study did not fully capture the effect of aspect on soil respiration.

We found that landscape attributes such as slope and UAA impacted soil respiration at our study site, however similar relationships may not simply apply in areas with differences in hydrology, vegetation, etc. For example, *Hanson et al.* (1993) measured increased upland efflux in an oak forest in Tennessee, which contrasts with our measurements in the TCEF. As differences in valley and upland SWC were small at the study site of *Hanson et al.* (1993) (relative to the TCEF), this may be the result of differences in soil root density, as a strong correlation exists between root density and soil respiration (*Shibistova et al.*, 2002). Soil root density was higher in the riparian zones in the TCEF, but higher in the uplands at the study site of *Hanson et al.* (1993). *Sotta et al.* (2006) found little difference in CO<sub>2</sub> efflux between plateau, valley, and upper and lower slope positions in Brazil. Our results corroborate their findings at short timescales, however we found high spatial variability in cumulative growing season efflux in the TCEF. This difference in the spatial variability of efflux is likely due to differences in SWC (~15-30% at the study site of *Sotta et al.* (2006), compared to 10-85% in the TCEF), as the spatial coherence of SWC patterns often breaks down in dry areas (*Western et al.*, 1999; *Western and Grayson*, 2000). Due to the contrasting results between our study and those of *Hanson et al.* (1993) and *Sotta et al.* (2006), we suggest

that care must be taken when extrapolating observations to areas with differences in hydrology, landscape attributes, etc., and highlights the need for further investigations of soil respiration heterogeneity across a variety of ecosystems.

#### Implications for Up-scaling of Soil Respiration Measurements

In order to accurately quantify soil respiration over large areas (e.g. watershed or ecosystem scales), it is necessary to collect measurements over a wide range of landscape positions and across the full range of biophysical gradients, particularly in areas of complex terrain. As such data collection is often unfeasible, studies of landscape scale soil respiration must employ techniques to bridge the gap between point and landscape scale measurements. We thus advocate the use of landscape position analysis when scaling soil respiration measurements to larger areas.

Our results demonstrate that soil respiration and respiration driving variables differed across riparian-hillslope transitions in the upper-Stringer Creek Watershed. Cumulative efflux was generally higher and had a wider range in the riparian zones along each transect (Figure 2.9). This reflects the wide range of riparian zone SWC (35-85%, Figure 2.4), as well as more narrow (optimal) soil and vegetation C:N ratios (Figure 2.3). In contrast, the hillslopes had a smaller range of efflux in concert with a smaller range of SWC (10-40%, Figure 2.4) as well as much higher soil and vegetation C:N ratios (Figure 2.3). Our results also demonstrate the importance of using cumulative analysis in studies of soil respiration across strong SWC gradients. At short timescales, surface efflux can exhibit equifinality across landscape positions despite strong differences in SWC, suggesting SWC had little control on the spatial variability of soil respiration within the

TCEF. However, at longer timescales, cumulative efflux analysis indicates SWC likely controls the variability of surface CO<sub>2</sub> efflux across the landscape. Significantly higher efflux occurred at wetter landscape positions within the TCEF.

Soil CO<sub>2</sub> concentrations also differed across riparian and hillslope zones. Riparian soil CO<sub>2</sub> concentrations ranged broadly (often by over 20,000 ppm, Figure 2.4), also likely in response to the wide range of riparian SWC (Figure 2.4). This was in contrast to the hillslopes, where the range of soil CO<sub>2</sub> concentrations never exceeded 5,000 ppm (Figure 2.4). Further, higher cumulative efflux was found on upstream transects (Figure 2.10), where TWI values were larger in response to higher UAA and gentler slopes (Table 2.1). In contrast, the lowest cumulative efflux was measured on downstream transects where low UAA and steep slopes resulted in a low TWI. Our findings indicate the importance of landscape context for interpreting point and plot scale measurements. This concept is widely used in hydrologic modeling, in which landscape position similarity is often related to hydrologic behavior similarity (*McGlynn et al.*, 2004; *Beighley et al.*, 2005; *Seibert and McGlynn*, 2005). We suggest that landscape position can also be related to carbon dynamics, or “carbon context,” to interpret and extrapolate point-scale measurements of soil respiration to larger landscapes.

The use of landscape analysis and similarity concepts implies homogeneity among similar landscape positions, however additional heterogeneity must be considered (*Seibert and McGlynn*, 2005). For example, while cumulative growing season efflux was generally lower in the hillslopes along each transect (median values of 819 and 1135 g CO<sub>2</sub> m<sup>-2</sup> in the hillslope and riparian zones across all transects, respectively), much

higher cumulative efflux was observed at T1-2 ( $1774 \text{ g CO}_2 \text{ m}^{-2}$ , Figure 2.9). This high efflux was likely in response to a fallen tree and subsequent increase in litterfall, which can stimulate soil respiration due to large organic matter contributions to the soil. However, while such local heterogeneities and exceptions can exist in addition to landscape position-induced biophysical variable differences, we suggest that landscape structure leads to organized heterogeneity at the TCEF. Therefore, landscape analysis can provide a way forward in up-scaling soil respiration measurements and be useful when modeling soil respiration to reduce potentially large uncertainty in scaling measurements to landscape and regional scales (*Riveros-Iregui, 2008b*).

### Conclusions

Measurements of growing season (June-August) SWC, soil temperature, soil and vegetation C and N content, soil  $\text{CO}_2$  concentrations, and surface  $\text{CO}_2$  efflux across eight topographically distinct riparian-hillslope transitions within the upper-Stringer Creek Watershed suggested that:

- 1) Instantaneous soil surface  $\text{CO}_2$  efflux was not significantly different both within and between riparian and hillslope zones at monthly timescales according to ANOVA analysis. This was likely due to differential mechanistic controls on  $\text{CO}_2$  production and transport that resulted in efflux equifinality at short timescales.
- 2) Cumulative growing season efflux was 25% higher in the riparian zones than the adjacent hillslopes, which demonstrates that large differences in soil respiration existed between riparian and hillslope zones over longer

timescales, and highlights the importance of cumulative analysis in comparisons of surface CO<sub>2</sub> efflux across the landscape.

- 3) Landscape attributes such as slope, UAA, and vegetation cover affected soil respiration driving variables such as SWC and SOM, and therefore should be accounted for when investigating landscape-level respiration heterogeneity.
- 4) Landscape position can be related to carbon dynamics and may be a valid approach to interpret and extrapolate point/plot scale measurements of soil respiration to larger portion of landscapes.

This research indicates that landscape position and contextual variables such as slope, UAA, and vegetation cover can impact soil respiration. Differential controls of topographically variable respiration drivers such as SWC, SOM availability, and soil gas diffusivity can lead to organized heterogeneity in cumulative surface CO<sub>2</sub> efflux as a function of landscape position. Our results highlight the need for further investigations of the spatial variability of soil respiration in complex terrain across a range of biophysical gradients and landscape positions in order to elucidate the primary controls of respiration heterogeneity across the landscape.

#### Acknowledgements

We gratefully acknowledge field assistance from Kelsey Jencso, Becca McNamara, Kelley Conde, and Austin Allen. We would like to thank the Tenderfoot Creek Experimental Forest and the USDA, Forest Service, Rocky Mountain Research Station, especially Ward McCaughey, for logistical support and research site access.

This work was funded by the NSF Integrated Carbon Cycle Research Program (ICCR, NSF Grant EAR0404130, EAR0403924, and EAR0403906) and fellowships awarded to VJ Pacific from the Big Sky Institute NSF GK-12 program, Inland Northwest Research Alliance (INRA), and the Montana Water Center Student Research Grant Program.

References

- Anderson, M. G. and T. P. Burt (1978) Role of topography in controlling throughflow generation, *Earth Surface Processes and Landforms*, 3, 331-344.
- Andrews, J. A. and W. H. Schlesinger (2001) Soil CO<sub>2</sub> dynamics, acidification, and chemical weathering in a temperate forest with experimental CO<sub>2</sub> enrichment, *Global Biogeochemical Cycles*, 15, 149-162.
- Baldocchi, D., J. Tang, and L. Xu (2006) How switches and lags in biophysical regulators affect spatial-temporal variation of soil respiration in an oak-grass savanna, *Journal of Geophysical Research*, 111, G02008, doi: 10.1029/2005JG000063.
- Beighley, R. E., T. Dunne, and J. M. Melack (2005) Understanding and modeling basin hydrology: interpreting the hydrogeological signature, *Hydrological Processes*, 19, 1333-1353.
- Beven, K. J., and M. J. Kirkby (1979) A physically-based variable contributing area model of basin hydrology, *Hydrological Sciences Bulletin*, 24, 43-69.
- Bonell, M. (1998) Selected challenges in runoff generation research in forests from the hillslope to headwater drainage basic scale, *Journal of the American Water Resources Association*, 34, 765-785.
- Conant, R. T., J. M. Klopatek, R. C. Malin, and C. C. Klopatek (1998) Carbon pools and fluxes along an environmental gradient in northern Arizona, *Biogeochemistry*, 43, 43-61.
- Cosanday, A. C., V. Maitre, and C. Guenat (2003) Temporal denitrification patterns in different horizons of two riparian soils, *European Journal of Soil Science*, 54, 25-38.
- Davidson, E. A., E. Belk, and R. D. Boone (1998) Soil water content and temperature as independent or confounded factors controlling soil respiration in a temperate mixed hardwood forest, *Global Change Biology*, 4, 217-227.
- Davidson, E. A., L. V. Verchot, J. H. Cattanio, I. L. Ackerman, and J. E. M. Carvalho (2000) Effects of soil water content on soil respiration in forests and cattle pastures of eastern Amazonia, *Biogeochemistry*, 48, 53-69.
- Dunne, T., and R. D. Black (1970) Partial area contributions to storm runoff in a small New England watershed, *Water Resources Research*, 6, 1296-1311.

- Fang, C., and J. B. Moncrieff (1999) A model for soil CO<sub>2</sub> production and transport 1: Model development, *Agricultural and Forest Meteorology*, 95, 225-236.
- Fang, C., and J. B. Moncrieff (2001) The dependence of soil CO<sub>2</sub> efflux on temperature, *Soil Biology and Biochemistry*, 33, 155-165.
- Fang, C., J. B. Moncrieff, H. L. Gholz, and K. L. Clark (1998) Soil CO<sub>2</sub> efflux and its spatial variation in a Florida slash pine plantation, *Plant and Soil*, 205, 135-146.
- Farnes, P.E., R. C. Shearer, W. W. McCaughey, and K. J. Hanson (1995) Comparisons of Hydrology, Geology and Physical Characteristics between Tenderfoot Creek Experimental Forest (East Side) Montana, and Coram Experimental Forest (West Side) Montana. Final Report RJVA-INT-92734. USDA Forest Service, Intermountain Research Station, Forestry Sciences Laboratory, Bozeman, Montana, 19 pp.
- Gulledge, J., and J. P. Schimel (2000) Controls on soil carbon dioxide and methane fluxes in a variety of taiga forest stands in interior Alaska, *Ecosystems*, 3, 269-282.
- Gurwick, N. P., P. M. Groffman, J. B. Yavitt, A. J. Gold, G. Blazejewski, and M. Stolt (2008) Microbially available carbon in buried riparian soils in a glaciated landscape, *Soil Biology and Biochemistry*, 40, 85-96.
- Hanson, P. J., S. D. Wullschleger, S. A. Bohlman, and D. E. Todd (1993) Seasonal and topographic patterns of forest floor CO<sub>2</sub> efflux from an upland oak forest, *Tree Physiology*, 13, 1-15.
- Happell, J. D., and J. P. Chanton (1993) Carbon remineralization in a north Florida swamp forest: effects of water level on the pathways and rates of soil organic matter decomposition, *Global Biogeochemical Cycles*, 7, 475-490.
- Hill, A. R. (1996) Nitrate removal in stream riparian zones, *Journal of Environmental Quality*, 25, 743-755.
- Hill, A. R., and M. Cardaci (2004) Denitrification and organic carbon availability in riparian wetland soils and subsurface sediments, *Soil Science Society of America Journal*, 68, 320-325.
- Hill, A. R., P. G. F. Vidon, and J. Langat (2004) Denitrification potential in relation to lithology in five headwater riparian zones, *Journal of Environmental Quality*, 33, 911-919.

- Holdorf, H. D. (1981) Soil Resource Inventory, Lewis and Clark National Forest – Interim In-Service Report. On file with the Lewis and Clark National Forest, Forest Supervisor’s Office, Great Falls, MT.
- Jencso, K. J., B. L. McGlynn, M. N. Gooseff, S. M. Wondzell, and K. E. Bencala (2009) Hydrologic connectivity between landscapes and streams: transferring reach and plot scale understanding to the catchment scale, *Water Resources Research*, 10.1029/2008WR007225
- Ju, W., and J. M. Chen (2005) Distribution of soil carbon stocks in Canada’s forests and wetlands simulated based on drainage class, topography and remotely sensed vegetation parameters, *Hydrological Processes*, 19, 77-94.
- Kang, S., D. Lee, J. Lee, and S. Running (2006) Topographic and climatic controls on soil environments and net primary production in a rugged temperate hardwood forest in Korea, *Ecological Resources*, 21, 64-74.
- Kellman, L., H. Beltrami, and D. Risk (2007) Changes in seasonal soil respiration with pasture conversion to forest in Atlantic Canada, *Biogeochemistry*, 82, 101-109, doi: 10.1007/s10533-006-9056-0.
- Khomik, M., M. A. Arain, and J. H. McCaughey (2006) Temporal and spatial variability in soil respiration, *Agricultural and Forest Meteorology*, 140, 244-256.
- Liu, H. S., and F. M. Li (2005) Root respiration, photosynthesis and grain yield of two spring wheat in response to soil drying, *Plant Growth Regulations*, 46, 233-240.
- McCarthy, D. R., and K. J. Brown (2006) Soil respiration responses to topography, canopy cover, and prescribed burning in an oak-hickory forest in southeastern Ohio, *Forest Ecology and Management*, 237, 94-102.
- McGlynn, B. L., and J. J. McDonnell (2003) Role of discrete landscape elements in controlling catchment dissolved organic carbon dynamics, *Water Resources Research*, 39, doi:10.1029/2002WR001525.
- McGlynn, B. L., and J. Seibert (2003) Distributed assessment of contributing area and riparian buffering along stream networks, *Water Resources Research*, 39, doi:10.1029/2002WR001521.
- McGlynn, B. L., J. J. McDonnell, J. Seibert, and C. Kendall (2004) Scale effects on headwater catchment runoff timing, flow sources, and groundwater-streamflow relations, *Water Resources Research*, 40, doi:10.1029/2003WR002494

- Merot, P., B. Ezzahar, C. Walter, and P. Arousseau (1995) Mapping waterlogging of soils using digital terrain models, *Hydrological Processes*, 9, 27-34.
- Millington, R. J. (1959) Gas diffusion in porous media, *Science*, 130, 100-102.
- Mincemoyer, S. A., and J. L. Birdsall (2006) Vascular flora of the Tenderfoot Creek Experimental Forest, Little Belt Mountains, Montana, *Madrono*, 53, 211-222.
- Moldrup, P., T. Olsen, P. Schjønning, T. Yamaguchi, and D. E. Rolston (2000) Predicting the gas diffusion coefficient in undisturbed soil from soil water characteristics, *Soil Science Society of America Journal*, 64, 94-100.
- Moldrup, P., T. Olsen, T. Komatsu, P. Schjønning, and D. E. Rolston (2001) Tortuosity, diffusivity, and permeability in the soil liquid and gaseous phases, *Soil Science Society of America Journal*, 65, 613-623.
- Mourier, B., C. Walter, and P. Merot (2008) Soil distribution in valleys according to stream order, *Catena*, 72, 395-404.
- Ohashi, M., and K. Gyokusen (2007) Temporal change in spatial variability of soil respiration on a slope of Japanese cedar (*Cryptomeria japonica* D. Don) forest, *Soil Biology and Biochemistry*, 39, 1130-1138.
- Ostendorf, B. (1996) Modeling the influence of hydrological processes on spatial and temporal patterns in CO<sub>2</sub> soil efflux from an arctic tundra catchment, *Arctic and Alpine Research*, 28, 318-327.
- Pacific, V. J., B. L. McGlynn, D. A. Riveros-Iregui, D. L. Welsch, and H. E. Epstein (2008) Variability in soil respiration across riparian-hillslope transitions, *Biogeochemistry*, doi: 10.1007/s10533-008-9258-8.
- Parkin, T. B., T. C. Kasper, Z. Senwo, J. H. Prueger, and J. L. Hatfield (2005) Relationship of soil respiration to crop and landscape in the Walnut Creek Watershed, *Journal of Meteorology*, 6, 812-824.
- Phillips, D. H., J. E. Fossa, C. A. Stiles, C. C. Trettin, and R. J. Luxmoore (2001) Soil-landscape relationships at the lower reaches of a watershed at Bear Creek near Oak Ridge, Tennessee, *Catena*, 44, 205-222.
- Pierzynski, G.M., J. T. Sims, and G. F. Vance (eds.) (2000), *Soils and Environmental Quality*. CRC Press: New York, N.Y. 480 pp.
- Pinol, J., J. M. Alcaniz, and R. Roda (1995) Carbon dioxide efflux and pCO<sub>2</sub> in soils of three *Quercus ilex* montane forests, *Biogeochemistry*, 30, 191-215.

- Raich, J. W., and A. Tufekcioglu (2000) Vegetation and soil respiration: correlations and controls, *Biogeochemistry*, 48, 71-90.
- Raich, J. W., and K. J. Nadelhoffer (1989) Belowground carbon allocation in forest ecosystems: Global trends, *Ecology*, 70, 1346-1354.
- Raich, J. W., and W. H. Schlesinger (1992) The global carbon dioxide flux in soil respiration and its relationship to vegetation and climate, *Tellus*, 44B, 81-99.
- Raich, J.W., C. S. Potter, and D. Bhagawati (2002) Interannual variability in global soil respiration, 1980-94, *Global Change Biology*, 8, 800-812.
- Rayment, M. B., and P. G. Jarvis (2000) Temporal and spatial variation of soil CO<sub>2</sub> efflux in a Canadian boreal forest, *Soil Biology and Biochemistry*, 32, 35-45.
- Risch, A. C., and D. A. Frank (2007) Effects on increased soil water availability on grassland ecosystem carbon dioxide fluxes, *Biogeochemistry*, 86, 91-103.
- Risk, D., L. Kellman, and H. Beltrami (2002) Soil CO<sub>2</sub> production and surface flux at four climate observatories in eastern Canada, *Global Biogeochemical Cycles*, 16, 69-1 – 69-11, doi:10.1029/2001GB001831.
- Riveros-Iregui, D. A., B. L. McGlynn, H. E. Epstein, and D. L. Welsch (2008a) Interpretation and evaluation of combined measurement techniques for soil CO<sub>2</sub> efflux: discrete surface chambers and continuous soil CO<sub>2</sub> concentration probes, *Journal of Geophysical Research – Biogeosciences*, doi:10.1029/2008JG000811
- Riveros-Iregui, D. A. (2008b) Hydrologic-Carbon Cycle Linkages in a Subalpine Catchment. PhD Dissertation. 220 pp. Montana State University-Bozeman.
- Riveros-Iregui, D. A., R. E. Emanuel, D. J. Muth, B. L. McGlynn, H. E. Epstein, D. L. Welsch, V. J. Pacific, and J. M. Wraith (2007) Diurnal hysteresis between soil temperature and soil CO<sub>2</sub> is controlled by soil water content, *Geophysical Research Letters*, doi: 10.1029/2007GL030938.
- Robinson, D. A., S. B. Jones, J. M. Wraith, D. Or, and S. P. Friedman (2003) A review of advances in dielectric and electrical conductivity measurements in soils using time domain reflectometry, *Vadose Zone Journal*, 2, 444-475.
- Schimel, D., T. G. F. Kittel, S. Running, R. Monson, A. Turnipseed, and D. Anderson (2002) Carbon sequestration studied in western U.S. mountains, *Eos Transactions, AGU*, 83, 445-456.

- Schuur, E. A. G., and S. E. Trumbore (2006) Partitioning sources of soil respiration in boreal black spruce forest using radiocarbon, *Global Change Biology*, 12, 165-176.
- Schwendenmann, L., E. Veldkamp, T. Brenes, J. J. O'Brien, and J. Mackensen (2003) Spatial and temporal variation in soil CO<sub>2</sub> efflux in an old-growth neotropical rain forest, La Selva, Costa Rica, *Biogeochemistry*, 64, 111-128.
- Scott-Denton, L. E., K. L. Sparks, R. K. Monson (2003) Spatial and temporal controls of soil respiration rate in a high-elevation, subalpine forest, *Soil Biology and Biochemistry*, 35, 525-534.
- Scott-Denton, L. E., T. N. Rosenstiel, and R. K. Monson (2006) Differential controls by climate and substrate over the heterotrophic and rhizospheric components of soil respiration, *Global Change Biology*, 12, 205-216.
- Seibert, J., and B. L. McGlynn (2005) Landscape element contributions to storm runoff. *Encyclopedia of Hydrological Sciences*, Wiley.
- Seibert, J., and B. L. McGlynn (2007) A new triangular multiple flow-direction algorithm for computing upslope areas from gridded digital elevation models, *Water Resources Research*, 43, W04501, doi:10.1029/2006WR005128.
- Shibistova, O., J. Lloyd, S. Evgrafova, N. Savushkina, G. Zrazhevskaya, A. Arneeth, A. Knohl, and O. Kolle (2002) Seasonal and spatial variability in soil CO<sub>2</sub> efflux rates for a central Siberian *Pinus sylvestris* forest, *Tellus*, 54B, 552-567.
- Sjogersten, S., R. van der Wal, and S. J. Woodin (2006) Small-scale hydrological variation determines landscape CO<sub>2</sub> fluxes in the high Arctic, *Biogeochemistry*, 80, 205-216.
- Smith, D. L., and L. Johnson (2004) Vegetation-mediated changes in microclimate reduce soil respiration as woodlands expand into grasslands, *Ecology*, 85, 3348-3361.
- Sotta, E. D., E. Veldkamp, B. R. Guinaraes, R. K. Paixao, M. L. P. Ruivo, and S. S. Almeida (2006) Landscape and climatic controls on spatial and temporal variation in soil CO<sub>2</sub> efflux in an Eastern Amazonian Rainforest, Caxiuana, Brazil, *Forest Ecology and Management*, 237, 57-64.

- Sotta, E. D., E. Veldkamp, L. Schwendenmann, B. R. Guimaraes, R. K. Paixao, M. P. Ruivo, A. C. DaCosta, and P. Meirs (2007) Effects of an induced drought on soil carbon dioxide (CO<sub>2</sub>) efflux and soil CO<sub>2</sub> production in an Eastern Amazonian rainforest, Brazil, *Global Change Biology*, 13, 1-12, doi: 10.1111/j.1365-2486.2007.01416.x
- Tang, J., and D. D. Baldocchi (2005) Spatial-temporal variation in soil respiration in an oak-grass savanna ecosystem in California and its partitioning into autotrophic and heterotrophic components, *Biogeochemistry*, 73, 183-207.
- Tang, J., D. D. Baldocchi, Y. Qi, and L. Xu (2003) Assessing soil CO<sub>2</sub> efflux using continuous measurements of CO<sub>2</sub> profiles in soils with small solid-state sensors, *Agricultural and Forest Meteorology*, 118, 207– 220.
- Washington, J. W., A. W. Rose, E. J. Ciolkosz, and R. R. Dobos (1994) Gaseous diffusion and permeability in four soil profiles in central Pennsylvania, *Soil Science*, 157, 65-76.
- Welsch, D. L., and G. M. Hornberger (2004) Spatial and temporal simulation of soil CO<sub>2</sub> concentrations in a small forested catchment in Virginia, *Biogeochemistry*, 71, 415-436.
- Western, A. W., and R. B. Grayson (2000). Soil moisture and runoff processes at Tarrawarra. *Spatial Patterns in Catchment Hydrology: Observations and Modelling*, Cambridge University Press.
- Western, A. W., R. B. Grayson, G. Bloschl, G. R. Willgoose, and T. A. McMahon (1999) Observed spatial organization of soil moisture and its relation to terrain indices, *Water Resources Research*, 35, 797-810.
- Xu, M., and Y. Qi (2001) Soil-surface CO<sub>2</sub> efflux and its spatial and temporal variations in a young ponderosa pine plantation in northern California, *Global Change Biology*, 7, 667-677.
- Xu, W., and S. Wan (2008) Water- and plant-mediated response of soil respiration to topography, fire, and nitrogen fertilization in semiarid grassland in northern China, *Soil Biology and Biochemistry*, 40, 679-687.
- Yuste, J. C., D. D. Baldocchi, A. Gershenson, A. Goldstein, L. Mission, and S. Wong (2007) Microbial soil respiration and its dependency on carbon inputs, soil temperature and moisture, *Global Change Biology*, 13, 1-18, doi: 10.1111/j.1365-2486.2007.01415.x

Table 2.1: Landscape characterization of upslope accumulated area (UAA), riparian zone width, predominate slope of hillslope, approximate vegetative groundcover (visually estimated in 3 m<sup>2</sup> area surrounding each measurement nest), and topographic wetness index (TWI). UAA and slope were calculated using 3 m digital elevation models (*Seibert and McGlynn, 2007*).

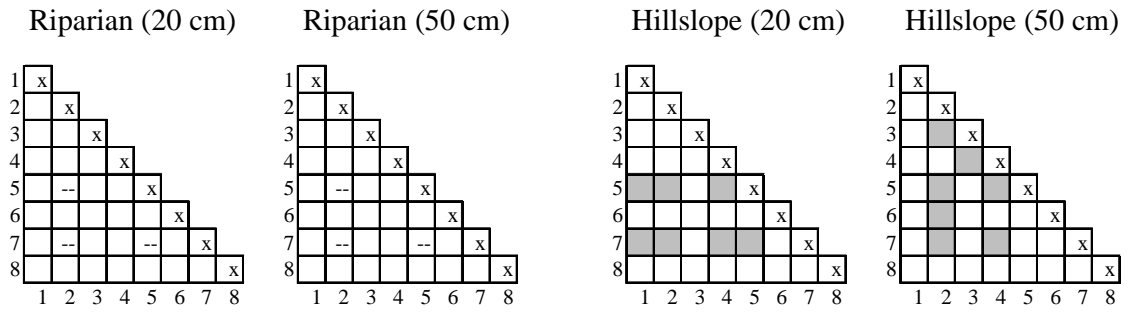
| Transect | UAA<br>m <sup>2</sup> | Riparian<br>Width<br>m | Hillslope<br>slope<br>% | Vegetation<br>Cover<br>% | TWI  |
|----------|-----------------------|------------------------|-------------------------|--------------------------|------|
| 1        | 2249                  | 12.7                   | 18.1                    | 80                       | 9.4  |
| 2        | 1804                  | 11.8                   | 13.6                    | 60                       | 9.5  |
| 3        | 14304                 | 21.0                   | 14.6                    | 90                       | 11.5 |
| 4        | 14783                 | 8.3                    | 30.0                    | 60                       | 10.8 |
| 5        | 14304                 | 11.7                   | 24.0                    | 20                       | 11.0 |
| 6        | 1023                  | 6.5                    | 21.4                    | 80                       | 8.5  |
| 7        | 1373                  | 4.7                    | 41.7                    | 40                       | 8.0  |
| 8        | 1755                  | 9.9                    | 42.5                    | 30                       | 8.3  |

Table 2.2: Analysis of variance statistics ( $\alpha = 0.05$ ) for riparian versus hillslope 20 and 50 cm soil carbon and nitrogen content, and respective soil C:N ratios. Bold numbers indicate statistically significant differences, and  $n = 8$  for all analyses. Riparian and hillslope average and standard deviation across all transects are provided.

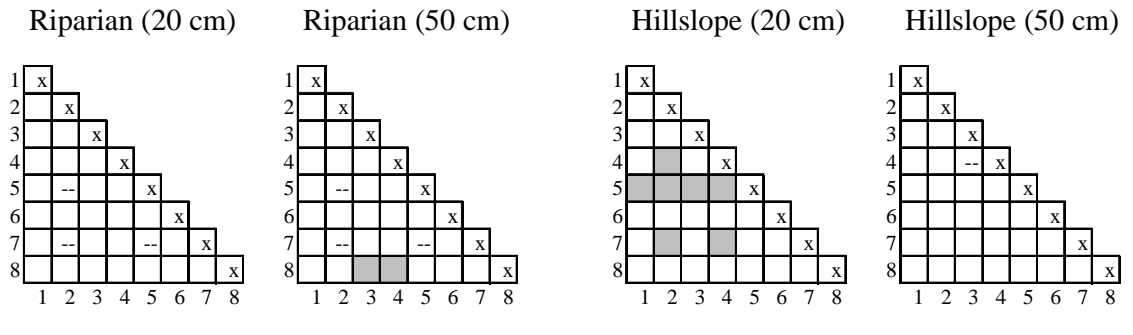
| Transect  | C-20 | C-50        | N-20        | N-50        | C:N - 20    | C:N - 50            |
|-----------|------|-------------|-------------|-------------|-------------|---------------------|
| 1         | 0.49 | 0.91        | 0.31        | 0.86        | <b>0.05</b> | 0.33                |
| 2         | 0.24 | 0.34        | 0.54        | 0.57        | 0.45        | 0.69                |
| 3         | 0.48 | 0.27        | 0.40        | 0.13        | <b>0.02</b> | <b>0.01</b>         |
| 4         | 0.68 | <b>0.04</b> | 0.40        | <b>0.02</b> | <b>0.03</b> | <b>&lt;&lt;0.01</b> |
| 5         | 0.25 | 0.22        | <b>0.02</b> | 0.07        | 0.14        | 0.25                |
| 6         | 0.93 | 0.50        | 0.20        | 0.21        | 0.12        | 0.15                |
| 7         | 0.14 | 0.58        | 0.36        | 0.49        | 0.37        | 0.49                |
| 8         | 0.67 | 0.75        | 0.84        | 0.97        | 0.32        | 0.42                |
| RIP: avg  | 2.34 | 1.77        | 0.17        | 0.12        | 14.1        | 15.4                |
| st dev    | 1.33 | 0.89        | 0.09        | 0.06        | 2.8         | 3.0                 |
| HILL: avg | 2.74 | 1.34        | 0.11        | 0.06        | 26.1        | 27.7                |
| st dev    | 1.8  | 0.69        | 0.86        | 0.04        | 9.7         | 11.9                |

Table 2.3: Analysis of variance statistics ( $\alpha = 0.05$ ) for transect-versus-transect comparisons A) soil carbon content; B) soil nitrogen content; and C) respective soil C:N ratios at 20 and 50 cm in both riparian and hillslope zones. Shaded boxes indicate significant differences. A dashed line indicates that statistical analysis could not be performed due to only one sample in each zone. n ranged from 3 to 8 due to reclassification of some nests as riparian or hillslope.

A) Carbon Content



B) Nitrogen Content



C) C:N Ratio

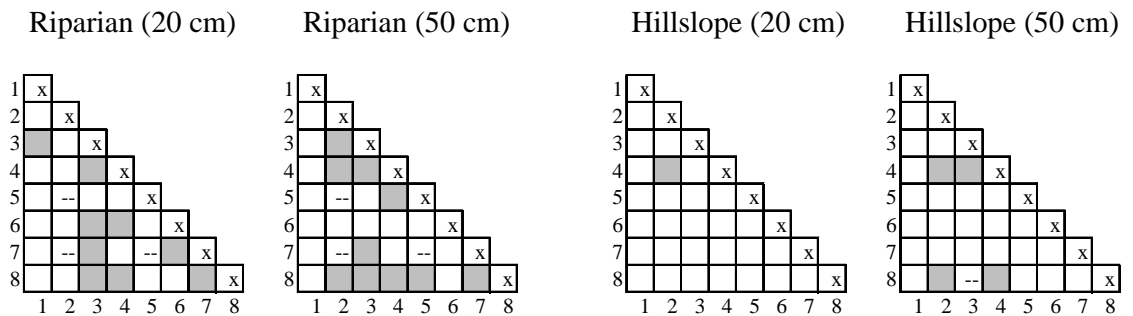


Table 2.4: Analysis of variance statistics ( $\alpha = 0.05$ ) for riparian versus hillslope soil CO<sub>2</sub> concentrations (20 and 50 cm), soil temperature, soil water content, surface CO<sub>2</sub> efflux, and soil gas diffusivity during A) June; B) July; and C) August, 2005. Bold numbers indicate statistically significant differences.

A) JUNE

| Transect | n  | CO <sub>2</sub> -20 | CO <sub>2</sub> -50 | Temp           | SWC            | Efflux         | Diff           |
|----------|----|---------------------|---------------------|----------------|----------------|----------------|----------------|
| 1        | 52 | << <b>0.01</b>      | << <b>0.01</b>      | 0.16           | << <b>0.01</b> | << <b>0.01</b> | << <b>0.01</b> |
| 2        | 52 | << <b>0.01</b>      | << <b>0.01</b>      | 0.21           | << <b>0.01</b> | 0.24           | << <b>0.01</b> |
| 3        | 52 | << <b>0.01</b>      | << <b>0.01</b>      | << <b>0.01</b> | << <b>0.01</b> | 0.67           | 0.43           |
| 4        | 52 | << <b>0.01</b>      | << <b>0.01</b>      | << <b>0.01</b> | << <b>0.01</b> | 0.12           | << <b>0.01</b> |
| 5        | 44 | << <b>0.01</b>      | 0.41                | 0.86           | << <b>0.01</b> | 0.82           | << <b>0.01</b> |
| 6        | 44 | << <b>0.01</b>      | << <b>0.01</b>      | 0.48           | << <b>0.01</b> | 0.74           | << <b>0.01</b> |
| 7        | 24 | << <b>0.01</b>      | << <b>0.01</b>      | 0.98           | << <b>0.01</b> | 0.21           | 0.09           |
| 8        | 24 | << <b>0.01</b>      | << <b>0.01</b>      | << <b>0.01</b> | << <b>0.01</b> | 0.50           | << <b>0.01</b> |

B) JULY

| Transect | n  | CO <sub>2</sub> -20 | CO <sub>2</sub> -50 | Temp           | SWC            | Efflux         | Diff           |
|----------|----|---------------------|---------------------|----------------|----------------|----------------|----------------|
| 1        | 80 | << <b>0.01</b>      | << <b>0.01</b>      | 0.57           | << <b>0.01</b> | 0.14           | << <b>0.01</b> |
| 2        | 80 | << <b>0.01</b>      | << <b>0.01</b>      | 0.41           | << <b>0.01</b> | << <b>0.01</b> | <b>0.04</b>    |
| 3        | 80 | << <b>0.01</b>      | << <b>0.01</b>      | 0.07           | << <b>0.01</b> | 0.30           | << <b>0.01</b> |
| 4        | 80 | << <b>0.01</b>      | 0.12                | << <b>0.01</b> | << <b>0.01</b> | 0.13           | << <b>0.01</b> |
| 5        | 36 | << <b>0.01</b>      | <b>0.04</b>         | 0.75           | << <b>0.01</b> | 0.33           | << <b>0.01</b> |
| 6        | 36 | << <b>0.01</b>      | << <b>0.01</b>      | 0.94           | << <b>0.01</b> | << <b>0.01</b> | <b>0.04</b>    |
| 7        | 28 | << <b>0.01</b>      | << <b>0.01</b>      | 0.66           | << <b>0.01</b> | << <b>0.01</b> | 0.12           |
| 8        | 28 | << <b>0.01</b>      | << <b>0.01</b>      | << <b>0.01</b> | << <b>0.01</b> | 0.09           | << <b>0.01</b> |

C) AUGUST

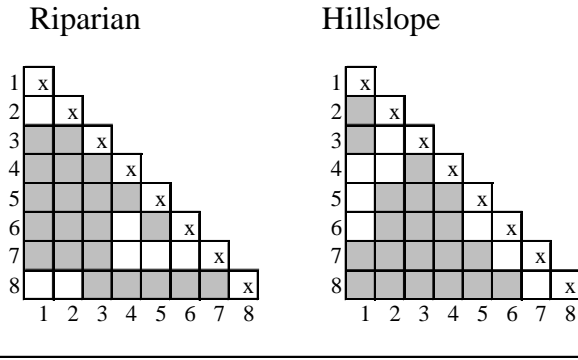
| Transect | n  | CO <sub>2</sub> -20 | CO <sub>2</sub> -50 | Temp | SWC            | Efflux         | Diff           |
|----------|----|---------------------|---------------------|------|----------------|----------------|----------------|
| 1        | 56 | << <b>0.01</b>      | << <b>0.01</b>      | 0.70 | << <b>0.01</b> | << <b>0.01</b> | << <b>0.01</b> |
| 2        | 56 | << <b>0.01</b>      | << <b>0.01</b>      | 0.62 | << <b>0.01</b> | << <b>0.01</b> | << <b>0.01</b> |
| 3        | 56 | << <b>0.01</b>      | << <b>0.01</b>      | 0.97 | << <b>0.01</b> | << <b>0.01</b> | << <b>0.01</b> |
| 4        | 56 | << <b>0.01</b>      | <b>0.01</b>         | 0.18 | << <b>0.01</b> | 0.52           | << <b>0.01</b> |
| 5        | 24 | << <b>0.01</b>      | << <b>0.01</b>      | 0.94 | << <b>0.01</b> | 0.09           | << <b>0.01</b> |
| 6        | 24 | << <b>0.01</b>      | << <b>0.01</b>      | 0.70 | << <b>0.01</b> | << <b>0.01</b> | << <b>0.01</b> |
| 7        | 24 | << <b>0.01</b>      | << <b>0.01</b>      | 0.64 | << <b>0.01</b> | << <b>0.01</b> | 0.11           |
| 8        | 24 | << <b>0.01</b>      | << <b>0.01</b>      | 0.22 | << <b>0.01</b> | << <b>0.01</b> | 0.67           |



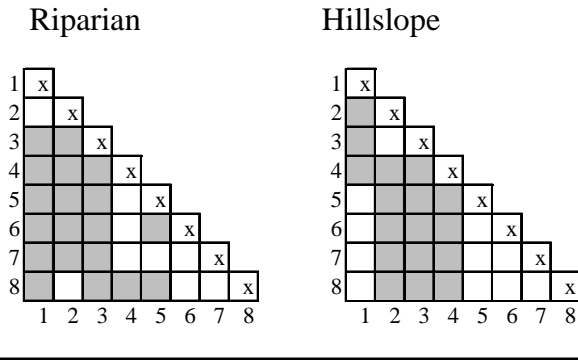
Table 2.6: Analysis of variance statistics ( $\alpha = 0.05$ ) for transect-versus-transect comparisons of riparian and hillslope soil water content during A) June; B) July; and C) August, 2005. Shaded boxes indicate significant differences. n ranged from 24 for T7 versus T8 in June to 80 for T1 versus T2 in July.

Soil Water Content

A) June



B) July



C) August

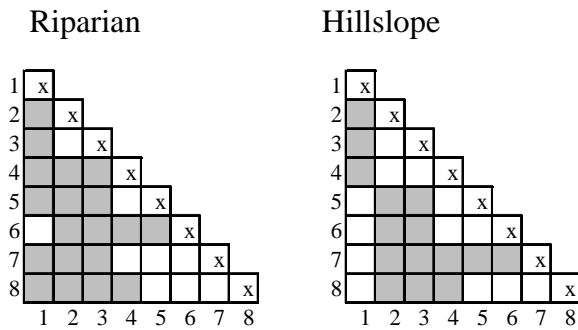
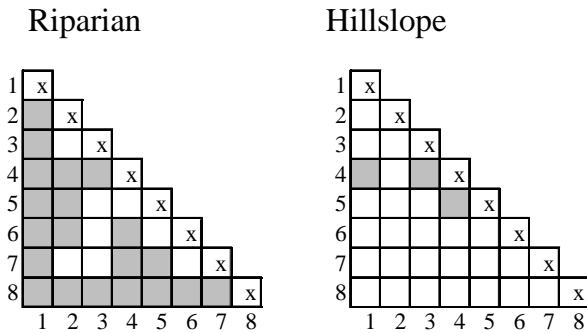


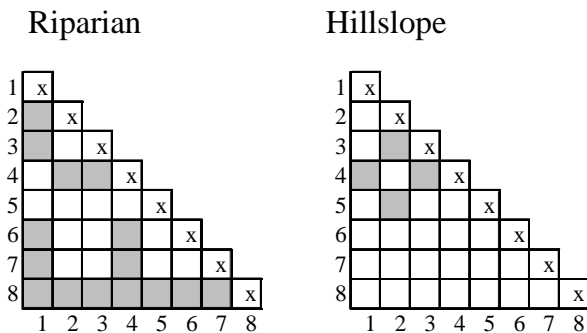
Table 2.7: Analysis of variance statistics ( $\alpha = 0.05$ ) for transect-versus-transect comparisons of riparian and hillslope soil water content during A) June; B) July; and C) August, 2005. Shaded boxes indicate significant differences. n ranged from 24 for T7 versus T8 in June to 80 for T1 versus T2 in July.

Soil Gas Diffusivity

A) June



B) July



C) August

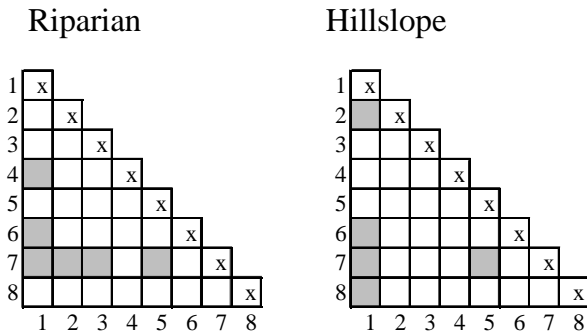
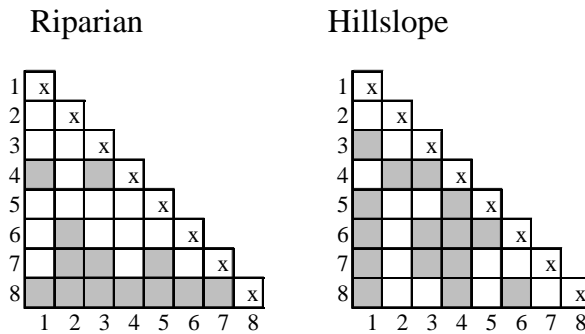


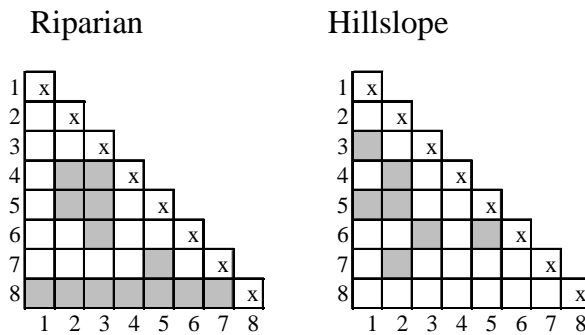
Table 2.8: Analysis of variance statistics ( $\alpha = 0.05$ ) for transect-versus-transect comparisons of riparian and hillslope soil CO<sub>2</sub> concentrations (20 cm) during A) June; B) July; and C) August, 2005. Shaded boxes indicate significant differences. n ranged from 24 for T7 versus T8 in June to 80 for T1 versus T2 in July.

Soil CO<sub>2</sub> Concentrations - 20 cm

A) June



B) July



C) August

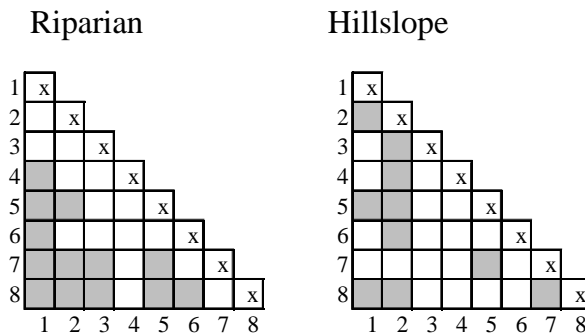
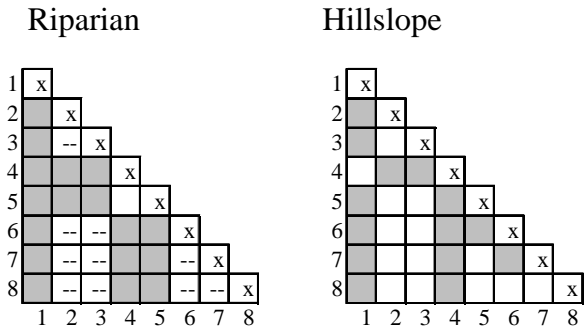


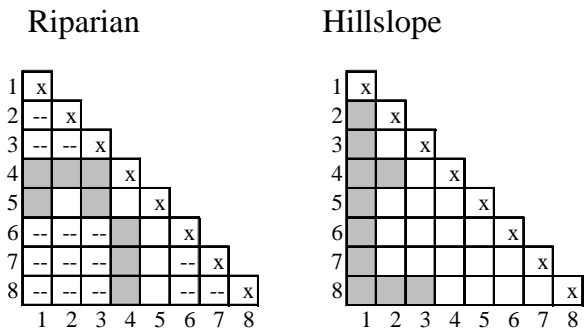
Table 2.9: Analysis of variance statistics ( $\alpha = 0.05$ ) for transect-versus-transect comparisons of riparian and hillslope soil CO<sub>2</sub> concentrations (50 cm) during A) June; B) July; and C) August, 2005. Shaded boxes indicate significant differences. n ranged from 24 for T7 versus T8 in June to 80 for T1 versus T2 in July.

Soil CO<sub>2</sub> Concentrations - 50 cm

A) June



B) July



C) August

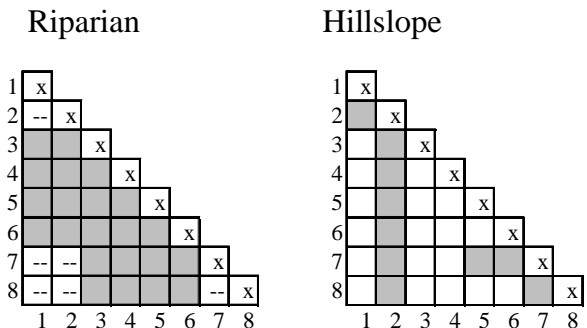
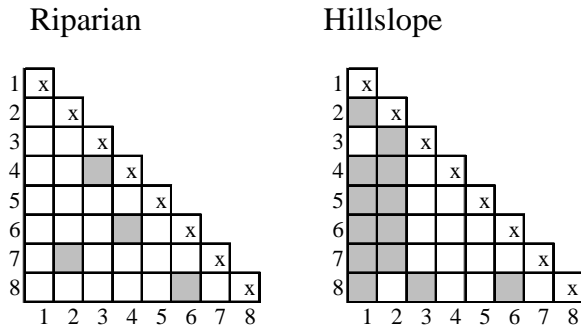


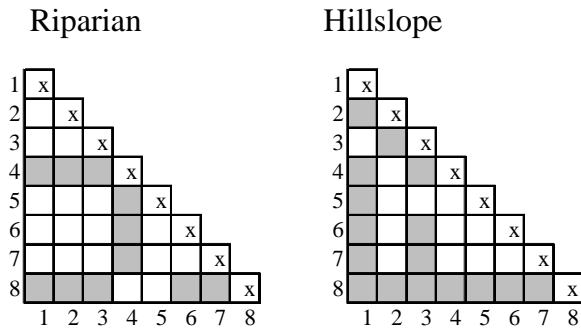
Table 2.10: Analysis of variance statistics ( $\alpha = 0.05$ ) for transect-versus-transect comparisons of riparian and hillslope soil surface CO<sub>2</sub> efflux during A) June; B) July; and C) August, 2005. Shaded boxes indicate significant differences. n ranged from 24 for T7 versus T8 in June to 80 for T1 versus T2 in July.

### Surface CO<sub>2</sub> Efflux

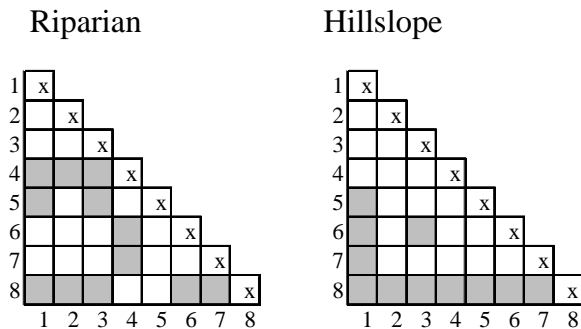
#### A) June



#### B) July



#### C) August



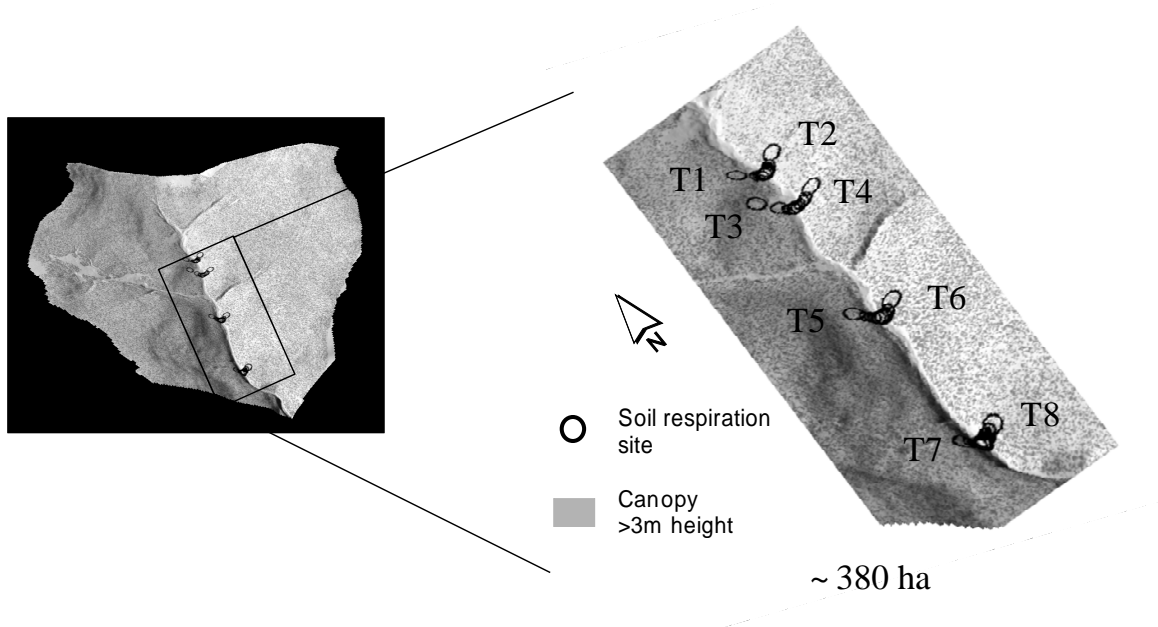


Figure 2.1: LIDAR (ALSM) topographic image (resolution < 1 m for bare earth and vegetation) of the upper-Stringer Creek Watershed within the Tenderfoot Creek Experimental Forest (Lewis and Clark National Forest), MT. Transect and soil respiration measurement locations are shown.

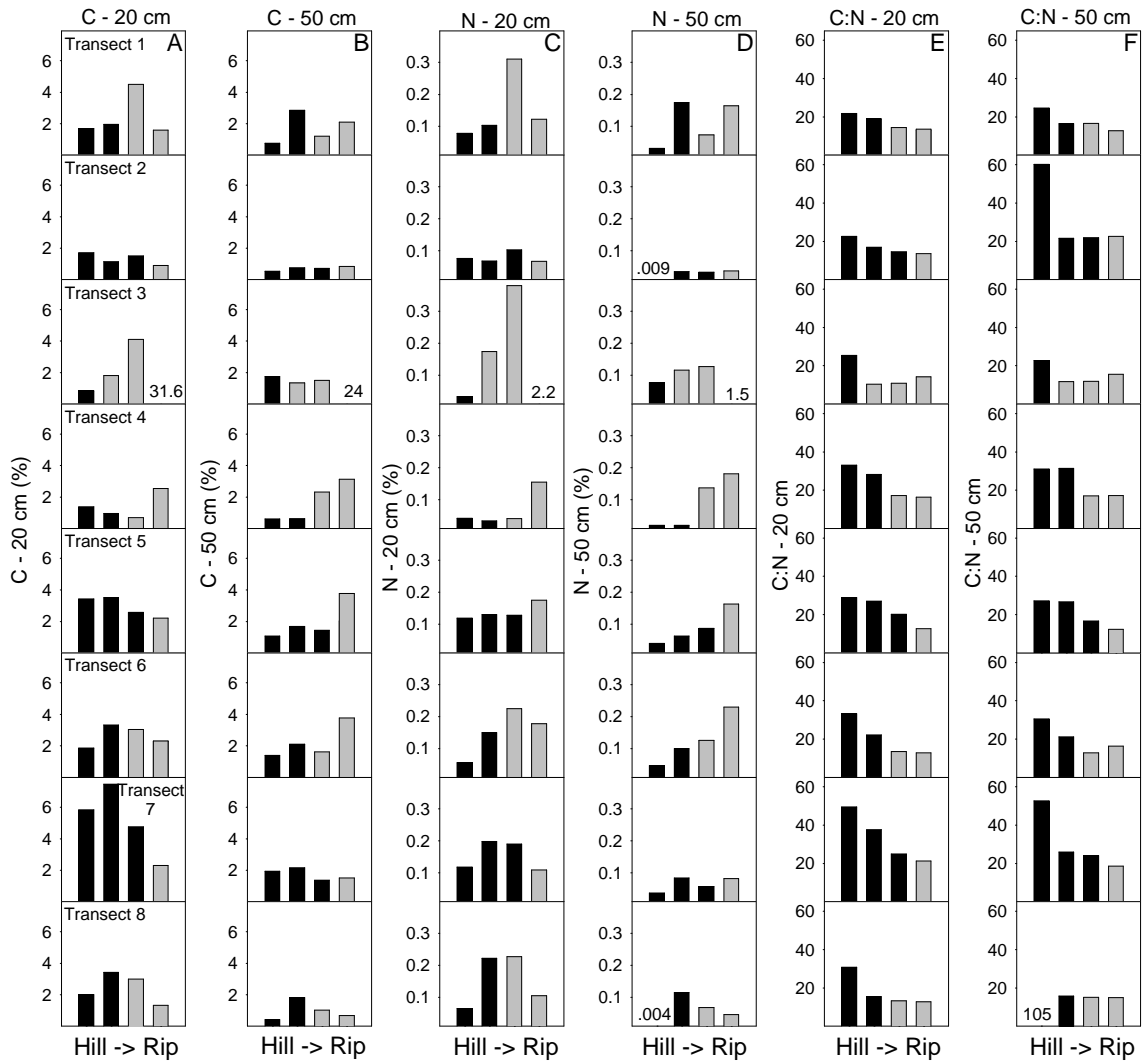


Figure 2.2: Bar graphs A) 20 cm soil C content; B) 50 cm soil C content; C) 20 cm soil N content; D) 50 cm soil N content; E) 20 cm soil C:N ratio; and F) 50 cm soil C:N ratio in hillslope (black) and riparian (grey) zones along each transect. Very small or large values are written instead of plotted as they affected the bar graph scale.

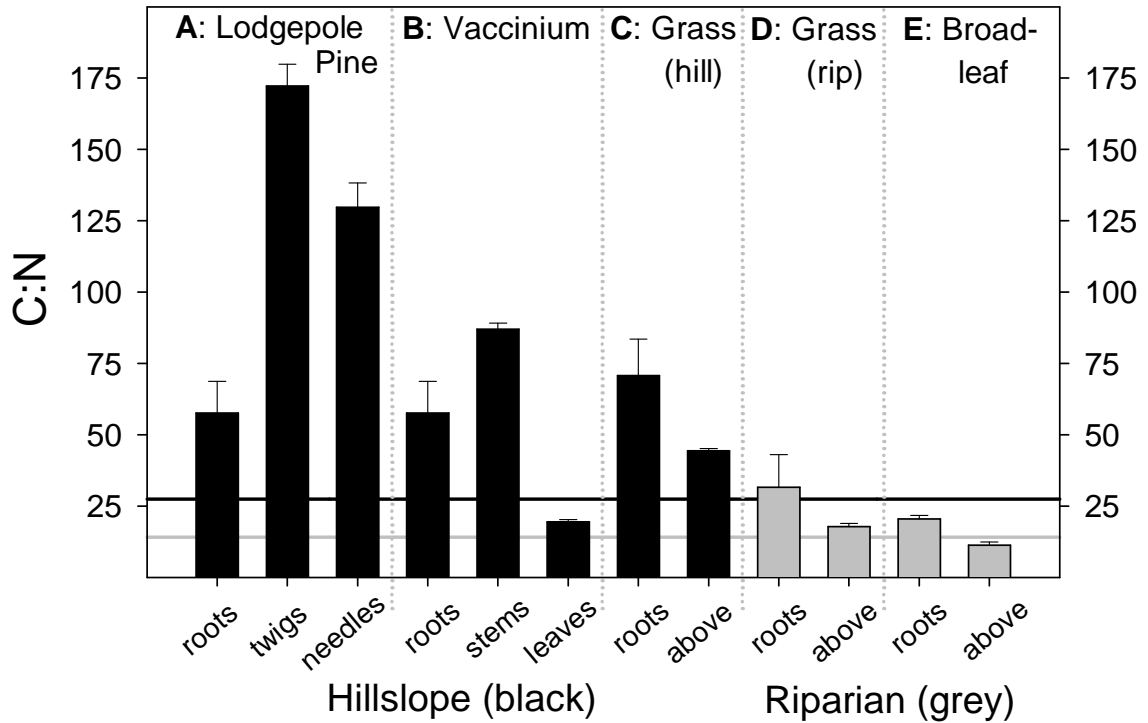


Figure 2.3: Bar graphs of vegetation C:N ratios in hillslope (black) and riparian (grey) zones: A) lodgepole pine (roots, twigs, and needles); B) vaccinium (roots, twigs, leaves); C) grass in the hillslopes (roots, and above-ground); D) grass in the riparian zones (roots and above-ground); and E) broad leaf plants (roots and above-ground). Whiskers represent one standard deviation based upon 3 replications. Average 20 cm soil C:N ratios (26:1 and 14:1 in the hillslope and riparian zone, respectively) are indicated by solid black (hillslope) and grey (riparian) lines.

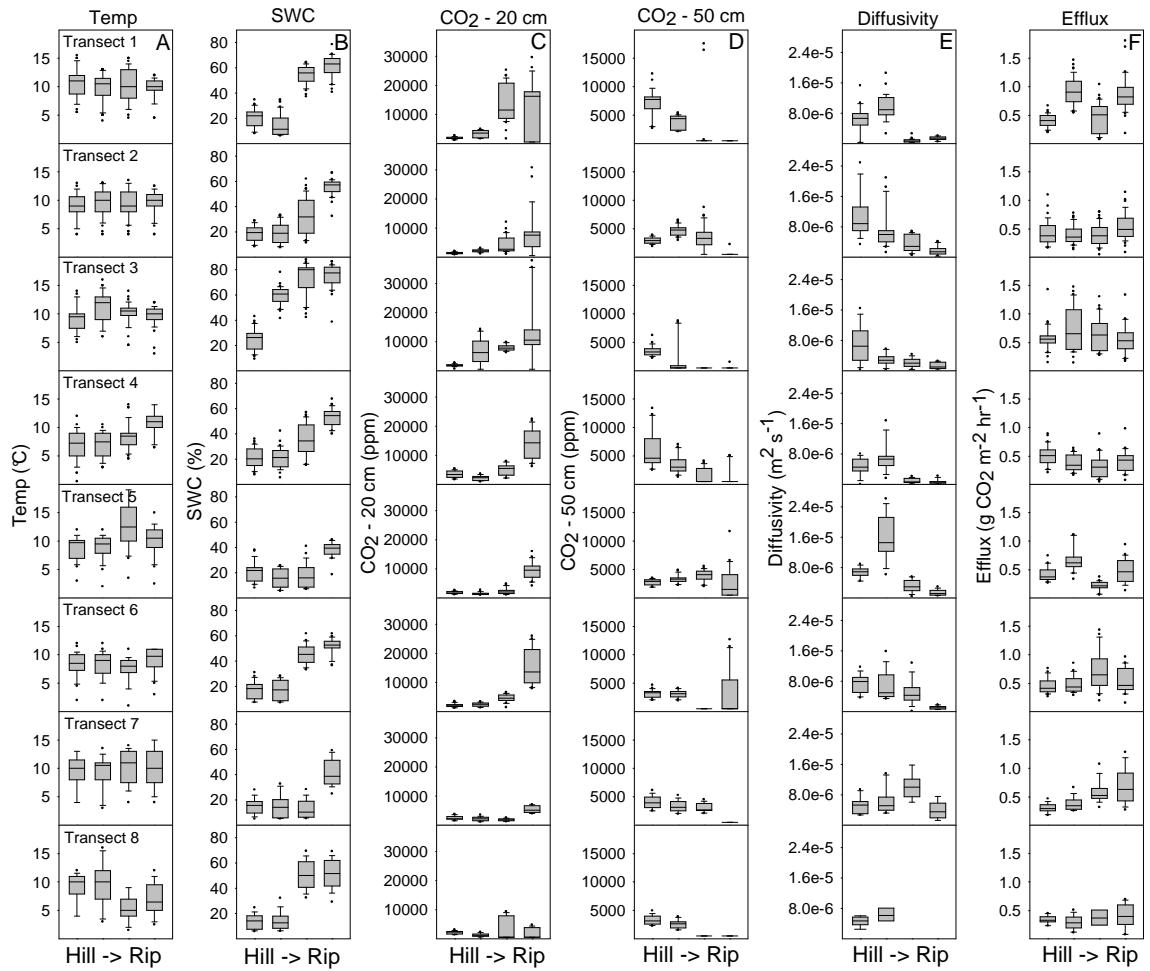


Figure 2.4: Box-plots of A) soil temperature; B) soil water content; C) soil CO<sub>2</sub> concentration – 20 cm; D) soil CO<sub>2</sub> concentration – 50 cm; E) soil gas diffusivity; and F) surface CO<sub>2</sub> efflux along each transect from June 14 to August 31, 2005.

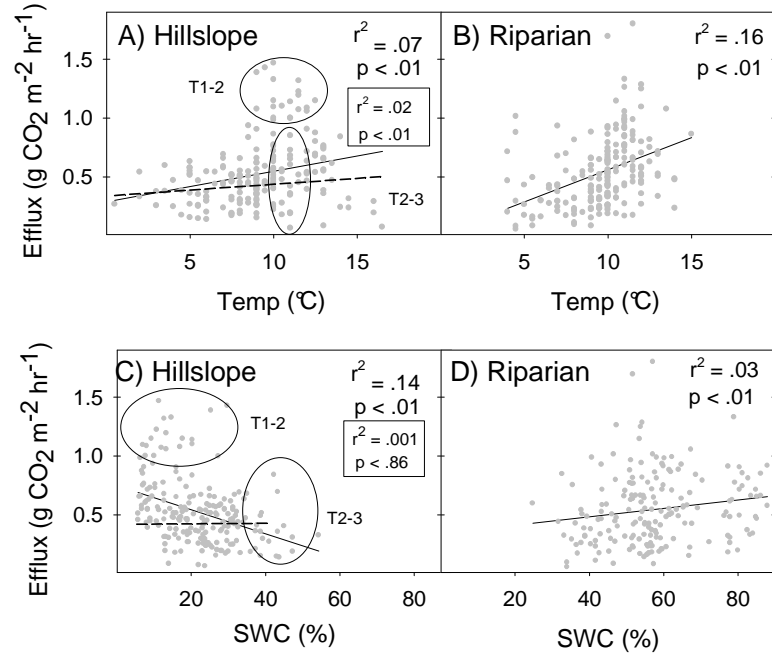


Figure 2.5: Bivariate plots of soil temperature and surface CO<sub>2</sub> efflux at A) riparian, and B) hillslope zones; and SWC and surface CO<sub>2</sub> efflux at C) riparian, and D) hillslope zones from all transects collected from June 9 to August 31, 2005. Solid line denotes linear regression, and p-values are provided for  $\alpha = 0.05$ . Circles show data from T1N2 and T2N3, boxes show  $r^2$  and p-values, and dashed line denotes linear regression, with these nests removed from analysis.

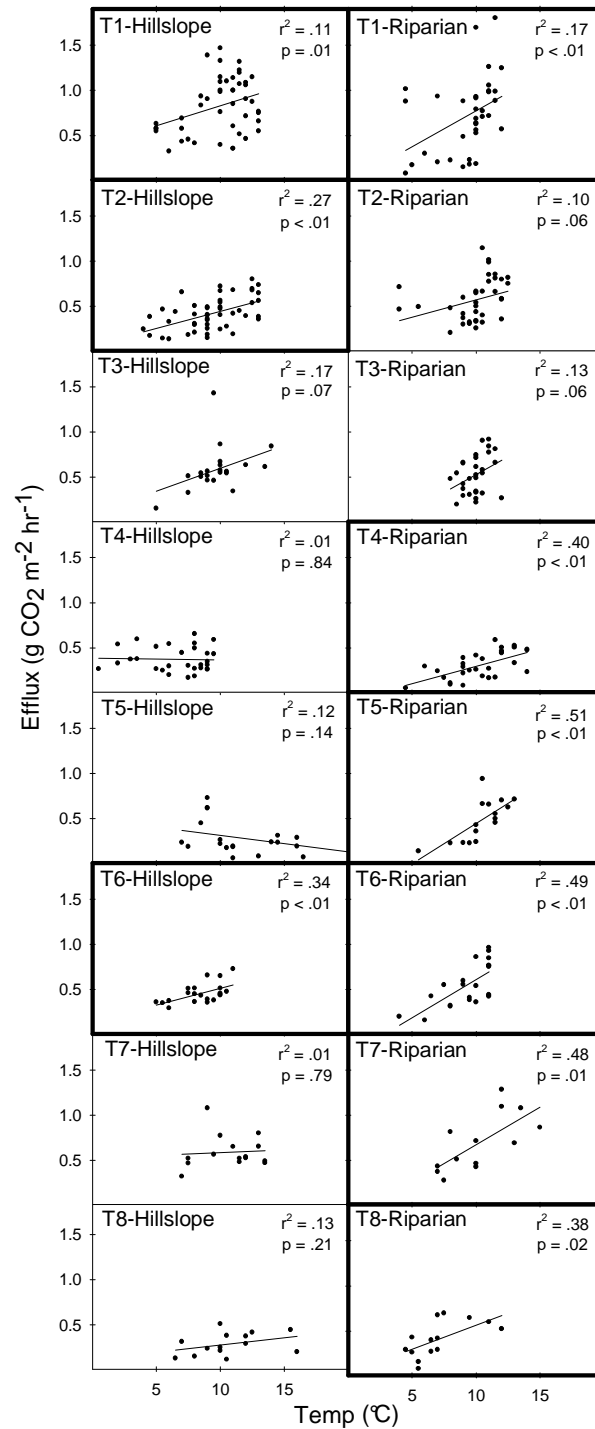


Figure 2.6: Bivariate plots of soil temperature and surface CO<sub>2</sub> efflux at riparian and hillslope zones along each transect, collected from June 9 to August 31, 2005. Solid line denotes linear regression, and p-values are provided for  $\alpha = 0.05$ . Dark boxes indicate a statistically significant relationship.

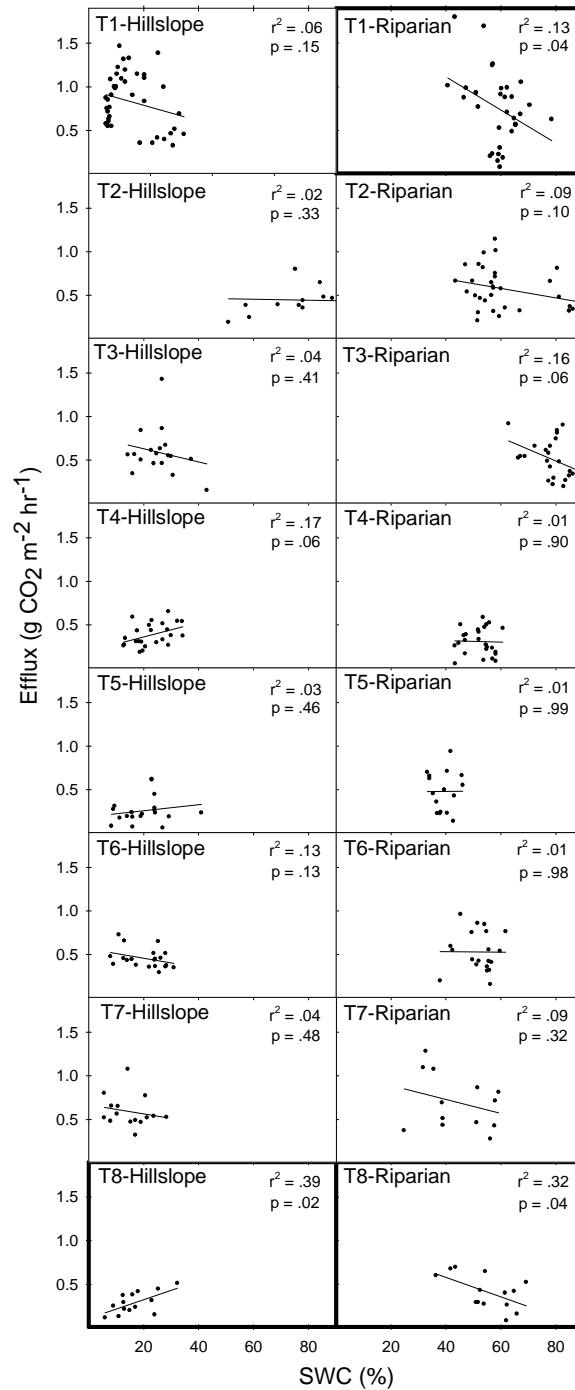


Figure 2.7: Bivariate plots of soil water content and surface CO<sub>2</sub> efflux at riparian and hillslope zones along each transect, collected from June 9 to August 31, 2005. Solid lines denote linear regression, and p-values are provided for  $\alpha = 0.05$ . Dark boxes indicate a statistically significant relationship.

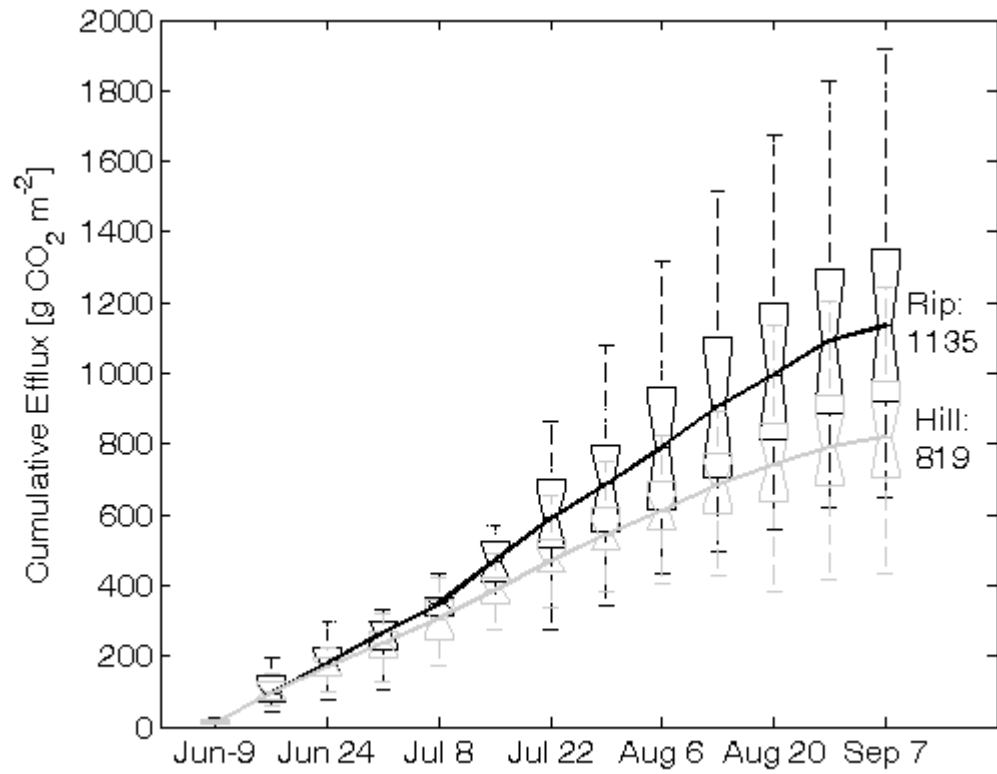


Figure 2.8: Box plots of cumulative growing season efflux (June 9 - August 31, 2005) from all riparian and hillslope locations.

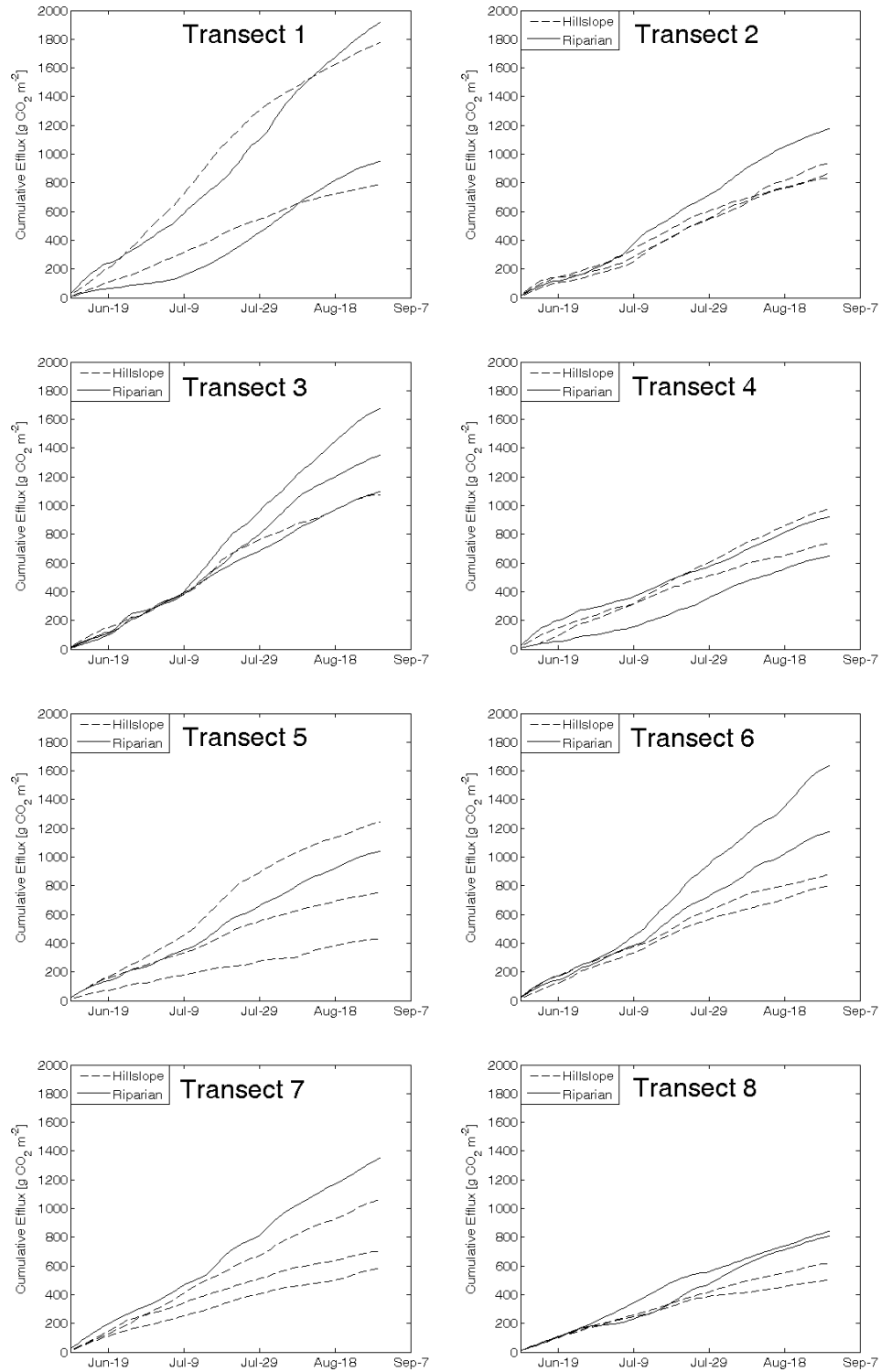


Figure 2.9: Cumulative growing season efflux (June 9 - August 31, 2005) plots for hillslope (dashed lines) and riparian (solid lines) zones across each transect.

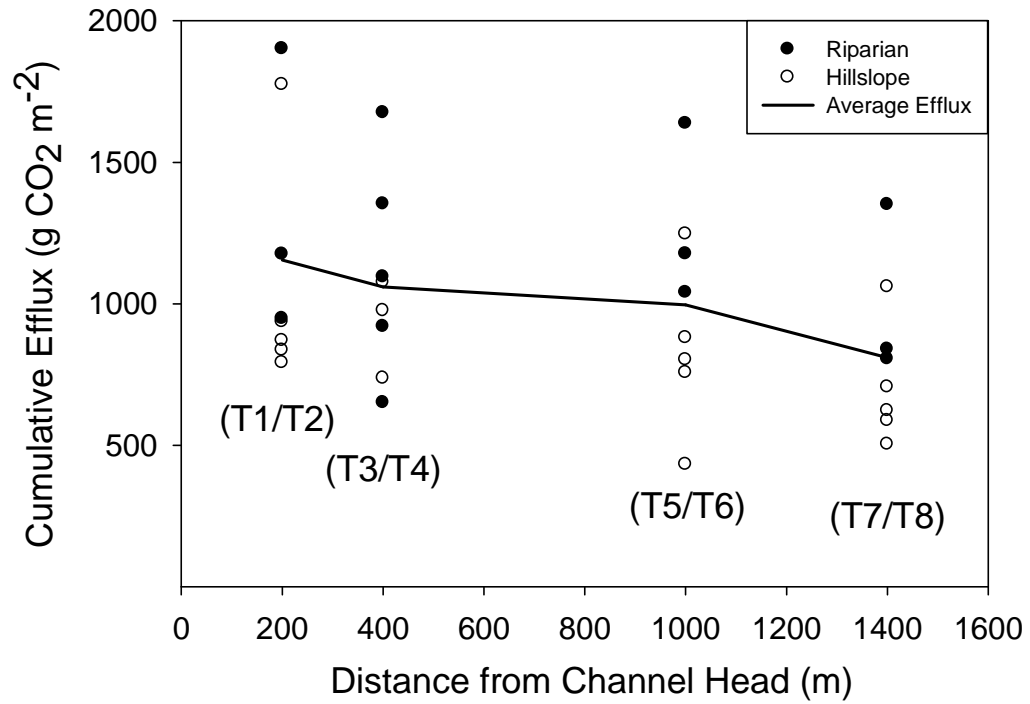


Figure 2.10: Cumulative growing season efflux (June 9 – August 31, 2005) from riparian and hillslope locations versus distance from channel head.

## CHAPTER 3

DIFFERENTIAL SOIL RESPIRATION RESPONSES TO CHANGING  
HYDROLOGIC REGIMES

*Adapted from: Pacific, V.J., B.L. McGlynn, D.A. Riveros-Iregui, H.E. Epstein, and D.L. Welsch (in review) Differential soil respiration responses to changing hydrologic regimes. Submitted for publication in Water Resources Research – Rapid Communications.*

Abstract

Soil respiration is tightly coupled to the hydrologic cycle (e.g. snowmelt and precipitation timing and magnitude). We examined riparian and hillslope soil respiration across a wet (2005) and a dry (2006) growing season in a subalpine catchment. When comparing the riparian zones, cumulative CO<sub>2</sub> efflux was 33% higher, and peak efflux occurred 17 days earlier during the dry growing season. In contrast, cumulative efflux in the hillslopes was 8% lower, and peak efflux occurred 10 days earlier during the drier growing season. Our results demonstrate soil respiration was more sensitive to drier growing season conditions in wet (riparian) landscape positions.

Introduction

Soil respiration is a critical component of ecosystem carbon source/sink status (Oechel *et al.*, 1993; Cox *et al.*, 2000; Heimann and Reichstein, 2008; Luysaert *et al.*, 2008) and is strongly controlled by soil water content (SWC) (Schaphoff *et al.*, 2006; Riveros-Iregui *et al.*, 2007; Pacific *et al.*, 2008), and therefore precipitation (Oechel *et al.*, 1993; Mu *et al.*, 2008). Over the last 100 years, estimated mean global precipitation

over the land surface has increased by 0.3-4% (*Yu et al.*, 2008). This intensification of the hydrologic cycle is predicted to increase by up to 20% in North America over the next century (*Christensen et al.*, 2007). Peak snowmelt-dominated streamflow is occurring 1-4 weeks earlier (*Stewart et al.*, 2005), and is predicted to occur an additional 3-5 weeks earlier over the next century (*Stewart et al.*, 2004). These alterations to the hydrologic cycle (at seasonal to annual timescales) will likely lead to strong changes in SWC, and therefore soil respiration. However, large uncertainty exists in the response of soil respiration to changes in SWC across different landscape positions (e.g. wet and dry areas).

Intermediate SWC is optimal for soil respiration (*Davidson et al.*, 2000; *Sjogersten et al.*, 2006). Soil respiration is limited at low SWC by root and microbial desiccation stress (*Orchard and Cook*, 1983; *Linn and Doran*, 1984) and at high SWC due to bidirectional limitations in diffusion of gas and nutrients to plants and microorganisms (*Skopp et al.*, 1990; *Moldrup et al.*, 2000). Previous research has indicated that higher soil water inputs can increase soil respiration at dry sites and decrease respiration at wet sites, and lead to similar soil CO<sub>2</sub> efflux across wet and dry landscape positions (*Davidson et al.*, 1998; *Savage and Davidson*, 2001). However, *Davidson et al.* (1998) and *Savage and Davidson* (2001) were limited by few sampling locations and small spatial coverage. Here we document dynamic and strongly contrasting soil respiration response at wet (riparian) and dry (hillslope) landscape positions to wetter and drier growing season conditions (and therefore different

approaches to and departures from optimal intermediate SWC) from 32 locations in a complex subalpine watershed.

### Methods

The study site was the upper-Stringer Creek Watershed (~380 ha), located in the U.S. Forest Service Tenderfoot Creek Experimental Forest (TCEF, Lewis and Clark National Forest, lat. 46°55' N., long. 110°52' W.) of central Montana. The spatial heterogeneity of this site offers an ideal scenario to address soil respiration variability due to strong, natural biophysical gradients in the drivers of soil respiration. The elevation is 1,840 to 2,421 m, with a mean of 2,205 m. Mean annual temperature is 0°C, and mean annual precipitation is 880 mm, with ~70% falling as snow from November through May. Air temperature, precipitation, snow depth, and snow water equivalent were collected from 1994-2006 from the Onion Park SNOTEL (snow survey telemetry) site (2258 m, located approximately 2 km to the south of the upper-Stringer Creek Watershed). Streamflow was measured by the U.S. Forest Service Rocky Mountain Research Station from 1996-2006 at the upper-Stringer Creek Flume (located within 400 m of the field plots along Stringer Creek).

Eight transects (approximately 50 m long) originating at Stringer Creek and extending up the fall line through the riparian and adjacent hillslope zone included two riparian and two hillslope measurement locations along each transect (32 total measurement locations). The overstory vegetation in the hillslopes is mainly lodgepole pine (*Pinus contorta*), the understory vegetation is grouse whortleberry (*Vaccinium scoparium*), and riparian vegetation is predominantly bluejoint reedgrass (*Calamagrostis*

*canadensis*). In the hillslopes, the major soil group is loamy skeletal, mixed Typic Cryochrepts, while the riparian zones are composed of highly organic clayey, mixed Aquic Cryoboralfs (Holdorf, 1981).

We collected measurements of soil temperature, SWC, and soil surface CO<sub>2</sub> efflux during contrasting wet (2005) and dry (2006) growing seasons. Measurements were taken from June 9 – August 31 during both years, which was the approximate time of the growing season (Schmidt and Friede, 1996) and period of frequent data collection (every 2-7 days) during both 2005 and 2006. Further, the magnitude of soil respiration outside of this range was small due to very low soil temperatures (Pacific et al., 2008). One measurement of soil temperature (12 cm soil thermometer, Reotemp Instrument Corporation, San Diego, California, USA; measurement range of -20°C to 120°C) and three measurements of volumetric SWC (cm<sup>3</sup> H<sub>2</sub>O/cm<sup>3</sup> soil, integrated over the top 20 cm of soil; Hydrosense portable SWC meter, Campbell Scientific Inc., Utah, USA) were collected on each sampling day at each of the 32 locations. Three surface CO<sub>2</sub> efflux measurements were collected at each measurement location with a soil respiration chamber (SRC-1 chamber with a footprint of 314.2 cm<sup>2</sup>, accurate to within 1% of calibrated range [0 to 9.99 g CO<sub>2</sub> m<sup>-2</sup> hr<sup>-1</sup>] in conjunction with an IRGA (EGM-4, accurate to within 1% of calibrated range [0 to 2,000 ppm]; PP Systems, Massachusetts, USA). The chamber was flushed with ambient air for 15 s then inserted 3 cm into the soil before each measurement began, and each measurement took ~120 s. Cumulative efflux (June 9 to August 31) was estimated by linearly interpolating between measurements collected every 2-7 days. This technique has been demonstrated to be a

robust approach for comparison of efflux measurements across multiple locations over extended periods of time (*Riveros-Iregui et al.*, 2008). Analysis of variance (ANOVA) statistics ( $\alpha = 0.05$ ) were employed to test for differences between riparian and hillslope cumulative surface CO<sub>2</sub> efflux, soil temperature, and SWC. The three measurements of SWC and surface CO<sub>2</sub> efflux collected at each location on all sampling days (to account for local variability) were averaged for data analysis.

### Results

Peak snowmelt-driven streamflow occurred on June 6 in 2005. This was 8 days later than the 10-year average of May 29 (extent of streamflow record, Figure 3.1), and 18 days later than in 2006. Growing season precipitation was 91% higher in 2005 than in 2006 (Figure 3.2), and 30% higher than the 13-year average of 20.6 cm (extent of precipitation record) (Figure 3.1). Cumulative soil water inputs (rain and snowmelt) were slightly greater in 2005 than 2006 (Figure 3.1), but a higher percentage fell as rain during the 2005 growing season (34% versus 20%). This combination of earlier peak streamflow and less growing season precipitation in 2006 relative to 2005 led to strong differences in SWC and therefore soil respiration across wetter (riparian) and drier (hillslope) landscape positions.

SWC was significantly higher in the riparian zones than the hillslopes during both growing seasons ( $p < 0.01$ ) (Figure 3.2). Maximum volumetric SWC in the riparian zones was similar between years (~65%, limited by porosity), while minimum riparian SWC was much lower during the dry growing season (13% compared to 37%).

Maximum and minimum SWC in the hillslopes were similar across both growing seasons

(~30% and 5%, respectively). Soil temperature was significantly higher during the wet growing season ( $p \ll 0.01$ ) (Figure 3.2). When comparing the riparian zones, cumulative surface CO<sub>2</sub> efflux was 33% larger during the dry year (2006) than the wet year (2005) (1344 versus 1012 g CO<sub>2</sub> m<sup>-2</sup>) ( $p \ll 0.01$ ). Peak efflux in the riparian zones occurred 17 days earlier in the dry growing season (July 1 versus July 18) (Figure 3.3). In contrast to the riparian zones, comparison of cumulative efflux from the hillslopes showed that efflux was 8% lower (749 versus 809 g CO<sub>2</sub> m<sup>-2</sup>) (insignificant,  $p = 0.92$ ), and peak hillslope efflux occurred 10 days earlier during the dry growing season (July 1 versus July 11). CO<sub>2</sub> efflux from the riparian zone was 25% greater than from the hillslope zone in the wet growing season (2005). In the dry growing season (2006), cumulative CO<sub>2</sub> flux from the riparian zone was 79% greater than from the hillslope zone.

### Discussion

Our results demonstrate that soil respiration varied considerably in response to changing hydrologic regimes, and that these changes were not monotonic across the landscape. Total soil water inputs (rain and snowmelt) were similar in 2005 and 2006, however peak snowmelt occurred 3 weeks later in 2005 (Figure 3.1), and precipitation was 91% higher during the wet 2005 growing season (Figure 3.2). While these differences in precipitation and snowmelt appear extreme, they were well within the range of the 10-13 year data record (Figure 3.1), in which precipitation varied by 169% and the timing of peak snowmelt varied by 30 days. We show that changes in hydrologic

regimes, even within the range observed over the last decade, can lead to large but differential soil respiration responses across landscape.

The combination of later snowmelt and higher precipitation during 2005 increased the duration of SWC in the riparian zones above the intermediate level optimal for soil respiration (*Davidson et al.*, 2000; *Sjogersten et al.*, 2006) (defined as 40-60% in the TCEF (*Pacific et al.*, 2008), indicated by grey boxes in Figure 3.2). High SWC can simultaneously decrease both soil CO<sub>2</sub> production and transport (*Pacific et al.*, 2008) due to bidirectional limitations in diffusion of CO<sub>2</sub>, oxygen, and nutrients (*Skopp et al.*, 1990; *Moldrup et al.*, 2000). SWC in the riparian zones was greater than 60% at the beginning of both growing seasons (Figure 3.2). However, SWC remained above intermediate (optimal) levels for ~2 weeks longer during the wet 2005 growing season, leading to a longer period of inhibited soil respiration in the riparian zones. When comparing riparian zones, cumulative efflux was 33% higher in the dry (2006) growing season than the wet (2005) growing season, and peak efflux occurred 17 days earlier during the dry growing season (Figure 3.3). Increased efflux in the riparian zones during the dry growing season was likely due to a shorter period of above-intermediate SWC, and therefore a longer duration of relatively high soil CO<sub>2</sub> production and diffusion (*Pacific et al.*, 2008). In contrast, comparison of efflux in the hillslopes between the wet and the dry growing season showed that cumulative efflux was 8% lower, and peak efflux in the hillslopes occurred 10 days earlier during the dry growing season, (Figure 3.3). These differences in the timing and magnitude of efflux in the hillslopes between the wet and the dry growing season was likely the result of the quicker decline from near-intermediate

hillslope SWC during the drier growing season, as inhibited soil CO<sub>2</sub> production can occur at low SWC from desiccation stress (*Orchard and Cook, 1983; Linn and Doran, 1984*). It is likely that changes in soil temperature had a small effect on the variability in soil respiration between 2005 and 2006. Soil temperatures were significantly higher during 2005 ( $p \ll 0.01$ ) (Figure 3.2), and would promote higher efflux (*Hamada and Tanaka, 2001; Raich et al., 2002; Pendall et al., 2004*). However, significantly lower efflux in the riparian zones during 2005 ( $p \ll 0.01$ ) suggest soil temperature did not control soil respiration heterogeneity at this site. Our results indicate that changes in the timing and magnitude of precipitation and snowmelt can cause spatial and temporal variability in the movement of SWC into or out of the intermediate range that is optimal for respiration, the degree of which can vary strongly by landscape position.

We suggest that differences in soil respiration across the landscape between 2005 and 2006 were the result of decreased SWC from earlier snowmelt and lower precipitation, however other interpretations are possible. For example, the frequency and timing of precipitation pulses may be more important than the total amount of precipitation (*Schwinnig and Sala, 2004*). Large increases in soil respiration (*Austin et al., 2004; Lee et al., 2004; Daly et al., 2008*) often follow precipitation events, the degree of which can vary with both storm frequency and type of vegetation (*Fierer and Schimel, 2002*). In 2005, there was a period of intense rainfall at the end of June (Figure 2), which may have stimulated soil respiration and led to the peak in efflux in the hillslopes on July 1 (Figure 3.3). The later peak in efflux in the riparian zones during 2005 (July 18) may be due to reduced gas diffusivity following the increase in SWC (*Pacific et al.,*

2008). These results suggest that the large precipitation events at the end of June controlled the timing of peak efflux. However, these peaks in riparian and hillslope efflux may be due to the rise in soil temperature at the same time periods (Figure 3.2), which can increase evaporation and therefore decrease SWC. This indicates that predicted rises in temperature may constrain the effects of increased precipitation. We suggest that further research is necessary to determine the control of precipitation pulses and interactions between soil temperature and SWC on soil respiration variability following changes in hydrologic regimes.

The results of this study can have large implications for ecosystem carbon balances. We observed large and disproportionate changes in efflux from wet (riparian) and dry (hillslope) landscape positions from a wet to a dry growing season in a subalpine forest in the northern Rocky Mountains of Montana. Mean annual precipitation is projected to increase by up to 20% over the next century in North America (*Christensen et al.*, 2007), and peak snowmelt-dominated streamflow is predicted to occur 20-40 days earlier (*Stewart et al.*, 2004). Therefore, it is likely that the divergence in the response of soil respiration to changes in SWC across the landscape will be exacerbated in the future, and that changes in hydrologic regimes may strongly impact carbon source/sink magnitude and status of wet and dry landscape positions. Low Arctic and boreal soils are historically large carbon sinks due to a cold climate and wet soils (*Chapin et al.*, 1980; *Ping et al.*, 2008). These soils account for 20-60% of the global soil carbon pool and contain 1-2 orders of magnitude more carbon than emitted from anthropogenic activities (*Ping et al.*, 2008; *Schuur et al.*, 2008). Arctic and boreal soils are predicted to switch to

carbon sources as global temperatures increase (*Oechel et al.*, 1993). When comparing wet landscape positions (riparian zones) between a wet and a dry growing season, we found significantly lower efflux during the wet growing season, despite higher soil temperatures. These results suggest that possible warming-induced increases in arctic and boreal soil respiration could be constrained by increasing precipitation. In contrast, the predicted rise in precipitation in arid and semi-arid ecosystems (*Christensen et al.*, 2007) could increase soil respiration in these water-limited areas. This is supported by our comparisons of soil respiration at dry landscape positions (hillslope zones) between a wet and a dry growing season, in which we found higher efflux during the wet growing season. Higher soil respiration across dry landscapes could have a large impact on the global carbon cycle, as arid and semi-arid lands cover 41% of the Earth's surface (*Reynolds et al.*, 2007). The results of our study demonstrate that soil respiration responses to changes in SWC are not monotonic across the landscape. Rather, changes in soil respiration at wet and dry landscape positions can occur in opposing directions and with different magnitudes. The greatest changes may occur with drying of wet landscape positions.

### Conclusions

Based upon measurements and analysis of riparian and hillslope soil surface CO<sub>2</sub> efflux, SWC, and soil temperature across contrasting wet and dry growing seasons with large differences in snowmelt and precipitation timing and magnitude, we conclude that:

1. Wetter landscape positions were more sensitive to drier growing season conditions. When comparing the riparian zones, cumulative soil CO<sub>2</sub> efflux

was 33% higher during the dry (2006) growing season. In contrast, comparison of hillslope zones showed that cumulative efflux was 8% lower during the dry growing season.

2. Drier growing season conditions led to earlier peaks in both riparian and hillslope cumulative soil CO<sub>2</sub> efflux, with the greatest changes in wet (riparian) landscape positions. Peak riparian and hillslope efflux occurred 17 and 10 days earlier during the drier growing season.

This research provides insight into the coupling of soil respiration to alterations in the hydrologic cycle (e.g. snowmelt and precipitation timing and magnitude). We suggest wetter landscape positions could show the greatest changes in soil CO<sub>2</sub> efflux and therefore the greatest shifts in carbon source/sink status.

#### Acknowledgements

We gratefully acknowledge field assistance from K. Jencso, B. McNamara, K. Conde, and A. Allen. We would like to thank W. McCaughey of the USDA, Forest Service, Rocky Mountain Research Station and the Tenderfoot Creek Experimental Forest for extensive logistical support and research site access. This work was funded by the NSF Integrated Carbon Cycle Research Program (ICCR, NSF Grant EAR0404130, EAR0403924, and EAR0403906) and fellowships awarded to V. J. Pacific from the Big Sky Institute NSF GK-12 program and the Inland Northwest Research Alliance (INRA). We are also grateful for very informative comments from three anonymous reviewers, whose suggestions significantly improved an earlier version of this manuscript.

References Cited

- Austin, T. A., M. L. Yahdjian, J. M. Stark, J. Belnap, A. Porporato, I.C. Burke, U. Choromanska, D. Ravetta, and S. M. Schaeffer (2004) Water pulses and biogeochemical cycles in arid and semiarid ecosystems, *Oecologia*, 141, 221-235.
- Chapin, F. S., P. C. Miller, W. D. Billings, and P. I. Coyne (1980) Carbon and nutrient budgets and their control in coastal tundra, in *An Arctic Ecosystem: The Coastal Tundra at Barrow, Alaska*, edited by J. Brown, P. C. Miller, L. L. Tieszen, and F. L. Bunnell, pp. 458–483, Dowden, Hutchinson, & Ross, Stroudsburg, PA.
- Christensen, J. H., B. Hewitson, A. Busuioc, A. Chen, X. Gao, I. Held, R. Jones, R. K. Kolli, W. T. Kwon, R. Laprise, V. Magaña Rueda, L. Mearns, C. G. Menendez, J. Räisänen, A. Rinke, A. Sarr, and P. Whetton (2007) Regional climate projections, In *Climate Change 2007: The Physical Science Basis. Contribution of Working Group I to the Fourth Assessment Report of the Intergovernmental Panel on Climate Change*, edited by S. Solomon, D. Qin, M. Manning, Z. Chen, M. Marquis, K. B. Averyt, M. Tignor, H. L. Miller, 847-940, Cambridge University Press, Cambridge and New York.
- Cox, P. M., R. A. Betts, C. D. Jones, S. A. Spall, and I. J. Totterdell (2000) Acceleration of global warming due to carbon-cycle feedbacks in a coupled climate model, *Nature*, 408, 184-187.
- Daly, E., A. C. Oishi, A. Porporato, G. G. Katul (2008) A stochastic model for daily subsurface CO<sub>2</sub> concentration and related soil respiration, *Advances in Water Resources*, 31, 987-994.
- Davidson, E. A., E. Belk, and R. D. Boone (1998) Soil water content and temperature as independent or confounded factors controlling soil respiration in a temperate mixed hardwood forest, *Global Change Biology*, 4, 217-227.
- Davidson, E. A., L. V. Verchot, J. H. Cattanio, I. L. Ackerman, and J. E. M. Carvalho (2000) Effects of soil water content on soil respiration in forests and cattle pastures of eastern Amazonia, *Biogeochemistry*, 48, 53-69.
- Fierer N., and J. P. Schimel (2002) Effects of drying-wetting frequency on soil carbon and nitrogen transformations, *Soil Biology and Biochemistry*, 34, 777-787.
- Hamada, Y. and T. Tanaka (2001) Dynamics of carbon dioxide in soil profiles based on long-term field observation, *Hydrological Processes*, 15, 1829-1845.
- Heimann, M. and M. Reichstein (2008) Terrestrial ecosystem carbon dynamics and climate feedbacks, *Nature*, 451, 289-292, doi: 10.1038/nature06591.

- Holdorf, H. D. (1981) Soil Resource Inventory, Lewis and Clark National Forest – Interim In-Service Report, *on file with the Lewis and Clark National Forest, Forest Supervisor's Office, Great Falls, MT.*
- Lee, X., H. J. Wu, J. Singler, C. Oishi, and T. Siccama (2004) Rapid and transient response of soil respiration to rain, *Global Change Biology*, 10, 1017–26.
- Linn, D. M. and J. W. Doran (1984) Effect of water-filled pore space on carbon dioxide and nitrous oxide production in tilled and nontilled soils, *Soil Science Society of America Journal*, 48, 1267-1272
- Luysaert, S., E. D. Schulze, A. Borner, A. Knohl, D. Hessenmoller, B. E. Law, P. Ciais, and J. Grace (2008) Old-growth forests as global carbon sinks, *Nature*, 455, 213-215, doi: 10.1038/nature07276.
- Moldrup, P., T. Olsen, P. Schjønning, T. Yamaguchi, and D. E. Rolston (2000) Predicting the gas diffusion coefficient in undisturbed soil from soil water characteristics, *Soil Science Society of America Journal*, 64, 94-100.
- Mu, Q., M. Zhao, S. W. Running, M. Liu, and H. Tian (2008) Contribution of increasing CO<sub>2</sub> and climate change to the carbon cycle in China's ecosystems, *Journal of Geophysical Research*, 113, G01018, doi: 10.1029/2006JG000316.
- Oechel, W. C., S. J. Hastings, G. Vourlitis, M. Jenkins, G. Riechers, and N. Grulke (1993) Recent change of Arctic tundra ecosystems from a net carbon dioxide sink to a source, *Nature*, 361, 520-523.
- Orchard, V. A., and F. Cook (1983) Relationship between soil respiration and soil moisture, *Soil Biology and Biochemistry*, 15, 447-453.
- Pacific, V. J., B. L. McGlynn, D. A. Riveros-Iregui, D. L. Welsch, and H. E. Epstein (2008) Variability in soil respiration across riparian-hillslope transitions, *Biogeochemistry*, doi: 10.1007/s10533-008-9258-8.
- Pendall, E., S. Bridgman, P. Hanson, B. Hungate, D. W. Kicklighter, D. W. Johnson, B. E. Law, Y. Q. Luo, J. P. Megonigal, M. Olsrud, M. G. Ryan, and S. Q. Was (2004) Below-ground process response to elevated CO<sub>2</sub> and temperature: a discussion of observations, measurement methods, and models, *New Phytologist*, 162, 311-322.
- Ping, C., G. J. Michaelsoni, M. T. Jorgenson, J. M. Kimble, H. E. Epstein, V. E. Romanovsky, and D. A. Walker (2008) High stocks of soil organic carbon in the North American Arctic region, *Nature Geosciences.*, doi: 10.1038/ngeo284.

- Raich, J. W., C. S. Potter, and D. Bhagawati (2002) Interannual variability in global soil respiration, 1980-94, *Global Change Biology*, 8, 800-812.
- Reynolds, J. F., D. M. Stafford, D. M. Smith, E. F. Lambin, B. L. Turner, M. Mortimore, S. P. J. Batterbury, T. E. Downing, H. Dowlatabadi, R. J. Fernandez, J. E. Herrick, E. Huber-Sannwald, H. Jiang, R. Leemans, T. Lynam, F. T. Maestre, M. Ayarza, and B. Walker (2007) Global desertification: Building a science for dryland development, *Science*, 316, 847-851.
- Riveros-Iregui, D. A., R. E. Emanuel, D. J. Muth, B. L. McGlynn, H. E. Epstein, D. L. Welsch, V. J. Pacific, and J. M. Wraith (2007) Diurnal hysteresis between soil temperature and soil CO<sub>2</sub> is controlled by soil water content, *Geophysical Research Letters*, doi: 10.1029/2007GL030938.
- Riveros-Iregui, D. A., B. L. McGlynn, H. E. Epstein, and D. L. Welsch (2008) Interpretation and evaluation of combined measurement techniques for soil CO<sub>2</sub> efflux: discrete surface chambers and continuous soil CO<sub>2</sub> concentration probes, *Journal of Geophysical Research – Biogeosciences*, doi:10.1029/2008JG000811
- Savage, K. E., and E. A. Davidson (2001) Interannual variation of soil respiration in two New England forests, *Global Biogeochemical Cycles*, 15, 337-350.
- Schaphoff, S., W. Lucht, D. Gerten, S. Sitch, W. Cramer, and I. C. Prentice (2006) Terrestrial biosphere carbon storage under alternative climate projections, *Climate Change*, 74, 97-122, doi: 10.1007/s10584-005-9002-5.
- Schmidt, W.C. and J. L. Friede (1996) Experimental forests, ranges and watersheds in the Northern Rocky, Mountains: a compendium of outdoor laboratories in Utah, Idaho and Montana. General Technical Report INT-GTR 334. U.S. Department of Agriculture, Forest Service, Intermountain Research Station, Ogden, UT.
- Schuur, E. A. G., J. Bockheim, J. G. Canadell, E. Euskirchen, C. B. Field, S. V. Goryachkin, S. Hagemann, P. Kuhry, P. M. Lafleur, H. Lee, G. Mazhitova, F. E. Nelson, A. Rinke, V. E. Romanovsky, N. Shiklomanov, C. Tarnocai, S. Venevsky, J. G. Vogel, and S. A. Zimov (2008) Vulnerability of permafrost carbon to climate change: Implications for the global carbon cycle, *Bioscience*, 58, 701-714.
- Schwinning, S, and O. E. Sala (2004) Hierarchy of responses to resource pulses in arid and semi-arid ecosystems, *Oecologia*, 141, 211-220.
- Sjogersten, S., R. van der Wal, and S. J. Woodin (2006) Small-scale hydrological variation determines landscape CO<sub>2</sub> fluxes in the high Arctic, *Biogeochemistry*, 80, 205-216.

- Skopp, J., M. D. Jawson, and J. W. Doran (1990) Steady-state aerobic microbial activity as a function of soil water content, *Soil Science Society of America Journal*, 54, 1619-1625.
- Stewart, I. T., D. R. Cayan, and M. D. Dettinger (2004) Changes in snowmelt runoff timing in western North America under a “business as usual” climate change scenario, *Climate Change*, 62, 217-232.
- Stewart, I. T., D. R. Cayan, and M. D. Dettinger (2005) Changes towards earlier streamflow timing across western North America, *Journal of Climate*, 18 1136-1155.
- Yu, Y. Q., H. Zhi, B. Wang, H. Wan, C. Li, H. L. Mu, W. Li, W. P. Zheng, and T. J. Zhou (2008) Coupled model simulations of climate changes in the 20th century and beyond, *Advances in Atmospheric Science*, 2, 641-654.

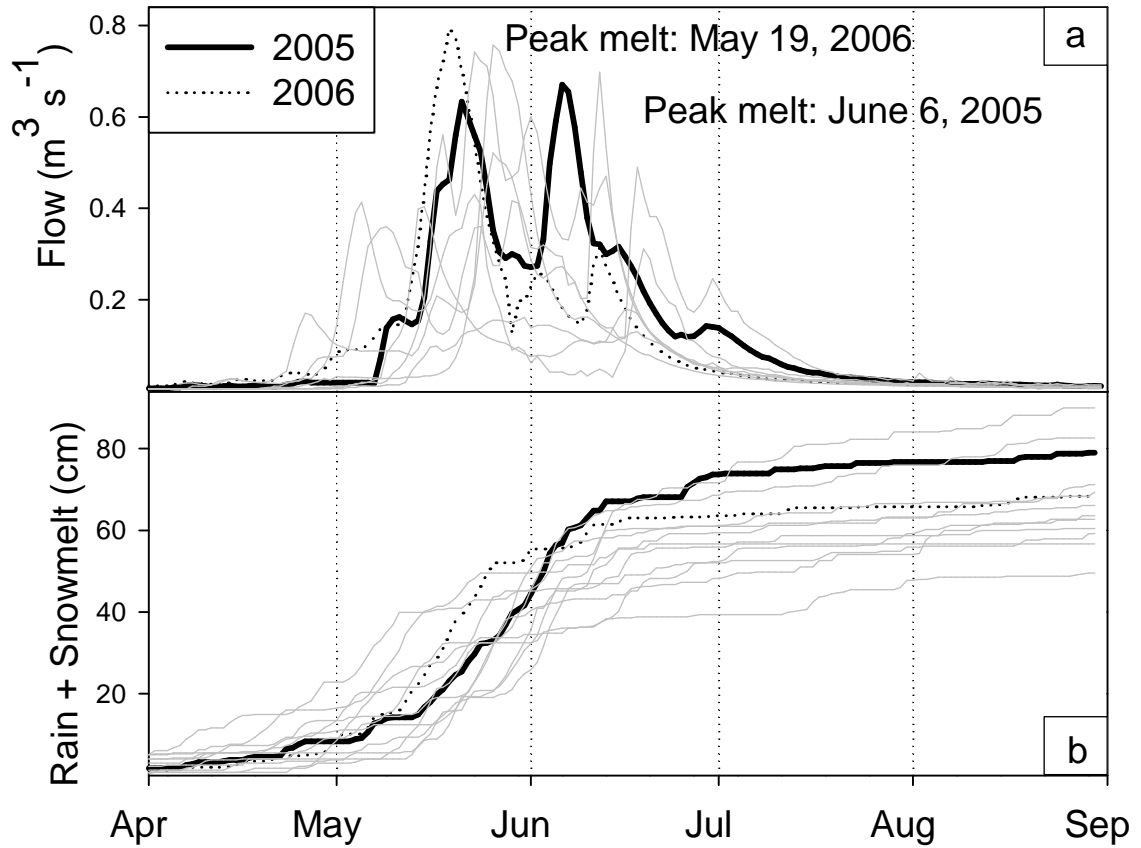


Figure 3.1: Streamflow and cumulative water inputs (rain and snowmelt). a) Streamflow during 2005 (solid line), 2006 (dashed line), and 1997-2006 data record (grey lines). b) cumulative water inputs (rain and snowmelt) during 2005 (solid line), 2006 (dashed line), and 1994-2006 data record (grey lines). Peak snowmelt occurred on June 6 in 2005, and May 19 in 2006 (10-year average was May 29). Cumulative water inputs were slightly higher in 2005 than 2006 (74.4 versus 69.3 cm), however a higher percentage fell as rain during the 2005 growing season (34% versus 20%).

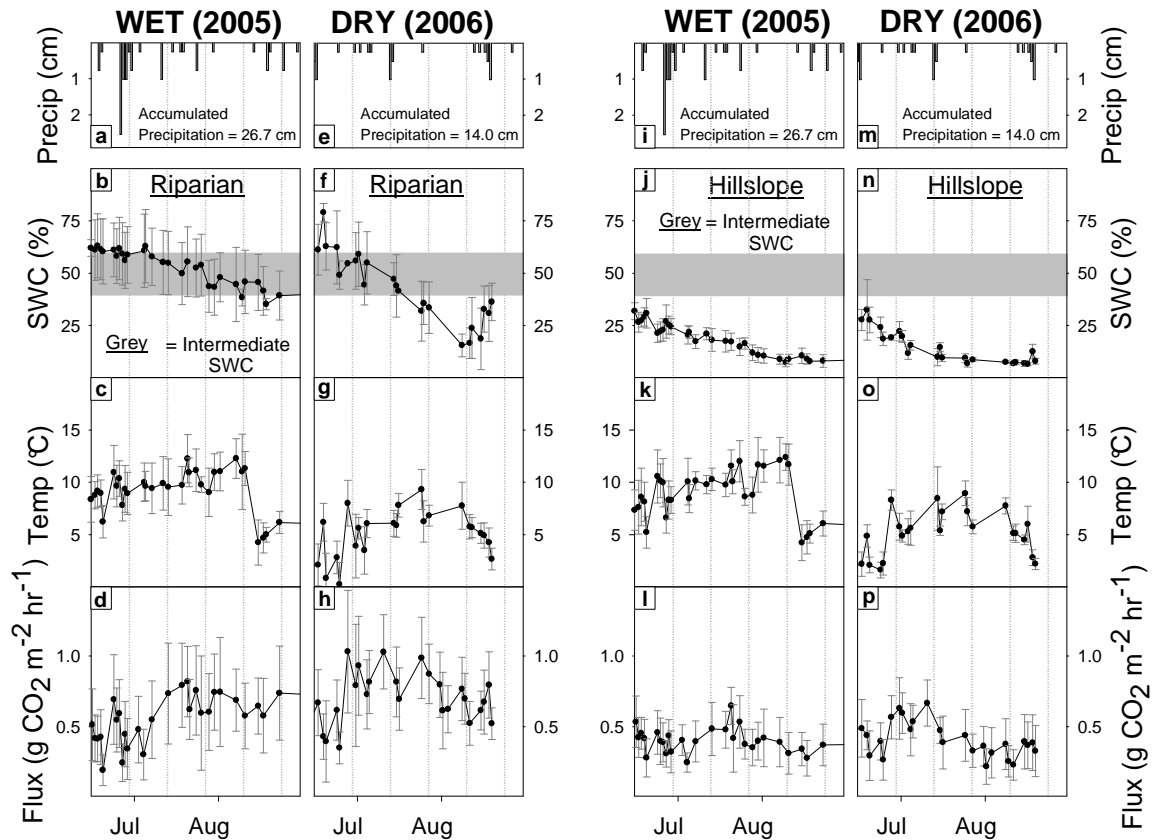


Figure 3.2: Riparian and hillslope precipitation, soil water content (SWC), and soil temperature during the 2005 (wet) and 2006 (dry) growing seasons. a-d: wet growing season riparian zone a) precipitation, b) SWC, c) soil temperature, and d) efflux. e-h: dry growing season riparian zone e) precipitation, f) SWC, g) soil temperature, and h) efflux. i-l: wet growing season hillslope zone i) precipitation, j) SWC, k) soil temperature, and l) efflux. m-p: dry growing season hillslope zone m) precipitation, n) SWC, o) soil temperature, and p) efflux. Measurements were collected between June 9 and August 31 during both 2005 and 2006 from 14 riparian and 18 hillslope measurement locations across 8 transects. Symbols indicate average values, and error bars indicate one standard deviation. n ranged from 8-32 on each sampling day. Across the 2005 and 2006 growing seasons, n = 366 and 252 in the riparian zones, respectively, and 450 and 292 in the hillslopes. Grey boxes denote intermediate SWC (optimal for soil respiration), defined as 40-60% in the TCEF (Pacific et al., 2008). Precipitation was 91% higher in 2005 than 2006.

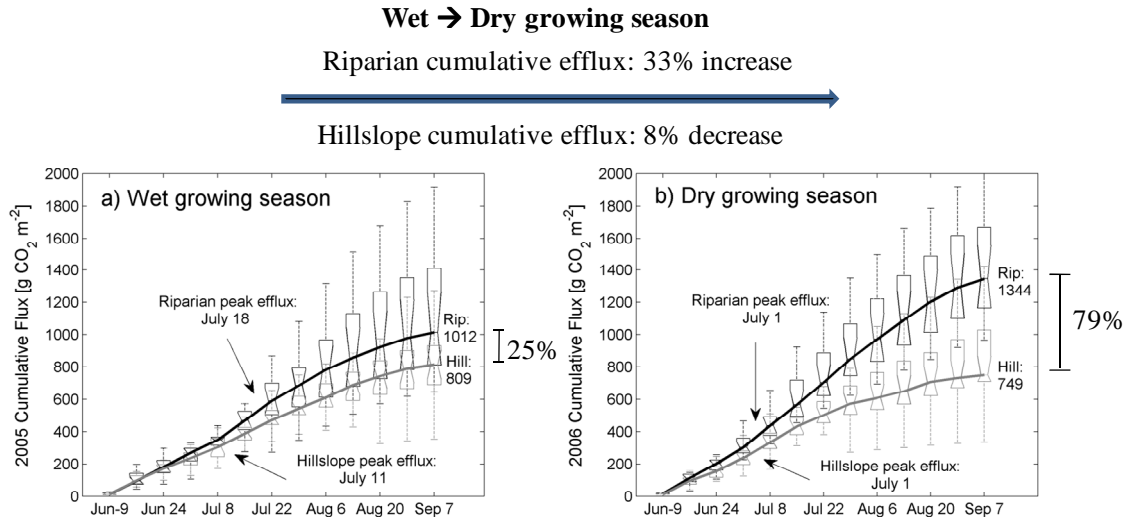


Figure 3.3: Cumulative riparian and hillslope growing season soil CO<sub>2</sub> efflux during the wet and dry growing seasons. Cumulative growing season efflux (measurements collected from June 9 - August 31) at riparian (black) and hillslope (grey) zones during the a) wet growing season (2005) and b) the dry growing season (2006). Boxes represent inter-quartile range, lines denote the cumulative median, and whiskers 1.5 times the inter-quartile range. Measurements are from 14 riparian and 18 hillslope locations across 8 transects. Total number of measurements (n) were 366 and 450 in the riparian and hillslope zones, respectively, in 2005, and 252 and 292 in 2006. The relative difference between riparian and hillslope efflux was 25% in 2005, and 79% in 2006.

## CHAPTER 4

VARIABLE FLUSHING MECHANISMS AND LANDSCAPE STRUCTURE  
CONTROL STREAM DOC EXPORT DURING SNOWMELT IN A SET OF NESTED  
CATCHMENTS

*Adapted from:* Pacific, V. J., K. G Jencso, and B. L. McGlynn (in review) Variable flushing mechanisms and landscape structure control stream DOC export during snowmelt in a set of nested catchments. *Submitted for publication in Biogeochemistry.*

Abstract

Stream DOC dynamics during snowmelt have been the focus of much research, and both one-dimensional (1D) and two-dimensional (2D) DOC export mechanisms have been proposed. However, control by landscape structure on the spatial and temporal variability of these DOC mobilization and delivery mechanisms from the soil to the stream remains poorly understood. We investigated stream, soil, surface, and groundwater DOC dynamics across 3 transects and 7 watersheds with a wide range of landscape settings during snowmelt (April 15 – July 15, 2007) in the U.S. Forest Service Tenderfoot Creek Experimental Forest in the northern Rocky Mountains, Montana. We found that the relative importance of 1D and 2D DOC flushing mechanisms was strongly controlled by landscape position and the degree of hydrologic connectivity between the stream, riparian, and hillslope zones. 1D flushing required a hydrologic connection across the riparian-stream interface, and likely occurred at landscape positions with a wide range of upslope accumulated area (UAA – the amount of land area draining to a particular location) and wetness status (such as at baseflow). In contrast, 2D flushing

appeared restricted to areas with a hydrologic connection across the entire hillslope-riparian-stream continuum, which generally occurred only at areas with high UAA, and/or at times of high wetness (such as at peak snowmelt). Further, the relative amount of DOC-rich riparian and wetland zones strongly influenced stream DOC export. Cumulative stream DOC export was highest from catchments with a large proportion of riparian:upland area, and ranged from 7.8 to 13.3 kg ha<sup>-1</sup> across the study period. This research suggests that the greatest stream DOC export during snowmelt in complex subalpine catchments occurs at areas with both high hydrologic connectivity and large DOC source areas.

### Introduction

Stream DOC export from watersheds is a significant component of the carbon cycle (*Laudon et al.*, 2004a; *Neill et al.*, 2006; *Johnson et al.*, 2006; *Waterloo et al.*, 2006; *Jonsson et al.*, 2007) and can strongly impact contaminant transport (*Imai et al.*, 2003; *Wei et al.*, 2008). In alpine and subalpine catchments, the majority of annual DOC flux often occurs during snowmelt (*Hornberger et al.*, 1994; *Boyer et al.*, 1997, 2000; *Laudon et al.*, 2004a). The process by which DOC is transported to the stream is commonly referred to as hydrologic nutrient flushing, in which solutes undergo a period of accumulation in the soil, and are then released to the stream during snowmelt or precipitation events (*Burns*, 2005). This flushing can lead to a characteristic peak in DOC concentrations on the rising limb of the event stream hydrograph (*Hornberger et al.*, 1994; *Boyer et al.*, 1997; *Hood et al.*, 2006; *van Verseveld et al.*, 2008). However,

the controls on DOC flushing at the hillslope, riparian, and catchment scale are poorly understood (*Weiler and McDonnell, 2006; van Verseveld et al., 2008*).

DOC flushing is often used to describe different, but related processes. At baseflow, stream DOC concentrations are generally low due to groundwater inflows through deep, low DOC mineral soil (Figure 4.1a) (*Hornberger et al., 1994*). However, rise in the groundwater table at the beginning of snowmelt or precipitation events can initiate the flushing process. One flushing mechanism refers to the intersection of a rising water table with shallow DOC-rich riparian soil layers (Figure 4.1b) (*Bishop et al., 1994; Hornberger et al., 1994; Boyer et al., 1997, 2000; Bishop et al., 2004; Laudon et al., 2004b*). This process can be augmented by transmissivity feedback, in which the rising water table enters soils with increasing hydraulic conductivity, leading to increased lateral flow contributions to runoff (*Bishop et al., 2004; Laudon et al., 2004b; Weiler and McDonnell, 2006*). Here, we define this rise of the water table into shallow soils a one-dimensional (1D) process. Often, there is a limited supply of DOC, and 1D flushing can result in decreased DOC concentrations through snowmelt or precipitation events (*Hornberger et al., 1994; Boyer et al., 1997*). More recently, *McGlynn and McDonnell (2003)* proposed a two-dimensional (2D) nutrient flushing mechanism, which is supported by *Bishop et al. (2004)* and *Hood et al. (2006)*. Here, catchment DOC export occurs as a function of the connectivity between near-stream and upland areas (Figure 4.1c), and activation of different source areas can control DOC export and stream concentrations over time. The initial rise in stream DOC concentrations occurs during the 1D rise of the water table into shallow organic-rich riparian soils. A second source of

high DOC on the rising limb of the stream hydrograph occurs as hillslopes become hydrologically connected to the riparian zones, allowing for quick transmission of hillslope water that is rich in DOC (*Bishop et al.*, 2004) along preferential flow paths (*McGlynn and McDonnell*, 2003). This high DOC initial hillslope runoff is then diluted with lower DOC matrix water, which can lead to lower stream DOC concentrations on the falling limb of the stream hydrograph (*McGlynn and McDonnell*, 2003).

We suggest that both 1D and 2D flushing mechanisms can influence the export of DOC from the soil to the stream, but that their relative importance shifts through space and time. For example, it is likely that rapid 1D flushing occurs in riparian areas at the initiation of snowmelt, resulting in an important early near-stream source of DOC (*Boyer et al.*, 1997). However, as uplands become hydrologically connected to riparian zones, 2D flushing can be initiated, thereby increasing the relative importance of upland nutrient sources (*McGlynn and McDonnell*, 2003; *Inamdar and Mitchell*, 2006; *Ocampo et al.*, 2006a, b). We suggest that in high elevation, snowmelt-dominated catchments, the relative control of 1D and 2D processes on stream DOC export can vary strongly through space and time and is largely dependent upon the degree of hydrologic connectivity between the stream and the riparian and hillslope zones, which is influenced by landscape structure (*Jencso et al.*, 2009).

Following *Jencso et al.* (2009), we define hydrologic connectivity as the time period when a groundwater connection exists between landscape elements (e.g. stream, riparian, and hillslope zones). For 1D flushing to occur, a hydrologic connection between the riparian zone and stream (RS) is necessary. However, 2D flushing requires a

hydrologic connection across the hillslope-riparian-stream (HRS) continuum (Figure 4.1c). Through a combination of extensive groundwater monitoring (> 120 recording groundwater wells) and landscape level topographic analysis, *Jencso et al.* (2009) found that the duration and timing of HRS hydrologic connectivity was a function of toeslope upslope accumulated area (UAA) - the amount of land area draining to a particular location. They found a strong positive relationship between HRS hydrologic connectivity and UAA ( $r^2 = 0.91$ ), with the highest and most persistent HRS hydrologic connectivity at landscape positions with large UAA. Here, we seek to investigate the relationship between landscape position and hydrologic connectivity on the spatial and temporal variability of DOC flushing mechanisms during snowmelt in a subalpine catchment in the northern Rocky Mountains. We present stream, soil, surface, and groundwater DOC dynamics during snowmelt (April 15 – July 15, 2007) across three transects and 7 sub-catchments with a range of landscape settings and hydrologic connectivity to address the following questions:

1. What are the dominant DOC mobilization and stream delivery mechanisms during snowmelt, and how do they vary with respect to landscape setting?
2. What is the spatial extent/frequency of dominant landscape settings, and what does this mean for DOC export at the catchment scale?

## Methods

### Site Description

The study site was the upper Tenderfoot Creek Watershed (2,280 ha), located within the U.S. Forest Service (USFS) Tenderfoot Creek Experimental Forest (TCEF)

(lat. 46°55' N., long. 110°52' W.) in the Little Belt Mountains of central Montana (Figure 4.2). Tenderfoot Creek drains into the Smith River, a tributary of the Missouri River. Elevation ranges from 1,840 to 2,421 m, with a mean of 2,205 m. Mean annual precipitation is 880 mm, with ~70% falling as snow from November through May (*Farnes et al.*, 1995). Monthly precipitation peaks in December or January (100 to 120 mm per month), and declines to 45 to 55 mm per month from July through October. Tenderfoot Creek runoff averages 250 mm per year, with peak flows typically in late May or early June. Mean annual temperature is 0°C, and mean daily temperatures range from -8.4°C in December to 12.8°C in July (*Farnes et al.*, 1995).

The geology is characterized by granite gneiss, shales, quartz porphyry, and quartzite (*Farnes et al.*, 1995). In the hillslopes, the major soil group is loamy skeletal, mixed Typic Cryochrepts, while the riparian zones are composed of mixed Aquic Cryoboralfs (*Holdorf*, 1981). Soil depths range from 0.5-1m in the hillslopes, and 1-2.0 m in the riparian zones (*Jencso et al.*, 2009).

Riparian vegetation is dominated by sedges (*Carex* spp.) and rushes (*Juncaceae* spp.) in the headwaters, where riparian soil is high in organic matter and fine silt and clay textured, and water tables are at or near the soil surface (*Jencso et al.*, 2009). In riparian areas with deeper water tables and coarsely textured soils, Willows (*Salix* spp.) are often present. In the uplands, Lodgepole pine (*Pinus contorta*) is the dominant overstory vegetation (*Farnes et al.*, 1995), and Grouse whortleberry (*Vaccinium scoparium*) primarily composes the understory vegetation (*Mincemoyer and Birdsall*, 2006).

There are 7 gauged sub-catchments in the TCEF. In general, all catchments have a gradual slope near the headwaters, with much steeper slopes near the catchment outlets. Middle Stringer Creek (MSC, 393 ha) and Lower Stringer Creek (LSC, 550 ha) have an intermediate amount of riparian and wetland area, and a median slope of 9°. Sun Creek (SC, 352 ha) is characterized by gentle slopes (median of 5.4°) and large seeps and wetland areas at the headwaters. Bubbling Creek (BC, 309 ha) also has gentle slopes (median of 5.8°), and a relatively small amount of riparian and wetland area. Spring Park Creek (SPC, 400 ha) has an extensive riparian and wetland area at the headwaters and steep slopes near the catchment outlet (median of 9.6°). Upper Tenderfoot Creek (UTC, 446) also has a large network of wetlands at the headwaters, and a median slope of 6.5°. Lower Tenderfoot Creek (LTC, 2260 ha) has an intermediate amount of wetland area, and moderate slopes (7.2°). The Stringer Creek Watershed (Middle and Lower) was utilized for more intensive data collection and divided into 4 sub-catchments for data analysis. These sub-catchments were the headwaters to Transect 1 (131 ha), Transect 1 to MSC (261.5 ha), MSC to Transect 5 (92.2 ha), and Transect 5 to LSC (68.2 ha). A description of the transects is provided below.

### Terrain Analysis

An ALSM (airborn laser swath mapping, commonly known as LIDAR, courtesy of the National Center for Airborn Laser Mapping - NCALM) derived 10 m digital elevation model (DEM) was used to calculate UAA (amount of land area draining to a particular location, calculated for the toeslope well position at the transition from hillslope to riparian zone) and slope (average slope along the fall line from the highest

hillslope location to the toeslope along each transect). Toeslope UAA was calculated using a triangular multiple flow-direction algorithm following the methods of *Seibert and McGlynn (2007)* and *Jencso et al. (2009)*. Riparian zone width was mapped with a GPS survey (Trimble GPS 5700 receiver - accurate to within 1-5 cm) and corroborated with the ALSM-derived DEM analysis (*Jencso et al., 2009*). The riparian-hillslope boundary was determined in the field, based upon break in slope and change in soil characteristics (depth, gleying, organic matter accumulation, texture) (*McGlynn and Seibert, 2003; Seibert and McGlynn, 2007; Pacific et al., 2008; Jencso et al., 2009*). See *Jencso et al. (2009)* for a more detailed description of terrain analyses in the TCEF. We calculated the percentage of time that HRS hydrologic connectivity existed by dividing the total number of days that a groundwater table was present along the HRS continuum by the total snowmelt period (91 days) (*Jencso et al., 2009*). For this study, we define the snowmelt period as April 15 to July 15, 2007, which bracketed pre-snowmelt, snowmelt, and the recession to baseflow ( $\sim 0.01 \text{ mm hr}^{-1}$ ) (Figure 3).

### Measurement Locations

This research was conducted concurrently with other research objectives and included locations and instrumentation both universal and specific to this study (*Pacific et al., 2008; Pacific et al., in review a, b; Riveros-Iregui et al., 2008, 2009, in review; Jencso et al., 2009*). Measurements were collected at the outlets of each of the sub-catchments within the TCEF (MSC, LSC, SPC, BC, SC, UTC, and LTC), as well as at Onion Park (headwaters of Tenderfoot Creek). In addition, 14 transects were located in the Stringer Creek Watershed, and 8 in the Tenderfoot Creek Watershed (Figure 4.2).

Three transects within the Stringer Creek Watershed were utilized for intensive monitoring in this study because they represented the range of landscape settings observed at TCEF. The Stringer Creek transects were located in 7 pairs, with each pair consisting of one transect on both the east (E) and west (W) side of Stringer Creek, which flows from the north to the south. The transects were numbered sequentially from upstream to downstream, followed by an E or W, designating the east or west side of Stringer Creek. On each transect, measurement locations were then designated with a number, with 1 being closest to the stream, and the highest number representing the location farthest up in the hillslope. Therefore, ST1-E1 refers to the riparian measurement location next to the creek on the east side of Transect 1. For this study, measurements were collected on ST1-E and ST1-W (most upstream transects, at the headwaters of the Stringer Creek), and ST5-W (just below the middle of the watershed).

#### Hydrometric Monitoring

Groundwater levels were recorded at 3-4 groundwater monitoring wells at each of the 3 focus transects along Stringer Creek. Wells were located in the riparian zone (1 m from stream channel), near the toe-slope (the transition point between the riparian and hillslope zone), and on the lower hillslope (1-5 m above the break in slope). The wells consisted of 3.8 cm (1.5 inch) inside-diameter PVC, screened across the completion depth (to bedrock) to 10 cm below the ground surface. Completion depths ranged from 0.5-1 m in the hillslopes and 1-1.5 m in the riparian zones. Groundwater levels were recorded every 30 min with water level capacitance rods (Trutrack, Inc.,  $\pm 1$  mm resolution). Capacitance rod measurements were corroborated with manual weekly

measurements using an electric water level tape. Soil tension lysimeters were installed at 20 and 50 cm depth at toeslope and lower hillslope positions on ST1-E and ST1-W and were constructed of a 3.8 cm (1.5 inch) inside-diameter PVC case attached to a porous ceramic cup (1 bar entry, Soilmoisture Equipment Corporation). The lysimeters were installed with a hand auger to the depth of interest, placing the lysimeter in a soil slurry made from native material. The lysimeters were in place and frequently vacuumed (to -0.35 bars) and purged over 9 months prior to this study. Overland and 10 cm flow cups were installed at all riparian measurement locations. The cups were constructed from 500 mL high-density polyethylene (HDPE) bottles, open at the top for surface flow, and with holes drilled to the depth of interest for 10 cm measurements.

Stream discharge was measured at flumes at the outlet of each of the 7 catchments. Stage at each flume was recorded at 15 min intervals with float potentiometers (installed and maintained by the USFS) and water level capacitance rods (Trutrack, Inc.,  $\pm 1$  mm resolution). Stage was also measured at the outlet of Onion Park, at the headwaters of Tenderfoot Creek. However, discharge could not be calculated as no flume was installed. Hourly measurements of precipitation, air temperature, snow depth, and snow water equivalent (SWE) were obtained from two Natural Resource Conservation Service snow survey telemetry (SNOTEL) stations located in TCEF, one at Onion Park (2,259 m, within 2 km and at approximately the same elevation as the headwaters of Stringer Creek), and one at LSC (1,996 m).

### Water Sampling

Water samples for DOC analysis were collected in 250 ml HDPE bottles. Samples were collected approximately every 2-4 days from the flumes during high flows (beginning of May through the beginning of June) as well as from the outlet of Onion Park, which flows into the headwaters of Tenderfoot Creek. Weekly samples were collected for the weeks before and after this time period. Water samples were collected from wells and lysimeters (when water was present) along each transect every 3-7 days. Wells, soil lysimeters, and 10 cm and surface cups were purged until dry the day before sampling occurred. Soil lysimeters were vacuumed to -0.35 bars after purging. The water samples were passed through a 0.45  $\mu\text{m}$  filter into 30 ml amber high density polyethylene (HDPE) bottles within 1-12 hours of collection (dependent upon location and time of sampling). Each sample was acidified to pH 1- 2 with 6N HCl, kept in a cooler during transport to Montana State University (MSU), and then frozen at - 20°C until analysis.

### DOC Analysis

Total DOC was analyzed with a high-temperature combustion technique at the MSU Watershed Hydrology Analytical Facility using a Shimadzu TOC-V C-analyzer (Shimadzu Corp., Kyoto, Japan). The instrument was calibrated at the beginning of every run with 3-5 standards ranging from 0.10 to 10.0 mg C L<sup>-1</sup> (prepared from reagent grade potassium hydrogen phthalate). Method detection limits were 0.1 mg L<sup>-1</sup>, and analytical precision was within 0.05 mg L<sup>-1</sup>.

### Cumulative DOC Export

We calculated cumulative stream DOC export for the 7 sub-catchments of the Tenderfoot Creek Watershed, and the 4 sub-catchments within the Stringer Creek Watershed. Daily stream DOC concentrations were estimated with linear interpolation between actual field measurements, and cumulative export was calculated for the 91-day study period (April 15 - July 15, 2007). Cumulative stream DOC export for each sub-catchment within the Stringer Creek Watershed was estimated with the stream DOC concentration and discharge at that sub-catchment outlet after subtracting the contribution from the upstream catchments. To aid in comparison with other studies, we also estimated annual stream DOC export for the Stringer Creek Watershed. For the time outside of our study period of April 15 to July 15, 2007, we used a baseflow DOC concentration of  $1.6 \text{ mg L}^{-1}$ , as measured before and after the snowmelt period.

## Results

### Landscape Analysis

Along the transects within the Stringer Creek Watershed, there were large differences in toeslope UAA, HRS hydrologic connectivity, riparian width, and slope (Table 4.1). ST5-W had the largest UAA, widest riparian zone, and steepest hillslope. Riparian zone width and steepness of the hillslope were similar on ST1-E and ST1-W, but UAA was higher on ST1-E. Within the 4 sub-catchments in the Stringer Creek Watershed, there were differences in the proportion of riparian to upland area. In the area between ST1 and MSC, the riparian zone comprised 3.79% of the catchment area. In the other sub-catchments, this value ranged from 1.3 to 1.42% (Table 4.2). The percentage

of the stream channel that had HRS hydrologic connectivity across the entire study period (April 15 – July 15) was similar across each sub-catchment in the Stringer Creek Watershed, ranging from 69-79% (Table 4.2). For the sub-catchments within the Tenderfoot Creek Watershed, there was also a wide range in the proportion of riparian:upland area (Table 3). In general, SC, BC, LSC had a small proportion of riparian:upland area (1.73-2.98%), MSC and LTC had an intermediate proportion (3.09-3.86%), and UTC and SP a high proportion of riparian:upland area (5.33-6.08%).

#### Snowmelt and Precipitation

We present SWE and precipitation data from the Onion Park SNOTEL site (Figure 3a, also shown in Figures 4-6) because it represents the elevation and biophysical variables most reflective of the greater TCEF. SWE peaked at 358 mm on April 20, 2007. The majority of the snowpack melted between April 27 and May 19, with average daily SWE losses of 15 mm and a maximum of 35 mm on May 13, 2007 (*Jencso et al.*, 2009). A late spring snowfall event and subsequent melting between May 24 and June 1 yielded an additional 97 mm of water. Four days after the end of snowmelt, a series of rain events occurred (June 4-7, and June 13-18, Figure 2), totaling 30 and 22 mm, respectively.

#### Transect Water Table Dynamics and DOC Concentrations

ST1-East: This transect had transient HRS hydrologic connectivity (totaling 38% of the study period) and both 1D and 2D flushing mechanisms were evident.

*ST1-E1 (riparian zone, next to stream)*: the groundwater table was ~20 cm below the ground surface at the beginning and end of the snowmelt period, but remained within 10 cm of the ground surface from the beginning of May to the end of June (Figure 4.3b). Well DOC concentrations were ~3 mg L<sup>-1</sup> throughout snowmelt, but briefly declined to 0.7 mg L<sup>-1</sup> on May 14 coincident with the rise in the water table. Riparian overland flow was present on sampling events between May 9 and June 12, concurrent with stream peak discharge, and DOC concentrations ranged from 3.7 to 6 mg L<sup>-1</sup>. Similar DOC concentrations were observed in the 10 cm flow cups during the same time period, with slightly greater fluctuations than in the surface water.

*ST1-E2 (riparian zone, near toeslope)*: the groundwater table quickly developed on April 25 and reached the ground surface by May 2 (Figure 4.3c). It remained within 10 cm of the ground surface until May 13, and then declined to 33 cm by May 25. The water table then quickly rose to 5 cm below the ground surface on May 28, at which point it began a slow decline to 85 cm by the middle of July. Well DOC concentrations were relatively stable at ~2 mg L<sup>-1</sup> until the end of May. Here, DOC concentrations increased coincident with the rise in the water table at the end of May, peaked at 3.4 mg L<sup>-1</sup> on June 12 during the recession to baseflow, then remained at ~3 mg L<sup>-1</sup> throughout the rest of the study period. Similar DOC concentrations were observed at the 50 cm lysimeter. Water was never present in the 20 cm lysimeter, which was likely the result of a crack or poor seal.

*ST1-E3 (hillslope zone)*: the transient groundwater table was initiated at the end of April and rose to 50 cm below the ground surface on May 5, then declined to 70 cm by

May 7 (Figure 4.3d). A second rise (to 30 cm below the ground surface) occurred on May 10, followed by a quick decline and cessation of the transient water table by May 20. On May 26, the water table rapidly rose to 30 cm below the ground surface and remained there for an 8 day period, then was not evident for the remainder of the study. During the initial water table rise, peak well and 50 cm lysimeter DOC concentrations were measured (5.8 and 7.3 mg L<sup>-1</sup>, respectively), then declined to approximately half that value by the middle of May. Increased DOC concentrations were measured on June 2, just after the final rise in the water table. Water was never present in the 20 cm lysimeter (likely a crack or poor seal).

ST1-West: This transect never developed a hydrologic connection across the HRS continuum (0% HRS connectivity) and it is likely that only 1D flushing occurred.

*ST1-W1 (riparian zone, next to the stream)*: the groundwater table was 17 cm below the ground surface at the beginning of snowmelt and rose to within 1 cm by May 5, when the peak well DOC concentration of 4.2 mg L<sup>-1</sup> was measured (Figure 4.4b). The water table then declined to 15 cm below the ground surface by May 8, and DOC concentrations declined to ~2.2 mg L<sup>-1</sup>, where they remained until the beginning of June. Concentrations declined to ~1.5 mg L<sup>-1</sup> by the middle of June concurrent with the gradual decline in the water table, where they remained until the end of the study period. Water was present in the 10 cm cup on only May 13, and had a DOC concentration of 5 mg L<sup>-1</sup>. Overland flow was present on the June 2 and June 12 sampling events, with DOC concentrations of ~6 mg L<sup>-1</sup>.

*ST1-W2 (riparian zone, near toeslope)*: Groundwater table dynamics were similar to that observed at ST1-W1. The water table was 15 cm below the ground surface at the beginning of snowmelt, and then rose to within 1 cm by April 28 (Figure 4.4c). It remained within 7 cm of the ground surface until the middle of June, and then gradually declined to 30 cm below the ground surface by the middle of July. At the beginning of the water sampling period, the DOC concentration was  $2.7 \text{ mg L}^{-1}$ , then peaked at  $4.2 \text{ mg L}^{-1}$  on May 5 following the rise in the water table. DOC concentrations fluctuated between  $\sim 2\text{-}3 \text{ mg L}^{-1}$  for the remainder of the snowmelt period. Similar DOC concentrations and temporal trends were observed in both the 20 and 50 cm soil lysimeters, although concentrations were  $\sim 1 \text{ mg L}^{-1}$  higher at the 20 cm lysimeter on all sampling events.

*ST1-W3 (hillslope)*: the water table never developed above the bedrock interface (100 cm below the ground surface) (Figure 4.4d).

ST5-West. This transect had 100% HRS hydrologic connectivity for the duration of this study and it is likely that the relative control of the 2D flushing on DOC export to the stream was high.

*ST5-W1 (riparian zone, next to stream)*: the groundwater table fluctuated between 50 and 60 cm below the ground surface for the duration of the snowmelt period (Figure 4.5b). In contrast, DOC concentrations were highly variable. Near the beginning of snowmelt, a DOC concentration of  $6.4 \text{ mg L}^{-1}$  was measured on May 4, and then quickly declined to a minimum concentration of  $1.7 \text{ mg L}^{-1}$  on May 9, coincident with the rise in

stream discharge. Concentrations then quickly increased and reached a maximum of  $7 \text{ mg L}^{-1}$  on May 25. Following a large decline in streamflow, DOC concentrations remained between  $5.5$  and  $7 \text{ mg L}^{-1}$  for the rest of the study period. Surface water was present between May 18 and July 9, with a peak DOC concentration of  $5.2 \text{ mg L}^{-1}$  on May 18 following the peak in streamflow, and then gradually declined to  $2.4 \text{ mg L}^{-1}$  on July 9.

*ST5-W2 (riparian zone, between the stream and the toeslope):* the groundwater table fluctuated between 20 and 30 cm below the ground surface for the majority of the snowmelt period, with 2-3 day peaks to 3 cm on ~May 2, May 10, and May 29 (Figure 4.5c). During the first sampling event on May 2, a DOC concentration of  $22 \text{ mg L}^{-1}$  was measured (note the difference in scale on the y-axis:  $0-25 \text{ mg L}^{-1}$ , compared to  $0-8 \text{ mg L}^{-1}$  at all locations other than ST5-W3), then declined by over an order of magnitude to  $1.5 \text{ mg L}^{-1}$  by May 9 coincident with peak discharge. DOC concentrations then increased to  $\sim 20 \text{ mg L}^{-1}$  by May 25 as discharge declined, where they remained for the remainder of snowmelt.

*ST5-W3 (riparian zone, near the toeslope):* the groundwater table was 10 cm below the ground surface at the beginning of snowmelt, then rose to within 3 cm by the end of April, where it remained for the remainder of the measurement period (note that water table measurements ended on June 23 due to equipment malfunction) (Figure 4.5d). Peak groundwater DOC concentrations ( $11 \text{ mg L}^{-1}$  – note the change in scale) were measured on May 2 coincident with the initial rise in the water table. Concentrations

gradually decreased to a minimum of  $5.4 \text{ mg L}^{-1}$  on May 25, then remained at  $\sim 7 \text{ mg L}^{-1}$  for the remainder of snowmelt.

*ST5-W4 (hillslope zone)*: the groundwater table was 10 cm below the ground surface at the beginning of snowmelt, and remained between 3 and 10 cm below the ground surface for the duration of the study period (Figure 4.5e). DOC concentrations were high at the beginning of snowmelt ( $6.5 \text{ mg L}^{-1}$ ), then declined as discharge decreased. When discharge increased at the beginning of May, DOC concentrations continued to decline, and reached a minimum of  $3.5 \text{ mg L}^{-1}$  by May 18. The DOC concentration rose to  $5.8 \text{ mg L}^{-1}$  by May 25 following the decrease in stream discharge, then remained between  $\sim 4$  and  $5 \text{ mg L}^{-1}$  for the remainder of the study period.

#### Stream Discharge and DOC Dynamics

Stream Discharge: Area-normalized stream discharge during our study period of April 15 – July 15, 2007 (which bracketed pre-snowmelt, snowmelt, and recession to baseflow:  $\sim 0.01 \text{ mm hr}^{-1}$ ) from LSC is shown in Figures 4.3-4.5 (water table and DOC dynamics from each of the individual transects), as well as Figures 4.6 and 4.8. Stream discharge from all catchments is presented in Figure 4.10. In general, stream discharge from all catchments had similar temporal dynamics. The lowest discharge was measured at SC, and the highest at LSC, with intermediate values at the other catchments. The first peak in discharge followed the initiation of snowmelt and occurred between May 3 and May 6 throughout all catchments, and ranged from  $0.18 \text{ mm hr}^{-1}$  at SC to  $0.43 \text{ mm hr}^{-1}$  at LSC (Figure 4.10). Stream discharge then declined to approximately half of that

measured at the initial peak as snowmelt slowed in response to a period of cold weather, where maximum temperatures remained below 5°C (compared to ~18°C during the previous week, as measured at the Onion Park SNOTEL site). Discharge then quickly increased, and peak flow occurred in all catchments between May 10 and May 14 (Figure 4.10). Maximum discharge ranged from 0.35 mm hr<sup>-1</sup> at SC to 0.55 mm hr<sup>-1</sup> at LSC. As soil water inputs from snowmelt decreased (black bars in Figure 4.2a), stream discharge declined to ~0.1-0.2 mm hr<sup>-1</sup> by May 25 in all catchments. A final snowfall event and subsequent melt occurred between May 24 and June 1, leading to a third and final peak in discharge during this time, which ranged from 0.20 mm hr<sup>-1</sup> at SC to 0.45 mm hr<sup>-1</sup> at LSC (Figure 4.10). Stream discharge then began the final snowmelt recessional period.

#### Stream DOC Concentrations.

*Stringer Creek:* DOC concentrations were highly variable along Stringer Creek (Figure 4.8). At ST1, near the headwaters, DOC concentrations were relatively stable at ~1.8 mg L<sup>-1</sup>, but rose to 2.5 mg L<sup>-1</sup> on May 5 associated with the first snowmelt-driven peak in stream discharge (Figure 4.8a). DOC concentrations then declined during the first streamflow recession, and continued to decline during the second rise in stream discharge near the middle of May (reaching a minimum concentration of 1.6 mg L<sup>-1</sup>). Stream DOC concentrations at ST1 increased during the third and final rise in discharge, and continued to rise during the recession to baseflow, with a peak concentration of 2.6 mg L<sup>-1</sup> on June 9.

At MSC, located between ST1 and ST5, stream DOC concentrations were more variable (Figure 4.8b). A baseflow concentration of 1.4 mg L<sup>-1</sup> was measured at the end

of April. DOC concentrations nearly doubled by May 2, associated with the first snowmelt-driven peak in discharge. Concentrations remained high until May 15, when they began to decline coincident with the decrease in runoff, and reached a minimum value of  $1.0 \text{ mg L}^{-1}$  on May 23. DOC concentrations then sharply increased, reaching a maximum of  $3.2 \text{ mg L}^{-1}$  by the beginning of June concurrent with the third snowmelt stream discharge peak. Concentrations remained at  $\sim 2.5 \text{ mg L}^{-1}$  throughout June, and then returned to the baseflow concentration of  $1.4 \text{ mg L}^{-1}$  by the beginning of July (Figure 4.8b).

At ST5, a peak streamflow DOC concentration of  $3.5 \text{ mg L}^{-1}$  was measured during the first sampling event on April 26 (Figure 4.8c). DOC concentrations then quickly declined to  $0.9 \text{ mg L}^{-1}$  by May 14, coincident with the peak in stream discharge. A sharp rise to  $2.5 \text{ mg L}^{-1}$  occurred on May 18 as discharge decreased. Stream DOC concentrations then declined to a minimum value of  $0.6 \text{ mg L}^{-1}$  on May 25, concurrent with the decrease in discharge at the end of May. By June 12, concentrations rose to  $2.1 \text{ mg L}^{-1}$  following the rise in stream discharge after the late-spring snow event, and then decreased to  $1.5 \text{ mg L}^{-1}$  by the middle of July during the recession to baseflow. Note that stream DOC concentrations are not available for the June 2 and June 9 sampling events (Figure 4.8c).

Stream DOC concentrations at LSC (catchment outlet), were  $2.4 \text{ mg L}^{-1}$  on the first sampling date at the end of April, rose slightly, and then declined to  $1 \text{ mg L}^{-1}$  by May 12, just before the peak in stream discharge (Figure 4.8d). A brief rise to  $2.1 \text{ mg L}^{-1}$  occurred on May 14 (at peak discharge), then concentrations returned to

1 mg L<sup>-1</sup> by the end of May as discharge decreased. DOC concentrations at LSC then quickly increased coincident with the rise in discharge at the end of May, and reached a peak of 3.3 mg L<sup>-1</sup> at the beginning of June. Stream DOC concentrations fluctuated between 2 and 3 mg L<sup>-1</sup> throughout June. DOC concentrations then declined during the recession to baseflow and reached 1.6 mg L<sup>-1</sup> by the middle of July (Figure 4.8d).

*Tenderfoot Creek:* DOC concentrations were also variable along Tenderfoot Creek. At Onion Park, which drains a large network of wetlands near the headwaters of Tenderfoot Creek, DOC concentrations were relatively high (Figure 4.6). Note that relative stage height and not discharge is shown at the outlet of Onion Park, as a flume was not installed here, and therefore no rating curve was available. While high DOC concentrations were observed during the early rise in flow (~4 mg L<sup>-1</sup>), peak concentrations were not measured until the beginning of June, following the peak in flow. DOC concentrations then decreased coincident with the decline in flow, and reached a minimum value of 1.1 mg L<sup>-1</sup> on July 9 (Figure 4.6).

At UTC, DOC concentrations were also high (Figure 4.10). The stream DOC concentration was ~3 mg L<sup>-1</sup> at the beginning of snowmelt, then increased by over 100% on the rising limb of the stream hydrograph. DOC concentrations fluctuated between 4 and 7 mg L<sup>-1</sup> until the beginning of June, when concentrations quickly declined coincident with the recession to baseflow, and reached a minimum of 2.1 mg L<sup>-1</sup> on July 9 (Figure 4.10). At LTC, a similar trend was observed, however DOC concentrations were approximately half that measured at UTF and generally fluctuated between 2 and 4 mg L<sup>-1</sup> (but decreased to 0.8 mg L<sup>-1</sup> on May 23 following the large

decline in discharge). The largest DOC concentration was measured on the falling limb of the last peak in discharge near the beginning of June.

*Spring Park Creek:* DOC concentrations were relatively low and similar to those measured at MSC and LSC (Figure 4.10). Concentrations generally fluctuated between 2 and 3 mg L<sup>-1</sup> throughout snowmelt, but declined to ~1 mg L<sup>-1</sup> on both the rising and falling limb of the peak in stream discharge at the middle of May.

*Sun Creek:* Relative to other catchments, stream DOC concentrations were high (Figure 4.10). At the beginning of snowmelt, a DOC concentration of 4 mg L<sup>-1</sup> was measured, followed by a quick rise to a peak concentration of 7 mg L<sup>-1</sup> on the rising limb of the initial peak in stream discharge. DOC concentrations declined to 2.8 mg L<sup>-1</sup> following the decline in peak discharge at the middle of May. DOC concentrations then remained at ~ 5 mg L<sup>-1</sup> until the beginning of June, when they decreased during the recession to baseflow, reaching a minimum of 2.5 mg L<sup>-1</sup> by the end of the study period (Figure 4.10).

*Bubbling Creek:* DOC concentrations were stable and remained between 3 and 4 mg L<sup>-1</sup> for the majority of the study period (Figure 4.10). A peak concentration of 5 mg L<sup>-1</sup> was measured at the beginning of May coincident with the rise in discharge at the beginning of snowmelt, and a minimum concentration of 2.3 mg L<sup>-1</sup> was measured at the end of the study period as the stream receded to baseflow (~1 mm hr<sup>-1</sup>) (Figure 4.10).

### Cumulative Stream DOC Export

During the study period of April 15 to July 15, 2007, cumulative stream DOC was high for the ST1-MSD sub-catchment ( $13.3 \text{ kg ha}^{-1}$ ), and ranged from  $7.3$  to  $8.7 \text{ kg ha}^{-1}$  at the other sub-catchments (Table 4.2, Figure 4.8e-f). For the larger sub-catchments of the Tenderfoot Creek Watershed, cumulative stream DOC export over the study period ranged from  $8.1$  to  $12.4 \text{ kg ha}^{-1}$  (Table 4.3). For the entire Stringer Creek Watershed, cumulative stream DOC for the 2007 water year was  $9.6 \text{ kg ha}^{-1}$ . There was a strong positive relationship ( $r^2 = 0.62$ ,  $p < 0.001$ ) between cumulative stream DOC export and the proportion of riparian to upland area across all sub-catchments (Figure 4.9).

### Discussion

#### What are the Dominant DOC Mobilization and Stream Delivery Mechanisms during Snowmelt, and how do they Vary with Respect to Landscape Setting?

Hydrologic flushing is commonly referred to as the mobilization process that leads to a large release of DOC to the stream channel during snowmelt or precipitation events (Burns, 2005), which often occurs on the rising limb of the stream hydrograph (Hornberger *et al.*, 1994; Boyer *et al.*, 1997; Inamdar *et al.*, 2004; Agren *et al.*, 2008; van Verseveld *et al.*, 2008). Both 1D and 2D nutrient flushing mechanisms have been proposed. In the 1D mechanism, a rising water table intersects shallow nutrient rich soil in the riparian zone (Figure 4.1b) (Hornberger *et al.*, 1994; Bishop *et al.* 1994; Boyer *et al.*, 1997, 2000; Laudon *et al.*, 2004b). In general, the riparian zone is the only DOC source area for export to the stream during 1D flushing. In contrast, upland DOC sources become increasingly important during 2D flushing as a hydrologic connection develops

between the riparian and the hillslope zone (Figure 4.1c) (*McGlynn and McDonnell, 2003; Bishop et al., 2004; Hood et al., 2006*). It is likely that both 1D and 2D flushing mechanisms occur during snowmelt, but that the relative control of each process on DOC export changes through space and time. We suggest these changes in DOC export mechanisms are strongly influenced by the timing and magnitude of riparian-stream (RS) and hillslope-riparian-stream (HRS) hydrologic connectivity. To investigate DOC mobilization and delivery mechanisms during snowmelt and the control of landscape structure, we collected measurements of DOC and stream and groundwater dynamics across 3 transects and 7 sub-catchments with distinct differences in landscape setting and RS and HRS hydrologic connectivity.

We observed both 1D and 2D flushing mechanisms in the subalpine, snowmelt dominated Stringer Creek Watershed, the occurrence of which was dependent upon landscape setting (toeslope UAA and riparian and wetland extent) and the degree of hydrologic connectivity. Our results suggest that 1D flushing likely occurred across the full range of landscape settings and hydrologic connectivity (both RS and HRS). In contrast, 2D flushing appeared restricted to only landscape settings with hydrologic connectivity across the entire HRS continuum. These areas generally had relatively high toeslope UAA (*Jencso et al., 2009*).

Our comparisons of DOC dynamics across 3 transects within the Stringer Creek Watershed illustrate the control of landscape structure on DOC export to the stream. ST1-W has a small toeslope UAA (1,563 m<sup>2</sup>) (Table 4.1), and the water table never developed in the hillslope (Figure 4.4). This lack of HRS hydrologic connectivity

suggested that only 1D flushing would occur (*McGlynn and McDonnell, 2003*). Our measurements of groundwater and DOC dynamics along ST1-W support this premise. DOC concentrations in both riparian wells followed fluctuations in the groundwater table (Figure 4.4b and c). At the beginning of snowmelt, concentrations increased as the water table rose to just below the ground surface and intersected shallow, organic-rich soils, then decreased during the initial decline in the water table. The relationship between increasing DOC concentrations and a rising water table indicated 1D flushing was the dominant DOC mobilization mechanism (*Hornberger et al., 1994; Boyer et al., 1997, 2000; Inamdar and Mitchell, 2006*). DOC concentrations again increased coincident with the rise in the water table after a snowstorm at the end of May, further supporting the occurrence of 1D flushing. We also observed surface water with high DOC concentrations (relative to groundwater) at the end of May and middle of June. High surface water concentrations indicated a 1D rise of the water table into shallow organic-rich soils, as overland flow would likely be dilute if only comprised of low DOC snowmelt (*Schiff et al., 1998; Laudon et al., 2004a, 2007; Buffam et al., 2007; Agren et al., 2008*). 2D flushing was not apparent on ST1-W, since there was never a hydrologic connection across the HRS continuum (i.e. no water table development in the hillslope well, Figure 4.4d). Our measurements of water table and DOC dynamics at ST1-W indicate that in areas of small UAA and no HRS hydrologic connectivity, 1D flushing is likely the only DOC mobilization and delivery mechanism to the stream.

In contrast, we observed both 1D and 2D flushing on ST1-E, which had intermediate toeslope UAA (10,165 m<sup>2</sup>), and transient HRS hydrologic connectivity (for

38% of the snowmelt period) (Table 4.1). 1D flushing was evident at ST1-E1 (riparian well next to stream). Here, groundwater DOC concentrations increased at the beginning of snowmelt (Figure 4.3b) as the water table rose into organic-rich shallow soils. High DOC concentrations were also observed in both the surface and 10 cm flow cups. These DOC dynamics indicated the occurrence of 1D flushing (*Hornberger et al.*, 1994; *Boyer et al.*, 1997, 2000). However, water table development in the hillslope well (ST1-E3, Figure 4.3d) resulted in hydrologic connectivity across the HRS continuum (*Jencso et al.*, 2009) and suggested that 2D flushing also impacted riparian DOC dynamics at this time. Our results support this premise. DOC concentrations at the beginning of snowmelt were high in the hillslope, and it is likely that this DOC-rich hillslope water was quickly transmitted along preferential flow paths (*Freer et al.*, 2002; *McGlynn and McDonnell*, 2003). This pulse of high-DOC hillslope water likely contributed to the increase in riparian groundwater DOC concentrations (Figure 4.3), and indicated the presence of 2D flushing (*McGlynn and McDonnell*, 2003). After this initial rise in riparian DOC concentrations, continued HRS hydrologic connectivity led decreased concentrations due to dilution by low DOC matrix water from the hillslope (*McGlynn and McDonnell*, 2003). Riparian zone DOC concentrations then increased on May 20 following cessation of the hillslope water table, and 2D dilution from low DOC hillslope groundwater ended. The hillslope water table developed again on May 26 after a late-spring snowstorm (Figure 4.3d). However, the water table in the hillslope persisted for only a short period of time and did not lead to a subsequent dilution of riparian zone DOC concentrations in this case. Our measurements of water table and DOC dynamics along ST1-E indicate the

presence of dynamic interactions between 1D and 2D DOC flushing mechanisms during snowmelt in an area of intermediate toeslope UAA and transient HRS hydrologic connectivity.

Similar to ST1-E, both 1D and 2D flushing mechanisms were observed on ST5-W, which had a very large toeslope UAA (46,112 m<sup>2</sup>) and was connected across the HRS continuum for the entire study period (Figure 4.5). 1D flushing was evident at ST5-W2 and ST5-W3, where DOC concentrations of 22 and 11 mg L<sup>-1</sup>, respectively, were measured at the beginning of snowmelt (note the difference in scale on Figure 4.6d and e). These concentrations were 3-4 times the maximum concentrations measured on other transects (~3-6 mg L<sup>-1</sup>). This was likely in response to high organic matter content near the ground surface, which is supported by observations of anoxic zones (*Megonigal et al.*, 1993) and hydromorphic soils (*Phillips et al.*, 2001; *Cosanday et al.*, 2003; *Mourier et al.*, 2008) at these locations. These elevated DOC concentrations were measured as the water table rose at the beginning of snowmelt and entered shallow organic soil, indicating the presence of 1D flushing (*Hornberger et al.*, 1994; *Boyer et al.*, 1997, 2000). However, a dynamic combination of 1D and 2D flushing mechanisms was evident between the beginning and middle of May when DOC concentrations quickly declined at ST5-W2. This decrease in DOC concentrations was coincident with the decline in the groundwater table, and indicated 1D flushing (*Hornberger et al.*, 1994; *Boyer et al.*, 1997, 2000). However, the control of 2D flushing is also apparent. DOC concentrations also declined at the same time at the hillslope well (ST5-W4, Figure 4.5e). 100% HRS hydrologic connectivity was present on ST5-W for the duration of this study and it is

likely that 2D transmission of groundwater from the hillslope impacted DOC concentrations in the riparian zone (*McGlynn and McDonnell, 2003*). The occurrence of 2D flushing on ST5-W was also evident at ST5-W1 (Figure 4.5b). In contrast to other riparian locations, DOC concentrations at ST5-W1 were relatively low. Here, the water table never rose above 50 cm below the ground surface (Figure 4.5b), and therefore remained in deeper, low DOC mineral soil (*Boyer et al., 1997; 2000*). However, increased DOC concentrations were measured at the beginning and end of May despite very little water table fluctuation. These increases in DOC followed a nearly identical trend as at ST5-W2, and indicated that changes in DOC concentrations at ST5-W1 were due to 2D inputs of DOC rich groundwater from the riparian zone further upslope. These results suggest that dynamic interactions between 1D and 2D flushing mechanisms can occur in areas with persistent yet still dynamic hydrologic connectivity.

Comparison of well and groundwater DOC dynamics on 3 transects with large differences in landscape setting and HRS hydrologic connectivity demonstrated the range of 1D and 2D flushing mechanisms that can occur through space and time in complex mountain watersheds. In areas with small UAA and 0% HRS hydrologic connectivity, only 1D flushing was apparent. In contrast, both 1D and 2D flushing mechanisms were evident in areas with higher UAA and transient to persistent HRS hydrologic connectivity. We suggest that in complex snowmelt-dominated catchments, measurements of water table and DOC dynamics are necessary from a range of landscape settings in order to ascertain DOC mobilization and delivery mechanisms to the stream at the catchment scale.

### Conceptual Model

Our conceptual model (Figure 4.7) illustrates that the relative control of DOC flushing mechanisms on the spatial and temporal variability of stream DOC export is strongly influenced by the degree of riparian-stream (RS) and hillslope-riparian-stream (HRS) hydrologic connectivity, which is partially dependent upon landscape structure and wetness status (*Jencso et al.*, 2009). 1D flushing can lead to DOC contributions from the riparian zone to the stream as the water table rises and intersects shallow, organic-rich soil layers (*Bishop et al.* 1994; *Hornberger et al.*, 1994; *Boyer et al.*, 1997, 2000; *Bishop et al.*, 2004; *Laudon et al.*, 2004b). DOC export during this rise of the water table is often augmented by transmissivity feedback (*Bishop et al.*, 2004; *Laudon et al.*, 2004b; *Weiler and McDonnell*, 2006). In contrast, 2D flushing can lead to changes in DOC source areas (e.g. from the riparian to the hillslope zone) throughout snowmelt or precipitation events (*McGlynn and McDonnell*, 2003; *Hood et al.*, 2006). Here, high DOC concentrations on the rising limb of the stream hydrograph are initially from the 1D rise of the water table into shallow riparian soil. A second large pulse of DOC occurs as the water table develops in the hillslope, and DOC-rich hillslope water is transmitted along preferential flowpaths to the stream (*McGlynn and McDonnell*, 2003). Stream DOC concentrations then decrease on the falling limb of the hydrograph from dilution by low-DOC hillslope soil matrix water. For 1D flushing to occur, there must be RS hydrologic connectivity, while a hydrologic connection across the entire HRS continuum is requisite for 2D flushing (*McGlynn and McDonnell*, 2003). While 1D DOC flushing can occur in any area of the watershed where a rising water table intersects shallow soil

layers, it is likely the only flushing mechanism present in areas with small toeslope UAA and little to no HRS hydrologic connectivity. In contrast, 2D flushing can occur only at catchment areas with HRS hydrologic connectivity, which are generally associated with landscape positions with higher toeslope UAA (*Jencso et al.*, 2009). We suggest that the relative control of 1D and 2D flushing mechanisms on stream DOC export changes over time. This is presented in our conceptual model (Figure 4.7), in which the darker areas under the connectivity curve denote the greatest 2D influence on stream DOC export. During dry times (such as baseflow – right side of the diagram where the area under the curve is nearly all white), few areas of the landscape have HRS hydrologic connectivity, and 1D flushing is the dominant DOC export mechanism. As the wetness status of the catchment increases (such as during snowmelt or precipitation events), 2D flushing becomes more prevalent and can occur over a wider range of UAA, as denoted by the increasing amount of dark area under the left side of the connectivity curve in our conceptual model (Figure 4.7). The relative importance of 2D flushing on DOC export is likely greatest at times of high wetness status, such as at peak runoff (Figure 4.7).

At our study site, both 1D (*Hornberger et al.*, 2004; *Boyer et al.*, 1997; *Bishop et al.* 1994, 2004; *Laudon et al.*, 2004b) and 2D (*McGlynn and McDonnell*, 2003; *Bishop et al.*, 2004; *Hood et al.*, 2006) flushing mechanisms likely controlled the mobilization and delivery of DOC to the stream, the relative importance of which changed through space and time. *Jencso et al.* (2009) found that in the TCEF, less than 4% of the stream network was hydrologically connected to the uplands at baseflow. These areas were generally restricted to landscape positions with high toeslope UAA. Therefore, the

relative influence of 2D flushing on DOC export at the catchment scale was low (right side of the connectivity curve in our conceptual model, where the area under the curve is almost entirely white – Figure 4.7). During low flows at the beginning and end of snowmelt, 1D flushing was likely the dominant DOC delivery process to the stream, and 2D export was limited to the small portion of the stream network with high UAA. However, as catchment wetness status increased during snowmelt, HRS hydrologic connectivity was present across a wider range of UAA, and the relative importance of 2D flushing on catchment DOC export increased. This is denoted by the increased amount of dark area under the left side of the connectivity curve, which signifies the time of highest wetness status (Figure 4.7). At peak snowmelt in the TCEF, 66% of the stream network was hydrologically connected across the HRS continuum (*Jencso et al.*, 2009). This was likely the time of the greatest influence of 2D flushing on stream DOC export (Figure 4.7). As snowmelt declined, the degree of HRS hydrologic connectivity decreased, and 2D flushing eventually became restricted to the small portion of the stream network with high UAA (right side of conceptual model diagram). At this time, only RS hydrologic connectivity was present along the majority of the stream network, and the relative influence of 1D flushing on stream DOC export returned to the high level observed during low flows prior to the onset of snowmelt. Our conceptual model suggests that in complex snowmelt-dominated catchments such as the TCEF, the spatial and temporal variability of 1D and 2D flushing mechanisms on stream DOC export is dependent upon landscape structure and wetness status, which strongly influence the degree of RS and HRS hydrologic connectivity.

What is the Spatial Extent/Frequency of  
Dominant Landscape Settings, and what does  
this Mean for DOC Export at the Catchment Scale?

The results of this study indicate that stream DOC export is dependent upon the spatial extent and organization of dominant landscape settings. Wetlands (*Hope et al.*, 1994; *Creed et al.*, 2003, 2008; *Agren et al.*, 2007, 2008) and shallow riparian zone soil horizons (*Bishop et al.*, 2004, *Hood et al.*, 2006; *Nakagawa et al.*, 2008) generally have high DOC content. Therefore, we can expect catchment areas with large riparian and wetland extent to be large sources of DOC to the stream. This premise was true in the TCEF, as illustrated in the comparison of DOC concentrations between the headwaters of Stringer Creek and Tenderfoot Creek (at Onion Park) (Figure 4.6). The headwaters of Stringer Creek have a relatively small riparian and wetland extent, and stream DOC concentrations were low ( $\sim 1.5\text{-}2.5 \text{ mg L}^{-1}$ ). In contrast, the headwaters of Tenderfoot Creek have an extensive riparian and wetland network (with intermittent hydrologic connectivity to the stream) and therefore greater contributions from organic-rich soils. DOC concentrations at the headwaters of Tenderfoot Creek were generally over  $4 \text{ mg L}^{-1}$  and therefore over 100% higher than at the headwaters of Stringer Creek. Further, there were large decreases in DOC concentrations in the headwaters of Tenderfoot Creek when flow decreased at the middle of April and then again at the middle of June (Figure 4.6). This was likely the result of transient hydrologic connectivity between riparian and wetland DOC source areas. In contrast, the limited extent of riparian and wetland area had little effect on stream DOC concentrations at the headwaters of Stringer Creek during the transition from high and low flow. Our comparisons of both the timing and

magnitude of stream DOC dynamics between the headwaters of Stringer Creek (little riparian and wetland area) and Tenderfoot Creek (large riparian and wetland area) indicate the strong influence that the spatial extent of organic-rich riparian and wetland areas can have on stream DOC export.

The influence of large DOC source areas on stream DOC export is also apparent when comparing the 4 sub-catchments of the Stringer Creek Watershed. Our results illustrate that even within a relatively small area (~550 ha), changes in the relative proportion of riparian to upland area can lead to strong differences in stream DOC export. At ST1, near the headwaters of Stringer Creek, stream DOC concentrations were low and relatively stable (Figure 8a). Cumulative stream DOC export during snowmelt (Figure 4.8e) was also relatively low ( $6.6 \text{ kg ha}^{-1}$ ). Low DOC at the headwaters of Stringer Creek likely reflects the relatively small percent of riparian to upslope area (1.42%) within this sub-catchment of the Stringer Creek Watershed (Table 4.2).

Stream DOC concentrations increased downstream between ST1 and MSC (Figure 4.8b). This increase was likely in response to the large increase in the percentage of riparian to upland area in this sub-catchment (3.79%), which was nearly three times higher than observed between the headwaters and ST1 (Table 4.2). This increase in the extent of organic riparian and wetland areas near the stream led to a large increase in cumulative stream DOC export ( $15.4 \text{ kg ha}^{-1}$ ), and demonstrates the influence of large DOC-source areas on stream DOC export. Cumulative stream DOC export was low at the 2 downstream sub-catchments (MSC to ST5, and ST5 to LSC) ( $6.2$  and  $7.5 \text{ kg ha}^{-1}$ , respectively). Compared to the large proportion of riparian to upland area observed

between ST1 and MSC (3.79%), these downstream sub-catchments had relatively low riparian to upland extent (1.32 and 1.3%). This combination of low stream DOC export with a low proportion of riparian to upland area further supports the premise that the relative amount of riparian and wetland area is a strong control on DOC export. High downstream DOC concentrations likely reflect inputs from large DOC source areas further upstream (as suggested by the higher percentage of riparian to upslope area, Table 4.2). The results of our study indicate that stream DOC concentrations measured at the outlet of a catchment can reflect a wide range of internal processes, controls, and space/time variability. Further, our results show the importance of estimating cumulative stream DOC export, rather than focusing solely on stream DOC concentrations, when comparing DOC dynamics from different catchments

The strong control of the relative amount of DOC source areas on stream DOC export at large scales is also apparent when comparing cumulative stream DOC to the riparian:upland proportion of each of the larger sub-catchments in the Tenderfoot Creek Watershed (Table 4.3). In general, the greatest DOC export occurred from catchments with high riparian:upland ratios. This trend is further supported when plotting cumulative DOC export versus the proportion of riparian:upland area from all of the sub-catchments in the Tenderfoot Creek Watershed (Figure 4.9). There was a strong positive relationship ( $r^2 = 0.62$ ,  $p < 0.001$ ) between DOC export and the relative amount of riparian:upland area, which is consistent with the results of other studies (*Dillon and Molot, 1997; Laudon et al., 2007*). These results are supported by *Hinton et al. (1998)* and *Inamdar and Mitchell (2006)*, who found that catchments with large wetland and

riparian areas consistently had higher DOC concentrations than catchments with little to no riparian and wetland extent.

Our estimate of annual cumulative stream DOC export from the entire Stringer Creek Watershed ( $9.6 \text{ kg ha}^{-1} \text{ yr}^{-1}$ ) is consistent with estimates from other studies. In a review of carbon export from nearly 100 catchments across the world, *Hope et al.* (1994) found a range of 10 to  $100 \text{ kg ha}^{-1} \text{ yr}^{-1}$  across a wide range of catchment sizes. Our estimate of cumulative DOC export from the Stringer Creek Watershed is consistent with those from catchments of similar size ( $\sim 5 \text{ km}^2$ ) and ecosystem type. *Laudon et al.* (2007) found that annual DOC export ranged from 35 to  $76 \text{ kg ha}^{-1} \text{ yr}^{-1}$  across 7 catchments in northern Sweden, and *Kortelainen et al.* (1997) found a similar range across catchments in Finland. The site locations used for these studies were boreal catchments, which have very large stores of DOC (as indicated by stream DOC concentrations of up to an order of magnitude higher than observed in Stringer Creek), and likely explains the higher export relative to our study site. The estimates by *Laudon et al.* (2007) and *Kortelainen et al.* (1997) are similar to those of boreal catchments presented by *Hope et al.* (1994). Our results indicate that while stream DOC export from subalpine catchments may not be as high as from boreal catchments, they can still contribute a large flux of DOC, which can have large implications for ecosystem carbon balances (*Laudon et al.*, 2004a; *Neill et al.*, 2006; *Johnson et al.*, 2006; *Waterloo et al.*, 2006; *Jonsson et al.*, 2007).

Hydrologic connectivity between the stream and riparian and hillslope zones was a strong control on DOC export from the landscape to the stream in the Stringer Creek Watershed. However, our calculations of cumulative stream DOC export illustrate that

the overall spatial extent of DOC source areas is also important. HRS hydrologic connectivity along the stream channel was high at all of the sub-catchments within the Stringer Creek Watershed, ranging from 69-79% (Table 4.2). Similarity in hydrologic connectivity along the stream channel suggested that stream DOC export would be high throughout the entire catchment. However, there were large differences in cumulative stream DOC export (Table 4.2, Figure 4.8). Cumulative stream DOC export was relatively low between the headwaters of Stringer Creek and ST1. While the degree of HRS hydrologic connectivity along this section of the stream was high (76% during the period of this study) (Table 4.2), it had a small percentage of riparian to upland area (1.42%). A similar trend (high HRS hydrologic connectivity, but low riparian area, and low cumulative stream DOC export) was also observed between MSC and ST5, and between ST5 and LSF. In contrast, the area between ST1 and MSC had high HRS hydrologic connectivity (69%) and a high proportion of riparian to upland area (3.79%). Cumulative stream DOC export from the ST1-MSC sub-catchment was over twice as high than from the other sub-catchments (Figure 4.8). Our results indicate that the intersection between large DOC source areas and high HRS hydrologic connectivity may lead to “hotspots” for stream DOC export in complex mountain watersheds.

The results of our study also demonstrate the integration of highly variable internal catchment dynamics in watershed outlet observations (Figure 4.10). The Tenderfoot Creek Watershed is composed of 7 sub-catchments, which varied in landscape structure (Jencso et al., 2009) and timing and magnitude of both stream discharge and DOC concentrations (Figure 4.10). Stream discharge was low in both SC

(Figure 4.10b) and UTC (Figure 4.10f), and almost never rose above  $0.3 \text{ mm hr}^{-1}$ . At these catchments, stream DOC concentrations were very high (maximum concentrations of over  $7 \text{ mg L}^{-1}$  were observed). In contrast, peak discharge was approximately twice as high in Stringer Creek (at both MSC and LSC), and stream DOC concentrations never exceeded  $4 \text{ mg L}^{-1}$  throughout the study period. Further, while DOC concentrations increased on the rising limb of the stream hydrograph at all catchments, there was variability in the timing of peak DOC concentrations across the catchments (Figure 4.10). There were also differences in DOC trends throughout the snowmelt period across the different catchments. In general, stream DOC concentrations were relatively stable in BC, MSC, and LSC, while concentrations were much flashier at the other catchments (Figure 4.10). At the outlet of Tenderfoot Creek (LTC), stream discharge and DOC dynamics were intermediate between the dynamics observed at the individual sub-catchments of Tenderfoot Creek, and reflect the integration of internal source waters with variability in landscape structure at the catchment outlet (*McGlynn and McDonnell, 2003; Jencso et al., 2009*). Our results indicate that measurements at the outlet of a catchment are often an unknown amalgamation of internal dynamics and may not be suitable for an unequivocal interpretation without data collection from a range of landscape positions within a catchment in order to ascertain the cause of stream dynamics observed at larger scales.

### Conclusions

Based upon catchment scale topographic analysis and measurements of stream, soil, surface, and groundwater DOC dynamics during snowmelt (April 15 – July 15)

across three transects and 7 watersheds with a range of landscape settings and hydrologic connectivity, we conclude that:

1. The relative importance of nutrient flushing mechanisms on stream DOC export was dependent upon landscape position and the degree of hydrologic connectivity between the stream, riparian, and hillslope zones. 1D flushing was restricted to areas with a hydrologic connection across the riparian-stream (RS) interface, while a hydrologic connection across the entire hillslope-riparian-stream (HRS) continuum was requisite for 2D flushing.
2. The relative importance of 1D versus 2D flushing mechanisms changed throughout space and time during snowmelt. In areas of small UAA and at times of low wetness status (such as baseflow), 1D flushing was the dominant DOC mobilization and delivery mechanism to the stream. In contrast, 2D flushing was restricted to areas of larger UAA and times of increased wetness status (such as peak snowmelt). The relative importance of 2D flushing increased after the initiation of snowmelt, with the greatest control likely at peak snowmelt when the spatial extent of HRS connectivity was highest throughout the catchment.
3. The intersection of hydrologic connectivity and high DOC source areas drove stream DOC export. The greatest DOC export occurred at areas with both high HRS hydrologic connectivity and large DOC source areas.

This research provides insight into the spatial and temporal controls of nutrient flushing mechanisms on stream DOC export during snowmelt. We suggest that landscape analysis may provide a way forward in determining the relative importance of 1D and 2D flushing mechanisms on stream DOC export, and what areas of the landscape likely provide the largest contributions of DOC to the stream. To continue to improve our understanding of DOC export at the catchment scale, future research is necessary across a range of landscape positions and characteristics, especially in complex terrain.

#### Acknowledgements

This work was funded by National Science Foundation (NSF) grant EAR-0337650 to B.L. McGlynn, and fellowships awarded to V.J. Pacific (from the Inland Northwest Research Alliance – INRA, and the Big Sky Institute NSF GK-12 Program) and K.J. Jencso (INRA). Extensive logistic collaboration was provided by the Tenderfoot Creek Experimental Forest and the USDA, Forest Service, Rocky Mountain Research Station, especially Ward McCaughey. Airborne Laser Mapping was provided by the NSF-supported Center for Airborne Laser Mapping (NCALM) at the University of California, Berkeley. We are grateful to Diego Riveros-Iregui for field assistance, and Galena Ackerman and John Mallard for performing laboratory analyses.

References Cited

- Agren, A., I. Buffam, M. Jansson, and H. Laudon (2007) Importance of seasonality and small streams for the landscape regulation of dissolved organic carbon export. *Journal of Geophysical Research*, 112, G03003, doi: 10.1029/2006JG000381.
- Agren, A., I. Buffam, M. Berggren, K. Bishop, M. Jansson, and H. Laudon (2008) Dissolved organic carbon dynamics in boreal streams in a forest-wetland gradient during the transition between winter and summer, *Journal of Geophysical Research*, 113, G03031, doi: 10.1029/2007JG000674.
- Bishop, K., C. Pettersson, B. Allard, and Y. H. Lee (1994) Identification of the riparian sources of aquatic dissolved organic carbon, *Environmental International*, 20, 11-19.
- Bishop, K., J. Seibert, S. Koher, and H. Laudon (2004) Resolving the double paradox of rapidly mobilized old water with highly variable response to runoff chemistry, *Hydrological Processes*, 18, 185-189.
- Boyer, E. W., G. M. Hornberger, K. E. Bencala, and D. M. McKnight (1997) Response characteristics of DOC flushing in an alpine catchment, *Hydrological Processes*, 11, 1635-1647.
- Boyer, E. W., G. M. Hornberger, K. E. Bencala, and D. M. McKnight (2000) Effects of asynchronous snowmelt on flushing of dissolved organic carbon: a mixing model approach, *Hydrological Processes*, 14, 3291-3308.
- Buffam, I., H. Laudon, J. Temnerud, C. M. Morth, and K. Bishop (2007) Landscape-scale variability of acidity and dissolved organic carbon during spring flood in a boreal stream network, *Journal of Geophysical Research*, 112, G01022, doi: 10.1029/2006JG000218.
- Burns, D. (2005) What do hydrologists mean when they use the term flushing? *Hydrological Processes*, 19, 1325-1327.
- Cosanday, A. C., V. Maitre, and C. Guenat (2003) Temporal denitrification patterns in different horizons of two riparian soils, *European Journal of Soil Science*, 54, 25-38.
- Creed, I. F., S. E. Sanford, F. D. Beall, L. A. Molot, and P. J. Dillon (2003) Cryptic wetlands: Integrating hidden wetlands in regression models of the export of dissolved organic carbon from forested landscapes, *Hydrological Processes*, 17, 3629-3648.

- Creed, I. F., F. D. Beall, T. A. Clair, P. J. Dillon, and R. H. Hesslein (2008) Predicting export of dissolved organic carbon from forested catchments in glaciated landscapes with shallow soils, *Global Biogeochemical Cycles*, 22, GB4024, doi: 10.1029/2008GB003294.
- Dillon, P. J. and L. A. Molet (1997) Effect of landscape form on export of dissolved organic carbon, iron, and phosphorus from forested stream catchments, *Water Resources Research*, 33, 2591-2600.
- Farnes, P. E., R. C. Shearer, W. W. McCaughey, and K. J. Hanson (1995) Comparisons of Hydrology, Geology and Physical Characteristics between Tenderfoot Creek Experimental Forest (East Side) Montana, and Coram Experimental Forest (West Side) Montana. Final Report RJVA-INT-92734. USDA Forest Service, Intermountain Research Station, Forestry Sciences Laboratory, Bozeman, Montana, 19p.
- Freer, J., J. J. McDonnell, K. J. Beven, N. E. Peters, D. A. Burns, R. P. Hooper, B. Aulenbach, and C. Kendall (2002) The role of bedrock topography on subsurface stormflow, *Water Resources Research*, 38, 10.1029/2001WR000872.
- Hinton, M. J., S. L. Schiff, and M. C. English (1998) Sources and flowpaths of dissolved organic carbon during storms in two forested watersheds of the Precambrian Shield, *Biogeochemistry*, 41, 175-197.
- Holdorf, H. D. (1981) Soil Resource Inventory, Lewis and Clark National Forest - Interim In-Service Report. On file with the Lewis and Clark National Forest, Forest Supervisor's Office, Great Falls, MT.
- Hood, E., M. N. Gooseff, and S. L. Johnson (2006) Changes in the character of stream water dissolved organic carbon during flushing in three small watersheds, Oregon, *Journal of Geophysical Research*, 111, G01007, doi: 10.1029/2005JG000082.
- Hope, D., M. F. Billet, and M. S. Cressner (1994) A review of the export of carbon in rivers: Fluxes and processes, *Environmental Pollution*, 84, 301-324.
- Hornberger, G. M., K. E. Bencala, D. M. McKnight (1994) Hydrologic controls on dissolved organic carbon during snowmelt in the Snake River near Montezuma, Colorado, *Biogeochemistry*, 25, 147-165.
- Imai, A., K. Matsushige, and T. Nagai (2003) Trihalomethane formation potential of dissolved organic matter in a shallow eutrophic lake, *Water Research*, 37, 4284-4294.

- Inamdar, S. P., S. Christopher, and M. J. Mitchell (2004) Flushing of DOC and nitrate from a forested catchment: Role of hydrologic flow paths and water sources, *Hydrological Processes*, 18, 2651-2661.
- Inamdar, S. P. and M. J. Mitchell (2006) Hydrologic and topographic controls on storm-event exports of dissolved organic carbon (DOC) and nitrate across catchment scales, *Water Resources Research*, 42, W03421, doi: 10.1029/2005WR004212.
- Jencso, K. G., B. L. McGlynn, M. N. Gooseff, S. M. Wondzell, K. E. Bencala, and L. A. Marshall (2009) Hydrologic connectivity between landscapes and streams: Transferring reach and plot scale understanding to the catchment scale, *Water Resources Research*, doi:10.1029/2008WR007225
- Johnson, M. S., J. Lehmann, E. C. Selva, M. Abdo, S. Riha, and E. Guimarães Couto (2006) Organic carbon fluxes within and streamwater exports from headwater catchments in the southern Amazon, *Hydrological Processes*, 20, 2599-2614.
- Jonsson, A., G. Algesten, A. K. Bergstrom, K. Bishop, S. Sobek, L. J. Tranvik, and M. Jansson (2007) Integrating aquatic carbon fluxes in a boreal catchment carbon budget, *Journal of Hydrology*, 334, 141-150.
- Laudon, H., S. Kohler, and I. Buffam (2004a) Seasonal TOC export from seven boreal catchments in northern Sweden, *Aquatic Science*, 66, 223-230.
- Laudon, H., J. Seibert, S. Kohler, and K. Bishop (2004b) Hydrological flowpaths during snowmelt: Congruence between hydrometric measurements and oxygen 18 in meltwater, soil water, and runoff, *Water Resources Research*, 40, W03102, doi: 10.1029/2003WR002455.
- Laudon, H., V. Sjöblom, I. Buffam, J. Seibert, and M. Morth (2007) The role of catchment scale and landscape characteristics for runoff generation of boreal streams, *Journal of Hydrology*, 344, 198-209.
- McGlynn, B. L. and J. J. McDonnell (2003) Role of discrete landscape units in controlling catchment dissolved organic carbon dynamics, *Water Resources Research*, 39, doi:10.1029/2002WR001525.
- McGlynn, B. L. and J. Seibert (2003) Distributed assessment of contributing area and riparian buffering along stream networks, *Water Resources Research*, 39, doi: 10.1029/2002WR001521.
- Megonigal, J. P., W. H. Patrick, and S. P. Faulkner (1993) Wetland identification in seasonally flooded forest soils: soil morphology and redox dynamics, *Soil Science Society of America Journal*, 57, 140-149.

- Mincemoyer, S. A. And J. L. Birdsall (2006) Vascular flora of the Tenderfoot Creek Experimental Forest, Little Belt Mountains, Montana, *Madrono*, 53, 211-222.
- Mourier, B., C. Walter, and P. Merot (2008) Soil distribution in valleys according to stream order, *Catena*, 72, 395-404.
- Nakagawa, Y., H. Shibata, F. Satoh, and K. Sasa (2008) Riparian control on NO<sub>3</sub><sup>-</sup>, DOC, and dissolved Fe concentrations in mountainous streams, northern Japan, *Limnology*, 9, 195-206. doi: 10.1007/s10201-008-0251-7.
- Neill, C., H. Elsenbeer, A. V. Krusche, J. Lehmann, D. Markewitz, and R. de O. Figueiredo (2006) Hydrological and biogeochemical processes in a changing Amazon: results from small watershed studies and the large-scale biosphere-atmosphere experiment, *Hydrological Processes*, 20, 2467-2476.
- Ocampo, C. J., C. E. Oldham, M. Sivapalan, and J. V. Turner (2006a) Hydrological versus biogeochemical controls on catchment nitrate export: A test of the flushing mechanism, *Hydrological Processes*, 20, 4269-4286.
- Ocampo, C. J., M. Sivapalan, and C. Oldham (2006b) Hydrological connectivity of upland-riparian zones in agricultural catchments: Implications for runoff generation and nitrate transport, *Journal of Hydrology*, 331, 643-658.
- Pacific, V. J., B. L. McGlynn, D. A. Riveros-Iregui, D. Welsch, and H. Epstein (2008) Variability in soil CO<sub>2</sub> production and surface CO<sub>2</sub> efflux across riparian-hillslope transitions, *Biogeochemistry*. doi: 10.1007/s10533-008-9258-8.
- Pacific, V. J., B. L. McGlynn, D. A. Riveros-Iregui, D. Welsch, and H. E. Epstein (in review) Soil respiration across riparian-hillslope transitions: Biophysical controls and the role of landscape position. *Journal of Geophysical Research - Biogeosciences*.
- Pacific, V. J., B. L. McGlynn, D. A. Riveros-Iregui, H. E. Epstein, and D. L. Welsch (in review) Differential soil respiration responses to changing hydrologic regimes. *Water Resources Research*.
- Phillips, D. H., J. E. Fossa, C. A. Stiles, C. C. Trettin, and R. J. Luxmoore (2001) Soil-landscape relationships at the lower reaches of a watershed at Bear Creek near Oak Ridge, Tennessee, *Catena*, 44, 205-222.
- Riveros-Iregui, D. A., B. L. McGlynn, H. E. Epstein, and D. L. Welsch (2008) Interpretation and evaluation of combined measurement techniques for soil CO<sub>2</sub> efflux: surface chambers and soil CO<sub>2</sub> concentration probes, *Journal of Geophysical Research – Biogeosciences*. doi: 10.1029/2008JG000811.

- Riveros-Iregui DA, BL McGlynn, HE Epstein, D Welsch, L Marshall (in review) A Critical Assessment of a Process Soil CO<sub>2</sub> Production and Transport Model. *Journal of Geophysical Research - Biogeosciences*.
- Riveros-Iregui, D. A. and B. L. McGlynn (in press) Landscape Structure Controls Soil CO<sub>2</sub> Efflux Variability in Complex Terrain: Scaling From Point Observations to Watershed Scale Fluxes. *Journal of Geophysical Research - Biogeosciences*.
- Schiff, S., R. Aravena, E. Mewhinney, R. Elgood, B. Warner, P. Dillon, and S. Trumbore (1998) Precambrian shield wetlands: Hydrologic control of the sources and export of dissolved organic matter, *Climate Change*, 40, 167-188.
- Seibert, J. and B. L. McGlynn (2007) A new triangular multiple flow direction algorithm for computing upslope areas from gridded digital elevation models, *Water Resources Research*, 43(4). W04501
- van Vevrseveld, W. J., J. J. McDonnell, and K. Lajtha (2008) A mechanistic assessment of nutrient flushing at the catchment scale, *Journal of Hydrology*, 358, 268-287.
- Waterloo, M. J., S. M. Oliveira, D. P. Drucker, A. D. Nobre, L. A. Cuartas, M. G. Hodnett, I. Langedijk, W. W. P. Jans, J. Tomasella, A. C. de Araújo, T. P. Pimentel, and J. C. M'unera Estrada (2006) Export of organic carbon in run-off from an Amazonian rainforest blackwater catchment, *Hydrological Processes*, 20, 2581-2597.
- Wei, Q., C. Feng, D. Wang, B. Shi, L. Zhang, Qia Wei, and H. Tang (2008) Seasonal variations of chemical and physical characteristics of dissolved organic matter and trihalomethane precursors in a reservoir: a case study, *Journal of Hazardous Materials*, 150, 257-264.
- Wieler, M. and J. McDonnell (2006) Testing nutrient flushing hypotheses at the hillslope scale: A virtual experiment approach, *Journal of Hydrology*, 319, 339-356.

Table 4.1: Stringer Creek transect characteristics of upslope accumulated area (UAA), hillslope-riparian-stream connectivity, riparian width, and slope of hillslope. Hydrologic connectivity across the hillslope-riparian-stream (HRS) continuum was calculated by dividing the number of days that a hillslope water table was present by the total snowmelt period (April 15 - July 15).

| Transect | UAA<br>(m <sup>2</sup> ) | HRS Connectivity<br>(% of snowmelt) | Riparian Width<br>(m) | Hillslope<br>(°slope) |
|----------|--------------------------|-------------------------------------|-----------------------|-----------------------|
| ST1-E    | 10165                    | 38                                  | 11.8                  | 15.6                  |
| ST1-W    | 1563                     | 0                                   | 12.7                  | 12.5                  |
| ST5-W    | 46112                    | 100                                 | 16.5                  | 20.8                  |

Table 4.2: Percentage of stream network with hillslope-riparian-stream (HRS) hydrologic connectivity, ratio of riparian:upland area, and cumulative stream DOC export from April 15 - July 15, 2007 for 4 sections of Stringer Creek: the headwaters to ST1, ST1 to the Middle Stringer Creek Flume (MSC), MSC to ST5, and ST5 to the Lower Stringer Creek Flume (LSC).

| Stream<br>Section | % of stream with<br>HRS connectivity | riparian:upland<br>(%) | cumulative stream<br>DOC export (kg ha <sup>-1</sup> ) |
|-------------------|--------------------------------------|------------------------|--|
| HW - ST1          | 76                                   | 1.42                   | 7.8  |
| ST1 - MSC         | 69                                   | 3.79                   | 13.3   |
| MSC - ST5         | 73                                   | 1.32                   | 7.3  |
| ST5 - LSC         | 79                                   | 1.30                   | 8.7  |

Table 4.3: Ratio of riparian:upland area and cumulative stream DOC export from April 15 to July 15, 2007 for the sub-catchments within the Tenderfoot Creek Watershed.

| Sub-catchment    | riparian:upland<br>(%) | cumulative stream<br>DOC export (kg ha <sup>-1</sup> ) |
|------------------|------------------------|--|
| Upper Tenderfoot | 5.33                   | 12.4   |
| Lower Tenderfoot | 3.86                   | 11.4   |
| Middle Stringer  | 3.09                   | 8.1  |
| Lower Stringer   | 2.98                   | 8.4  |
| Bubbling         | 2.46                   | 9.7  |
| Sun              | 1.73                   | 9.5  |
| Spring Park      | 6.08                   | 11.9   |

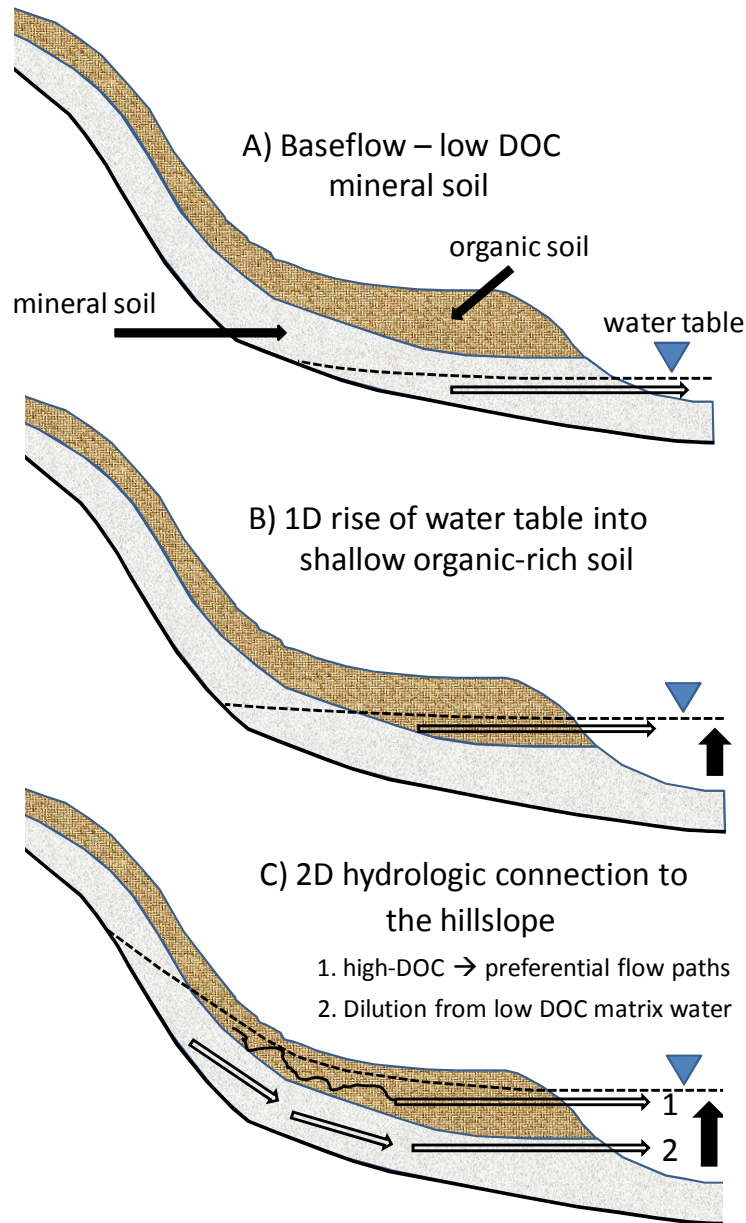


Figure 4.1: Conceptual model of DOC export from the soil to the stream. At times of low flow (baseflow) (A), groundwater travels through low DOC mineral soil, and stream DOC concentrations are low. As flow begins to increase (beginning of snowmelt) (B), the water table rises into shallow organic-rich riparian soil, and inputs of DOC from the soil to the stream increase, which we refer to as a one-dimensional process (1D flushing). As flow continues to increase (C), a hydrologic connection develops across the hillslope-riparian-stream continuum and initiates 2D flushing. A large pulse of DOC can occur as high DOC water from the hillslopes is transmitted downslope along preferential flow paths. Runoff from the hillslope is then diluted by low DOC matrix water traveling through mineral soil.

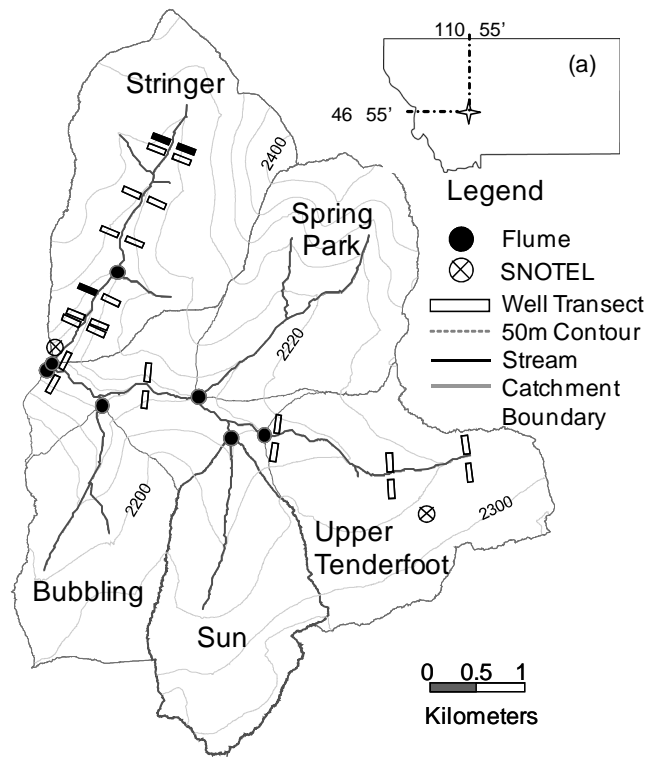


Figure 4.2: Location of the Tenderfoot Creek Experimental Forest (TCEF), with delineations of the sub-catchments, and locations of the flumes (at the outlet of each sub-catchment) and the Lower Stringer Creek SNOTEL site. Transect locations are denoted by rectangles, and the 3 utilized for this study within the Stringer Creek Watershed are shown in black.

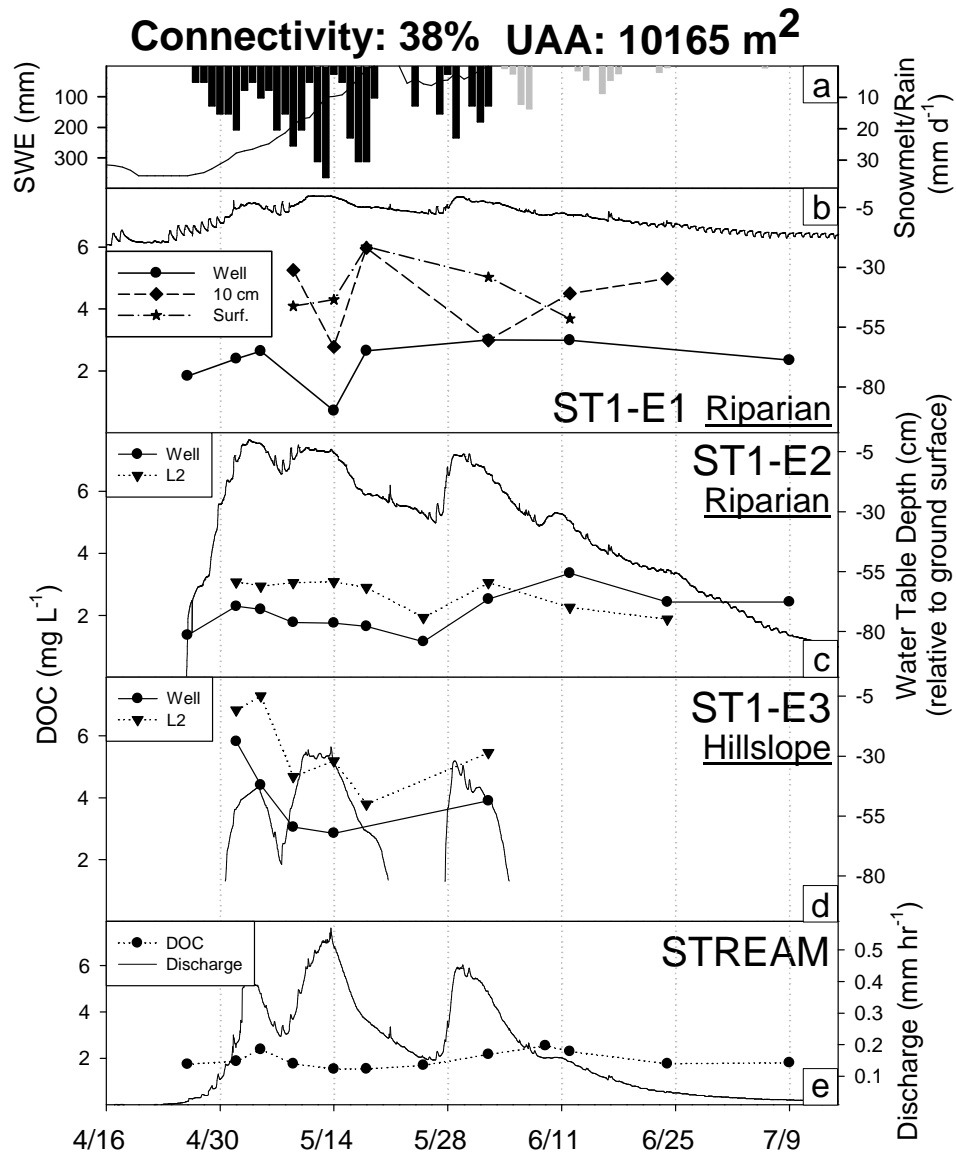


Figure 4.3: a) snow water equivalent (black line) and soil water inputs from snowmelt (black bars) and precipitation (grey bars); b) ST1-E1 (riparian) 10 cm, surface, and well DOC concentrations and groundwater height; c) ST1-E2 (riparian) lysimeter (20 cm), 10 cm and well DOC concentrations and groundwater height; d) ST1-E3 (hillslope) lysimeter (20 cm) and well DOC concentrations and groundwater height; and e) stream DOC concentrations and discharge from April 15 to July 15, 2007. The percentage of the study period that hillslope-riparian-stream connectivity existed, and upslope accumulated area (UAA) at the toeslope measurement location (E2) are listed at the top of the figure. Stream discharge is from the Lower Stringer Creek Flume.

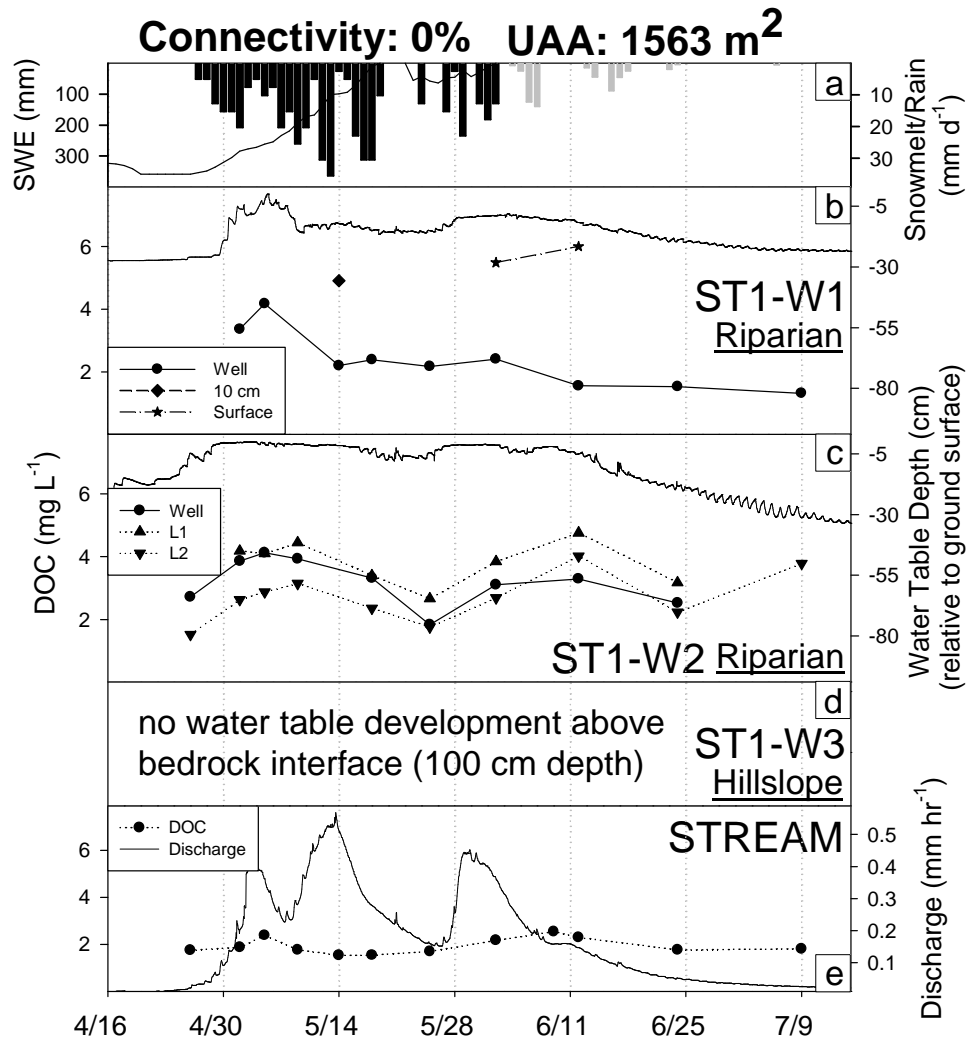


Figure 4.4: a) snow water equivalent (black line) and soil water inputs from snowmelt (black bars) and precipitation (grey bars); b) ST1-W1 (riparian) 10 cm, surface, and well DOC concentrations and groundwater height; c) ST1-W2 (riparian) lysimeter (L1 = 20 cm; L2 = 50 cm) and well DOC concentrations and groundwater height; d) statement of no hillslope water table development above the bedrock interface at 100 cm; and e) stream DOC concentrations and discharge from April 15 to July 15, 2007. The percentage of the study period that hillslope-riparian-stream connectivity existed, and upslope accumulated area (UAA) at the toeslope measurement location (W2) are listed at the top of the figure. Stream discharge is from the Lower Stringer Creek Flume.

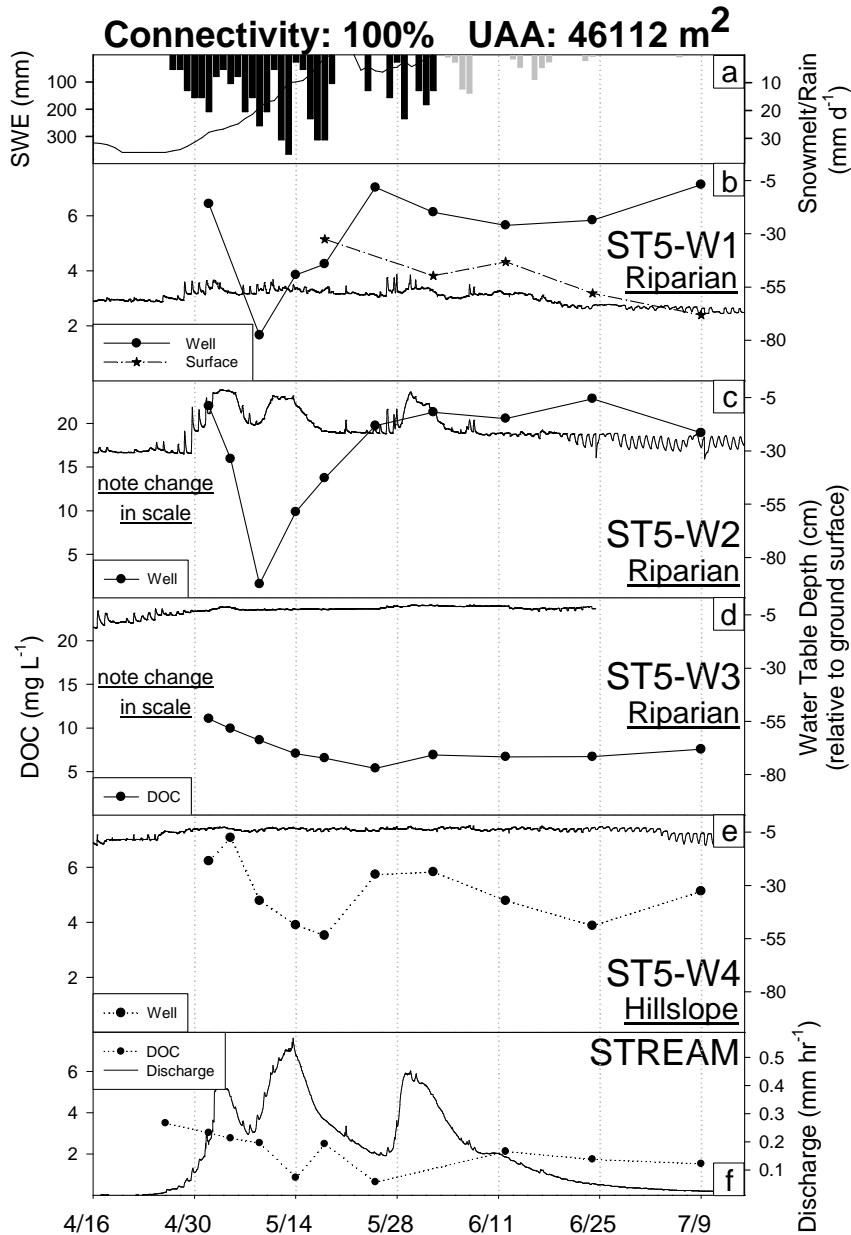


Figure 4.5: a) snow water equivalent (black line) and soil water inputs from snowmelt (black bars) and precipitation (grey bars); b) ST5-W1 (riparian) surface and well DOC concentrations and groundwater height; c) ST5-W2 (riparian) well DOC concentrations and groundwater height; d) ST5-W3 (riparian) surface and well DOC concentrations and groundwater height; e) ST5-W4 (hillslope) well DOC concentration and groundwater height; and h) stream DOC concentrations and discharge from April 15 to July 15, 2007. Note the difference in scale for DOC at (c) and (d). The percentage of the study period that hillslope-riparian-stream connectivity existed, and upslope accumulated area (UAA) at the toeslope measurement location (W3) are listed at the top of the figure. Stream discharge is from the Lower Stringer Creek Flume.

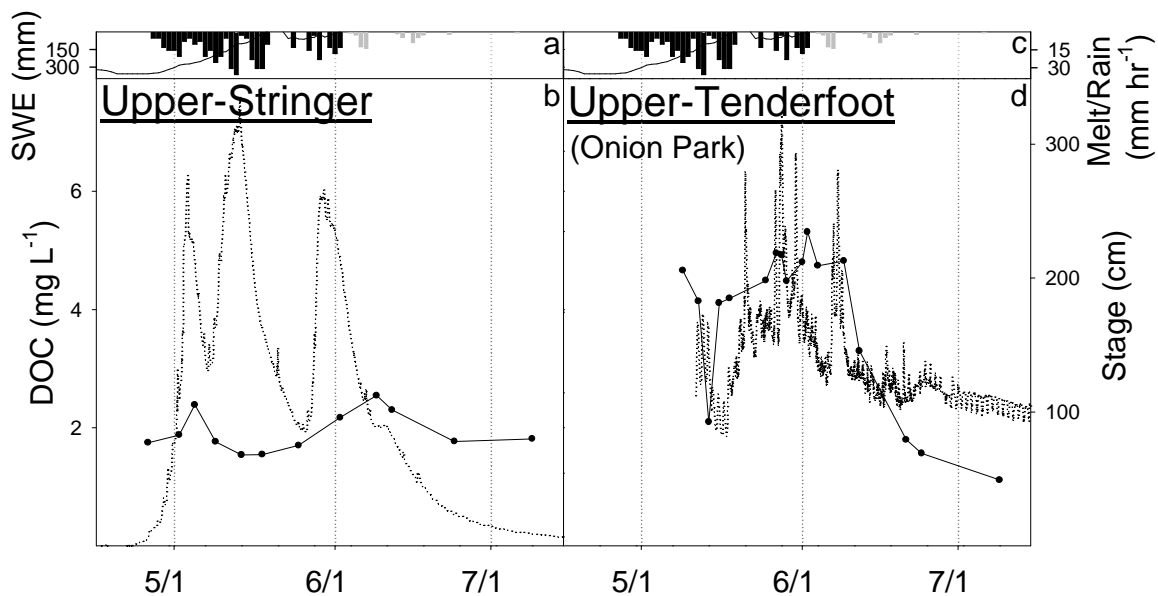


Figure 4.6: a) snow water equivalent (black line) and soil water inputs from snowmelt (black bars) and precipitation (grey bars); b) discharge and DOC concentrations at ST1 on Stringer Creek; c) snow water equivalent and snowmelt; and d) stage height and DOC concentrations at Upper Tenderfoot Creek (Onion Park) from April 15 to July 15, 2007. Discharge could not be calculated at Onion Park as no flume was installed.

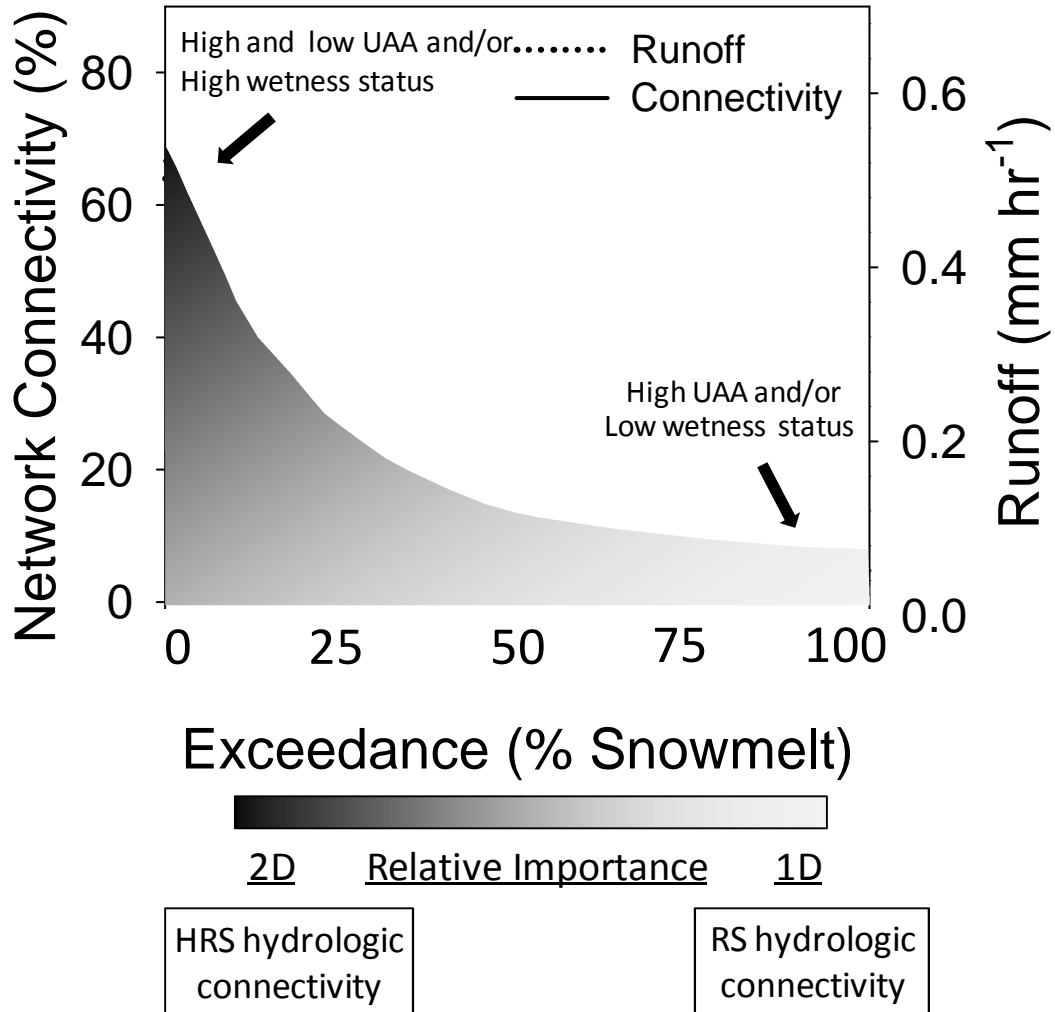


Figure 4.7: Conceptual model of 1D and 2D flushing mechanisms. Part (a) is adapted from Jencso et al. (2009), which shows data for the entire 2007 water year. Part (b) focuses on the snowmelt period, denoted by the grey box in Part (a). For 1D flushing to occur, a hydrologic connection is necessary between the riparian zone and the stream (RS). In contrast, a hydrologic connection across the entire hillslope-riparian-stream (HRS) continuum is requisite for 2D flushing. At baseflow and/or areas of high UAA, only a small portion of the stream network has HRS hydrologic connectivity, and 1D flushing is the dominant DOC mobilization and delivery mechanism to the stream. However, the relative importance of 2D flushing increases at areas of high UAA and during times of high wetness status (such as snowmelt or precipitation events). The greatest influence of 2D flushing on stream DOC export occurs at peak snowmelt when HRS hydrologic connectivity is highest.

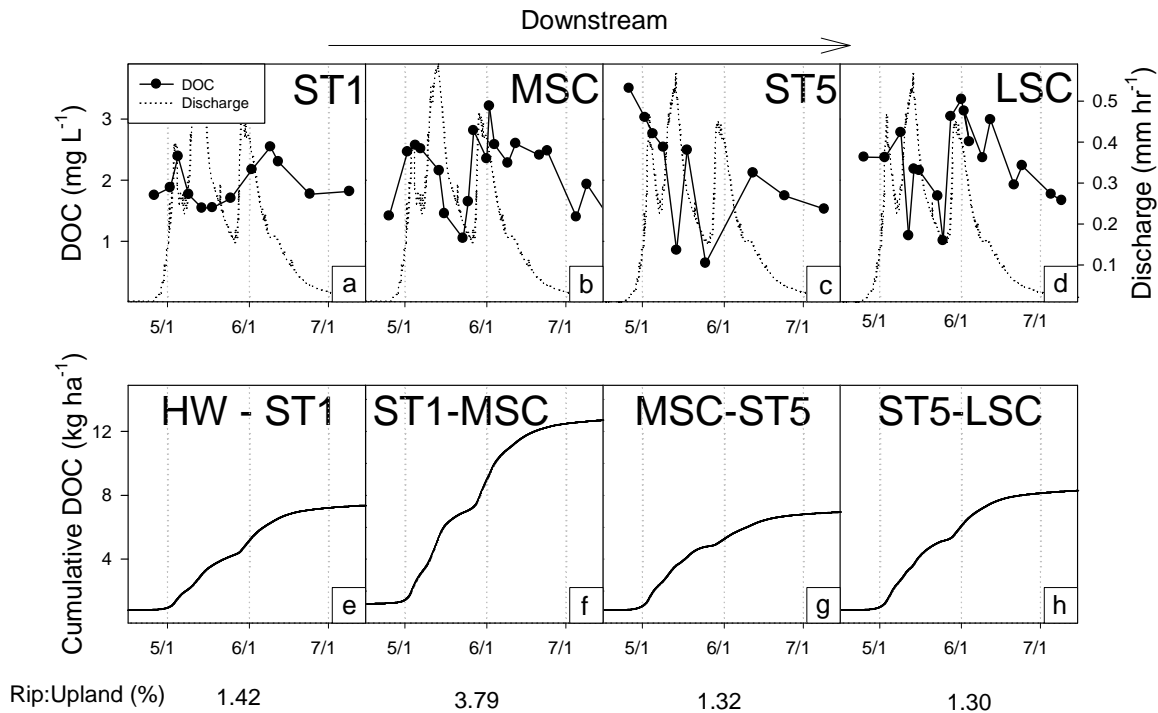


Figure 4.8: a-d) upstream to downstream Stringer Creek DOC concentrations at a) Transect 1; b) Middle Stringer Creek Flume (MSC); c) Transect 5; and d) Lower Stringer Creek Flume (LSC) from April 15 to July 15, 2007. e-h) cumulative DOC export from each sub-catchment. The percentage of riparian to upland area within each sub-catchment is also shown.

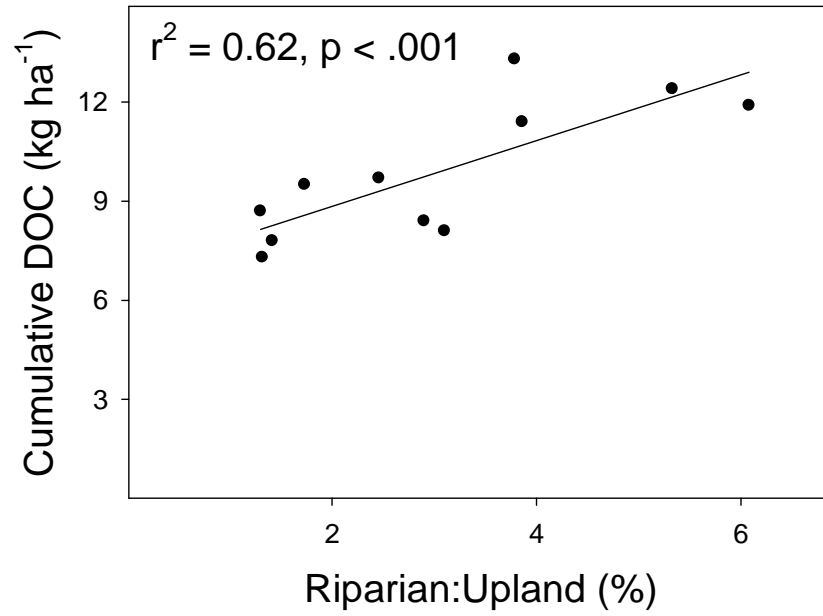


Figure 4.9: Cumulative DOC export between April 15 and July 15, 2007 at each of the sub-catchments in the Tenderfoot Creek Watershed (including the 4 catchments within the Stringer Creek Watershed - see Figure 8) as a function of riparian:upland ratio.

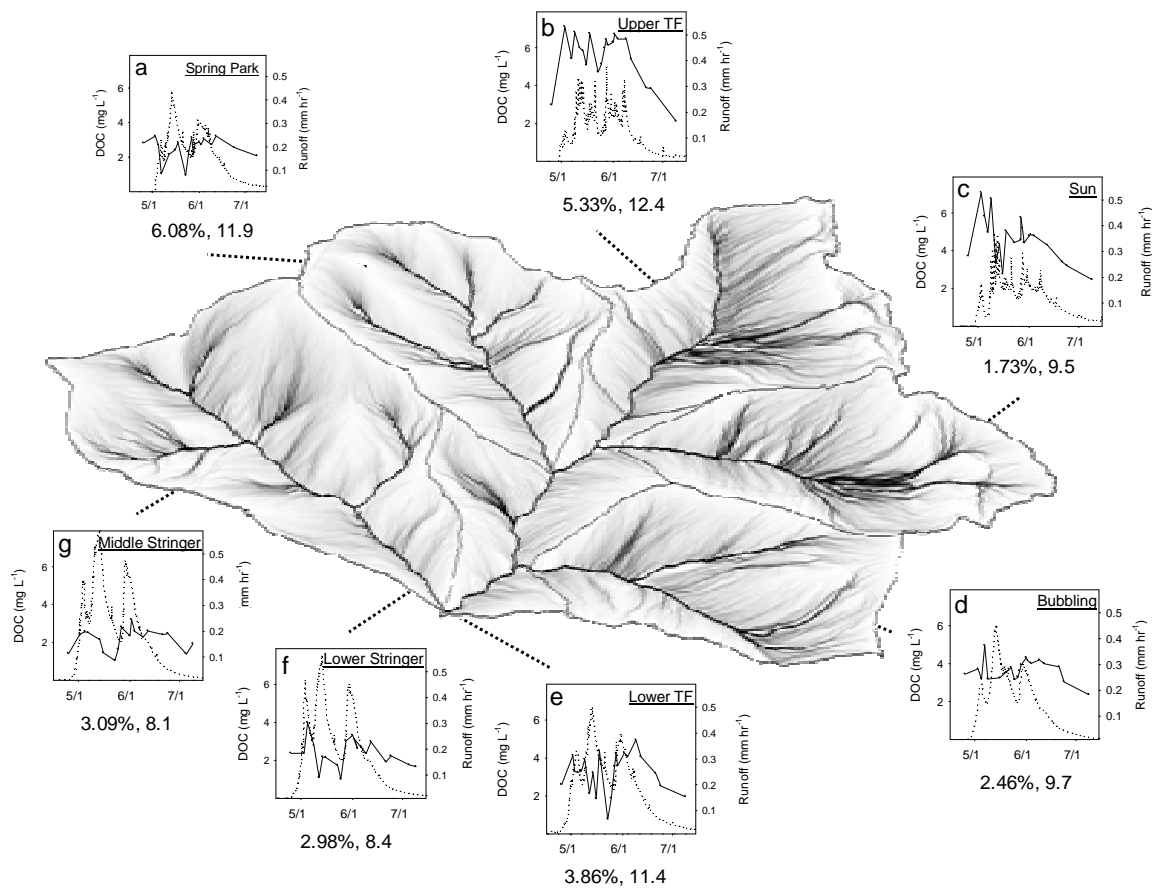


Figure 4.10: Comparison of discharge and DOC concentrations at the catchment outlet of a) Spring Park Creek; b) Upper Tenderfoot Creek; c) Sun Creek; d) Bubbling Creek; e) Lower Tenderfoot Creek; f) Lower Stringer Creek, and g) Middle Stringer Creek from April 15 to July 15, 2007. Riparian:upland extent and cumulative stream DOC export is given for each sub-catchment.

## CHAPTER 5

## SUMMARY

In this dissertation, I synthesized the controls of hydrology and landscape structure on two dominant avenues of carbon loss from high elevation mountain ecosystems: soil respiration and stream DOC export. Specifically, my research examined the biophysical controls and impact of changes in hydrologic regimes on soil respiration, and the control of landscape structure on stream DOC export across a range of spatial and temporal scales.

In Chapter 2, “Soil respiration across riparian-hillslope transitions: Biophysical controls and the role of landscape position,” I found that riparian and hillslope soil CO<sub>2</sub> efflux was not significantly different at short timescales, likely due to differential combinations of soil CO<sub>2</sub> production and transport. My results indicated that riparian zone soils had high CO<sub>2</sub> concentrations and low diffusivity in response to high SWC, while the opposite was true in the hillslopes. This resulted in similar CO<sub>2</sub> efflux across wet and dry landscape positions at short timescales. However, cumulative growing season CO<sub>2</sub> efflux was significantly higher from wet riparian landscape positions. I also determined that landscape position and attributes (e.g. slope, upslope accumulated area, and vegetation cover) could be related to soil respiration dynamics and led to organized heterogeneity in cumulative surface CO<sub>2</sub> efflux. These results may provide a way forward in reducing uncertainty in models of soil respiration across complex terrain and

highlight the need for further research of soil respiration across a wide range of biophysical gradients and landscape positions.

Chapter 3, “Differential soil respiration responses to changing hydrologic regimes,” built upon the knowledge gained in Chapter 2 by examining how changes in the timing and magnitude of snowmelt and precipitation affected soil respiration across wet and dry landscape positions. I found that cumulative growing season efflux peaked earlier during a drier growing season at both wet and dry landscape positions, but that the greatest changes occurred at wet areas of the landscape. These results suggest that predicted changes in soil respiration in response to higher temperatures may be constrained by concurrent changes in precipitation, which can strongly impact ecosystem carbon source/sink status.

In Chapter 4, “Variable flushing mechanisms and landscape structure control stream DOC export during snowmelt in a set of nested catchments,” I examined stream DOC export during snowmelt. Similar to soil respiration, I found that landscape structure strongly impacted stream DOC export due to its influence on hydrologic connectivity between the stream and riparian and hillslope zones and the importance of the relative amount of high DOC sources areas on cumulative stream DOC export. The greatest DOC export occurred at landscape positions with high hillslope-riparian-stream hydrologic connectivity and large riparian sources of DOC. These results suggest that landscape analysis may provide a way forward for determining which areas of the landscape are large contributors of DOC to the stream.

This dissertation focused on the intersection between hydrology, landscape structure, and carbon export, and to my knowledge, is the first study that examined carbon export via both soil surface CO<sub>2</sub> efflux and stream DOC in complex terrain. Each chapter elucidated the influence of hydrology and landscape structure on one of these specific avenues of carbon export. However, not until these chapters are integrated does it become apparent that hydrology and landscape structure influenced more than one carbon export mechanism, and that common themes existed. For example, I found that landscape position and attributes influenced the biophysical controls of soil respiration and resulted in higher CO<sub>2</sub> export from the soil to the atmosphere at wet riparian landscape positions. I then demonstrated that these wet riparian positions were also large sources of DOC to the stream, and that the relative amount of riparian area within a catchment and the degree of hillslope-riparian-stream hydrologic connectivity influenced catchment DOC export. In both studies, there existed a common theme of increased carbon export with increased upslope accumulated area. Further, I demonstrated that soil respiration response to changes in hydrologic regimes, such as snowmelt and precipitation timing and magnitude, differed across wet and dry landscape positions, with the greatest changes at wet landscape positions. Based upon the common theme of higher carbon export via both soil respiration and stream DOC at wet versus dry landscape positions, I suggest that the greatest changes in DOC export may also occur at wet landscape positions and from catchments with a large extent of riparian area. Thus, integration of the chapters presented in this dissertation demonstrates that hydrology and landscape structure influenced both soil respiration and stream DOC export, which are

two dominant avenues of ecosystem carbon export. With knowledge of these results, I propose that hydrology and landscape structure may also impact additional avenues of carbon loss, such as that from stream dissolved inorganic carbon (DIC) export or above-ground plant respiration. Collectively, these dissertation chapters suggest that studies of ecosystem carbon export need to account for both hydrology and landscape structure, particularly in areas of complex terrain, and highlights that landscape analysis may allow for increased confidence in estimations of ecosystem carbon export and balances.

Based upon the knowledge gained from my dissertation, I offer the following recommendations for future research:

1. Studies of soil respiration in complex terrain must be conducted across a wide range of biophysical variables (including soil water content, soil temperature, substrate, and soil physical properties) and from a variety of landscape positions in order to elucidate the primary controls of soil respiration heterogeneity through space and time.
2. Changes in hydrologic regimes, such as snowmelt and precipitation timing and magnitude, must be considered when examining interannual variability in carbon export processes. This needs to be a major focus of future carbon cycle research due to predictions of large changes in hydrologic regimes, particularly in high elevation mountain ecosystems, which can strongly impact ecosystem carbon source/sink status.
3. Studies of ecosystem carbon export should not be restricted to only one export process, and need to address whether the controls of one carbon export

mechanism is applicable to multiple avenues of carbon export. This may provide a way forward in simplifying the estimation of ecosystem carbon export and balances.

This dissertation addresses gaps in our current understanding of the interactions of the carbon and water cycle: the control of hydrology and landscape structure on carbon export from complex mountain catchments. Each chapter builds upon the knowledge gained in the previous chapter, and collectively highlight the need for an interdisciplinary approach to studies of carbon export. I suggest these disciplines should include, but not be limited to, hydrology, biogeochemistry, and ecology, the integration of which will broaden our knowledge on the controls of carbon export from complex mountain watersheds.